

N -jettiness in electroweak high-energy processes

Junegone Chay, Taewook Ha, and Taehyun Kwon

Department of Physics, Korea University, Seoul 02841, Korea

E-mail: chay@korea.ac.kr, hahah@korea.ac.kr, aieamfirst@korea.ac.kr

ABSTRACT: We study N -jettiness in electroweak processes at extreme high energies, in which the mass of the weak gauge bosons can be regarded as small. The description of the scattering process such as $e^-e^+ \rightarrow \mu^-\mu^+ + X$ is similar to QCD. The incoming leptons emit initial-state radiation and the resultant particles, highly off-shell, participate in the hard scattering, which are expressed by the beam functions. After the hard scattering, the final-state leptons or leptonic jets are observed, described by the fragmenting jet functions or the jet functions respectively. At present, electroweak processes are prevailed by the processes induced by the strong interaction, but they will be relevant at future e^-e^+ colliders at high energy. The main difference between QCD and electroweak processes is that the initial- and final-state particles should appear in the form of hadrons, that is, color singlets in QCD, while there can be weak nonsinglets as well in electroweak interactions. We analyze the factorization theorems for the N -jettiness in $e^-e^+ \rightarrow \mu^-\mu^+ + X$, and compute the factorized parts to next-to-leading logarithmic accuracy. To simplify the comparison with QCD, we only consider the $SU(2)_W$ gauge interaction, and the extension to the Standard Model is straightforward. Put it in a different way, it corresponds to an imaginary world in which colored particles can be observed in QCD, and the richer structure of effective theories is probed. Various nonzero nonsinglet matrix elements are interwoven to produce the factorized results, in contrast to QCD in which there are only contributions from the singlets. Another distinct feature is that the rapidity divergence is prevalent in the contributions from weak nonsinglets due to the different group theory factors between the real and virtual corrections. We verify that the rapidity divergence cancels in all the contributions with a different number of nonsinglet channels. We also consider the renormalization group evolution of each factorized part to resum large logarithms, which are distinct from QCD.

KEYWORDS: jettiness, electroweak processes, rapidity divergence, resummation

Contents

1	Introduction	2
2	SCET setup for the jettiness in $e^-e^+ \rightarrow \mu^-\mu^+X$	5
3	Factorization for the N-jettiness	7
3.1	SCET _I : $\mathcal{T}^2 \sim M^2 \ll p_c^2 \sim Q\mathcal{T} \ll Q^2$	7
3.1.1	The beam function	10
3.1.2	The jet function and the semi-inclusive jet function	11
3.1.3	The soft function	13
3.1.4	Factorized N -jettiness in SCET _I	14
3.2	SCET _{II} : $\mathcal{T}^2 \sim M^2 \sim p_c^2 \ll Q\mathcal{T} \ll Q^2$	15
4	Treatment of rapidity divergence	18
5	Collinear functions	20
5.1	Beam function and PDF	20
5.2	Semi-inclusive jet functions	26
5.3	Fragmentation functions and fragmenting jet functions	28
6	Hard function	31
7	Soft function	33
7.1	Hemisphere soft function	33
7.2	Soft anomalous dimensions	38
8	Renormalization group evolution	39
8.1	Hard function	39
8.2	Collinear functions	40
8.3	Soft function	41
9	Conclusion and outlook	42
A	Laplace transforms of the distributions	43
B	Beam functions and the matching coefficients for small M	45
C	Semi-inclusive jet functions and FJF for small M in SCET_I	46
C.1	Semi-inclusive jet functions	46
C.2	Fragmenting jet functions	47

D Color structures of the soft functions	48
D.1 Tree-level color matrices for the soft functions	48
D.2 No mixing in the soft function at order α	49

1 Introduction

The understanding of high-energy scattering has reached a state of the art with the advent of the effective theories such as soft-collinear effective theory (SCET) [1–4]. The basic picture to this understanding lies in the following procedure. The partons from the incoming protons, as in Large Hadron Collider, participate in the hard scattering and produce a plethora of final-state particles including hadrons, electroweak gauge bosons, Higgs particles and possibly heavy particles beyond the Standard Model. Quantum chromodynamics (QCD) plays a major role in comprehending collider physics phenomenology because the strong interaction acts in every stage of the scattering process with disparate energy scales.

The essence of disentangling the strong interaction is to construct factorization theorems which decompose the high-energy processes into hard, collinear and soft parts. SCET is the appropriate effective theory of QCD for high-energy processes, in which energetic, collinear particles form jets immersed in the sea of soft particles. In SCET we select the relevant collinear and soft modes and integrate out all the other degrees of freedom. Factorization of high-energy processes can be accomplished in SCET by decoupling the soft interaction from the collinear particles. Subsequently the collinear sectors in different directions do not interact with each other. Depending on the observables of interest, the phase space is divided by the definite properties of the specific modes and the factorization theorem is constructed according to how the modes or the phase spaces are organized. Each mode has its own characteristic scale, and typically there is a hierarchy of such scales. The scattering cross sections or event shape observables are expressed in terms of the logarithms of the ratios of the different energy scales, which necessitates the resummation of the large logarithms. Because each factorized part is governed by a single scale in each phase space, the large logarithms in each sector can be resummed to all orders using the renormalization group (RG) equations.

So far, we have described the factorization of high-energy processes in QCD. Here we change gears to employ SCET in extremely high-energy electroweak processes, in which all the masses of the particles including the weak gauge bosons can be regarded as small. By way of illustration, we consider the process $e^-e^+ \rightarrow \mu^- \text{ jet}, \mu^+ \text{ jet} + X$, where X denotes arbitrary final states, and the μ jet denotes the jet which includes the muon in the final state.¹ In order to simplify the situation, we consider only the weak $SU(2)_W$ gauge interaction by turning off all the other gauge interactions. Therefore we imagine a world with the $SU(2)_W$ weak gauge interaction out of the full $SU(3)_C \times SU(2)_W \times$

¹From now on, we will write $e^-e^+ \rightarrow \mu^- \mu^+ + X$ for the jets including muons. If we refer to the muons instead of the muon jets, we will explicitly state it.

$U(1)_B$ gauge interactions of the Standard Model. The extension to the Standard Model is complicated, but straightforward. In the high-energy limit, the incoming electron can be regarded as a collection of the “partons” which consist of leptons, weak gauge bosons. These partons undergo a hard collision and produce final-state energetic particles, along with soft particles.

This scenario may sound rather dull because everything mimics the processes in QCD, and one may wonder what, if any, can be learned from this imaginary world. The most interesting issue in this context is that the weak gauge interaction is not confining. It means that the incoming particles or the outgoing particles do not have to be gauge singlets. This is in contrast to QCD, where all the strongly-interacting particles are produced as color singlets, that is, hadrons. Due to this constraint, various matrix elements of the operators in QCD in, say, the parton distribution functions (PDF) or the jet functions are evaluated only for the color singlet configurations. However, the gauge singlets, as well as the gauge nonsinglets participate in weak high-energy processes. It makes the procedure of the factorization more sophisticated, and requires more care in analyzing the interwoven structure. Put it in a different way, it corresponds to imagining QCD without confinement and ask how the factorization works if there are free quarks and gluons. The underlying hard scattering processes can be traced directly and the measurement of the jets and the properties can be reconstructed explicitly by the constituents without worrying about hadronization.

We sketch electroweak high-energy processes by analogy with QCD. The incoming on-shell “partons” (electrons in our case) possess certain fractions of the energy from the initial particles and they radiate away gauge bosons to be far off-shell. This process is described by the electroweak beam functions. Then the energetic partons undergo a hard scattering and the final-state particles can be observed in terms of individual particles, described by the fragmentation functions, or jets by the jet functions or the fragmenting jet functions (FJF). And the soft interaction is interspersed between the collinear parts. In electroweak high-energy processes, gauge singlets and nonsinglets are involved in all these factorized components, which makes the analysis more intriguing. This study will be relevant in high-energy electron-positron colliders such as CEPC [5], ILC [6], FCC-ee [7], and CLIC [8]. Our analysis can be extended to include the production of the Higgs boson, weak gauge bosons and top quarks.

There appear many different energy scales, the energy of the hard scattering Q , the invariant masses of the initial- and final-states as a typical collinear scale, and the soft scale, and possibly more if we are interested in more differential processes describing event shapes. In addition, the mass of the weak gauge bosons M also enters into the picture as a physical mass. In radiative corrections, there are logarithms of the ratios of these scales and we need to resum the large logarithms to all orders. In SCET, the factorization is achieved by dissecting the phase space and devising the modes in that phase space such that the radiative corrections depend on a single scale in each phase space. Then the resummation is obtained by solving the RG equation.

Besides the conventional RG behavior, there is additional rapidity divergence because the phase space is divided into different regions. It is obviously absent in the full theory

because there is no separation of the phase space. Therefore it is a good consistency check for an effective theory to see whether the rapidity divergences are cancelled when all the factorized contributions are added. It is one of the goals in this paper to check this point even in the presence of the nonsinglets participating in the scattering.

Though the sum of the rapidity divergences cancels, the rapidity divergence remains in each sector and it affects the RG behavior of the factorized parts. The rapidity divergence has been regulated using diverse methods, such as the use of the Wilson lines off the lightcone [9], the δ -regulator [10, 11], the analytic regulator [12], the rapidity regulator [13, 14], the exponential regulator [15], and the pure rapidity regulator [16], etc.. Recently one of us has proposed a consistent scheme of applying rapidity regulators to the soft and collinear sectors [17]. It correctly produces the directional dependence in the soft function, which is essential in our case because there are four different collinear directions involved. The independence of the rapidity scale in the cross section critically depends on the interplay between the collinear and the soft functions.

The dependence on the rapidity scale in each sector becomes highly nontrivial and more interesting when gauge nonsinglets as well as singlets participate in high-energy scattering. First of all, let us describe the rapidity divergence for singlets, which is well understood in QCD. The rapidity divergence appears distinctively in SCET_I and SCET_{II}. In SCET_I, since collinear and soft particles have different offshellness, there is no overlap in rapidity between these modes, hence no rapidity divergence arises. In other words, the rapidity divergence cancels in each sector. On the other hand, in SCET_{II}, where collinear and soft particles have the same offshellness, they overlap near the rapidity boundary. The soft particles with small rapidity cannot perceive the large rapidity region which belongs to collinear sector, causing the rapidity divergence in the soft sector. In the collinear sector, according to our regularization scheme of the rapidity divergence, which will be described in detail, the rapidity divergence arises from the zero-bin subtraction [13, 14]. The zero-bin subtraction replaces the spurious rapidity divergence in the naive contribution. It is analogous to the pullup mechanism [18, 19] in the dimensional regularization, in which the IR divergence is replaced by the UV divergence. The rapidity divergence may survive in each sector, but their sum cancels. However, the persistent existence of the rapidity divergence in each sector offers additional evolution to complete the resummation.

In weak interaction, the structure of the rapidity divergence is more intricate. For gauge singlets, there is no rapidity divergence as in QCD. For gauge nonsinglets, regardless of SCET_I or SCET_{II}, the rapidity divergence is not cancelled in each sector when the weak charges of the initial or final states are specified. Nor are the Sudakov logarithms. The non-cancellation of the electroweak logarithms is known as the Block-Nordsieck violation in electroweak processes [20–23]. In contrast, the Sudakov logarithms in QCD cancel from virtual and real contributions in inclusive processes. It yields, for example, the Dokshitzer-Gribov-Lipatov-Altarelli-Parisi (DGLAP) evolution of the PDF. The non-cancellation in weak interaction affects the UV behavior as well as the rapidity behavior. Our result is, in some sense, a manifestation of the non-cancellation in considering the event shape through the jettiness.

In the framework of SCET, it was pointed out in ref. [24] that the nonsinglet elec-

troweak PDFs possess this property. It is also true for the beam function in the initial state, and for the jet functions, or the FJFs in the final state, and for the soft function. The purposes of this paper are to analyze the structure of the factorization in the weak processes, and to resum large logarithms by probing the structure of the divergences including the rapidity divergence from the nonsinglet contributions.

As a concrete example, we consider an event shape, especially the N -jettiness [25, 26] (in fact, 2-jettiness) in $e^-e^+ \rightarrow \mu^-\mu^+ + X$. By considering the jettiness, we can probe the hierarchy of scales in effective theories, and the characteristics of a measurement-dependent factorization can be discussed. In addition, we are interested in the case in which there are four distinct lightlike directions. For this reason, N -jettiness is better suited than the beam thrust in the Drell-Yan process [27] or the jet thrust in e^-e^+ collisions. In terms of QCD, it corresponds to the N -jettiness from the partonic subprocess $q\bar{q} \rightarrow q'\bar{q}' + X$.

The rest of the paper is organized as follows. In section 2, we explain the N -jettiness, and establish the power counting of the relevant momenta and the jettiness to choose the appropriate effective theories. In section 3, we first construct the factorization of the N -jettiness in SCET_I, in which the ingredients of the factorized parts are extracted and defined. The beam functions, the semi-inclusive jet functions, and the soft functions are constructed in the context of SCET_I with the weak singlet and nonsinglet contributions. Then we scale down to SCET_{II} and establish the factorization by probing the relations between the beam function in SCET_I, and the PDF in SCET_{II}, or those between the fragmenting jet functions and the fragmentation functions. In section 4, we examine the source of the rapidity divergence, set up the rapidity regulators in the collinear and the soft sectors and discuss their characteristics.

In section 5, we present the radiative corrections of the collinear parts at next-to-leading order (NLO), which consist of the beam functions, the PDFs, the jet functions, the fragmentation functions and the FJFs. In section 6, the hard functions are collected for the process $\ell_e\bar{\ell}_e \rightarrow \ell_\mu\bar{\ell}_\mu$ with the left-handed electron and muon doublets, and the hard anomalous dimension matrix is presented. The soft functions are analyzed in section 7, which are expressed in terms of the matrices in weak-charge space. In section 8, we combine all the factorized parts to show the RG evolution of the N -jettiness, and we conclude in section 9. Long technical calculations are relegated to appendices. In appendix A, we list the Laplace transforms of the distributions. In appendices B and C, we present how to obtain the collinear functions and the matching coefficients in the limit of small M . In appendix D, we illustrate the color matrices for the soft functions at tree level, and we show that there is no mixing at one loop for the soft functions with four nonsinglets.

2 SCET setup for the jettiness in $e^-e^+ \rightarrow \mu^-\mu^+X$

We consider the N -jettiness², which is defined as [25, 26]

$$\mathcal{T}_N = \sum_k \min \left\{ \frac{2q_i \cdot p_k}{\omega_i} \right\}, \quad (2.1)$$

²We keep using the terminology N -jettiness, bearing in mind that we actually consider the 2-jettiness \mathcal{T}_2 in our case.

where i runs over 1, 2 for the beams, and $3, \dots, N+2$ for the final-state jets. Here q_i are the reference momenta of the beams and the jets with the normalization factors $\omega_i = \bar{n}_i \cdot q_i$, and p_k are the momenta of all the measured particles in the final state.

$$q_{1,2}^\mu = \frac{1}{2} z_{1,2} E_{\text{cm}} n_{1,2}^\mu = \frac{1}{2} \omega_{1,2} n_{1,2}^\mu, \quad q_i^\mu = \frac{1}{2} \omega_i n_i^\mu, \quad (i = 3, \dots, N+2), \quad (2.2)$$

where $z_{1,2}$ are the momentum fractions of the beams. Here n_1 and n_2 are lightcone vectors for the beams, which are aligned to the z direction, $n_1^\mu = (1, 0, 0, 1)$, $n_2^\mu = (1, 0, 0, -1)$, and n_i are the lightcone vectors specifying the jet directions. Typically we write the lightlike vectors as $n_i = (1, \mathbf{n}_i)$, $\bar{n}_i = (1, -\mathbf{n}_i)$, where the unit vector \mathbf{n}_i denotes the direction of the spatial momentum \mathbf{p}_i . The N -jettiness in eq. (2.1) can also be expressed in terms of some arbitrary hard scales instead of the normalization factor ω_i .

In references [26, 28], the authors have considered the differential distribution with respect to the individual jettiness, which is defined as

$$\tilde{\mathcal{T}}_i = \sum_k \frac{2q_i \cdot p_k}{\omega_i} \prod_{i \neq j} \theta(n_j \cdot p_k - n_i \cdot p_k). \quad (2.3)$$

Here we consider the total N -jettiness \mathcal{T}_N , which is given by $\mathcal{T}_N = \sum_i \tilde{\mathcal{T}}_i$.

For $\mathcal{T}_2 \ll Q$, SCET can be applied to the process $e^- e^+ \rightarrow \mu^- \mu^+ + X$, but we should determine which effective theories are to be employed, depending on the hierarchy of the scales in the collinear and soft momenta and the magnitude of the jettiness. The n -collinear momentum scales as $p_c^\mu = (\bar{n} \cdot p_c, p_{c\perp}, n \cdot p_c) = (p_c^-, p_{c\perp}, p_c^+) \sim Q(1, \lambda, \lambda^2)$, where $\lambda \sim p_{c\perp}/\bar{n} \cdot p_c$ is the small parameter in SCET. We can consider either SCET_I, or continue down to SCET_{II}, depending on the power counting of the soft momentum.

In SCET_I, the ultrasoft (usoft) momentum scales as $p_{us}^\mu = (p_{us}^-, p_{us\perp}, p_{us}^+) \sim Q(\lambda^2, \lambda^2, \lambda^2)$, while the soft momentum in SCET_{II} scales as $p_s^\mu = (p_s^-, p_{s\perp}, p_s^+) \sim Q(\lambda, \lambda, \lambda)$. The gauge boson mass M is another mass scale which enters into the system. When the usoft or the soft gauge bosons are on their mass shell, $p_{us}^2 \sim p_s^2 \sim M^2$, it implies that the gauge boson mass M is power counted as $Q\lambda^2$ in SCET_I, and $Q\lambda$ in SCET_{II}.

The scale of the N -jettiness \mathcal{T}_N from eq. (2.1), is extracted from the lightcone component p^+ . Note, however, that the magnitudes of p^+ for the collinear and the usoft momenta in SCET_I are comparable to each other, hence the contribution to the N -jettiness comes both from the collinear and the usoft sectors. On the other hand, the magnitude of p^+ for the collinear momentum is much smaller than that for the soft momentum in SCET_{II}. In this case, the contribution to the N -jettiness comes only from the soft sector. Therefore we expect that the structure of the factorization takes different forms in SCET_I and in SCET_{II}.

In SCET_I, the hierarchy of the scales is given as $\mathcal{T}^2 \sim M^2 \ll p_c^2 \sim Q\mathcal{T} \ll Q^2$. The relevant modes scale as

$$\begin{aligned} n\text{-collinear} : p_c^\mu &\sim (Q, \sqrt{Q\mathcal{T}}, \mathcal{T}) \sim (Q, \sqrt{QM}, M) \sim (Q, p_\perp, p_\perp^2/Q), \\ \text{usoft} : p_{us}^\mu &\sim (\mathcal{T}, \mathcal{T}, \mathcal{T}) \sim (M, M, M). \end{aligned} \quad (2.4)$$

The N -jettiness probes the scale of order $p_c^+ \sim p_{us}^+ \sim Q\lambda^2 \sim \mathcal{T}$, hence both the collinear and the usoft parts contribute to the N -jettiness.

If we consider the kinematical situation in which $M^2 \ll p_c^2 \sim Q\mathcal{T}$, the framework of SCET_I suffices to describe the N -jettiness. However, we would like to include another kinematical case, in which the jet becomes narrower, and we reach the region $M^2 \sim p_c^2 \sim \mathcal{T}^2$. Then the plus component $p_c^+ \sim \mathcal{T}^2/Q$ does not contribute to the jettiness. However, there remains large logarithms associated with Q/M , which should be resummed. This can be achieved by going from SCET_I to SCET_{II} through the matching. The beam functions and the jet functions in SCET_I have virtuality $p_c^2 \sim QM$, and we need a second stage of matching to separate these scales. And the ultrasoft function is scaled down to the soft function, which develops the rapidity divergence. These necessitate the use of SCET_{II}.

In SCET_{II}, the hierarchy of scales is given by $\mathcal{T}^2 \sim M^2 \sim p_c^2 \ll Q\mathcal{T} \ll Q^2$. The hard-collinear, collinear and soft modes scale as

$$\begin{aligned} n\text{-hard-collinear} &: p_{hc}^\mu \sim (Q, \sqrt{Q\mathcal{T}}, \mathcal{T}) \sim (Q, \sqrt{QM}, M), \\ n\text{-collinear} &: p_c^\mu \sim (Q, \mathcal{T}, \mathcal{T}^2/Q) \sim (Q, M, M^2/Q) \sim (Q, p_\perp, p_\perp^2/Q), \\ \text{soft} &: p_s^\mu \sim (\mathcal{T}, \mathcal{T}, \mathcal{T}) \sim (M, M, M). \end{aligned} \tag{2.5}$$

In fact, the hard-collinear modes are not the dynamical degrees of freedom in SCET_{II}, but these are the modes from SCET_I to be integrated out to obtain SCET_{II}. The N -jettiness probes the scale of order $p_s^+ \sim Q\lambda \sim M$, and the collinear contribution with $p_c^+ \sim Q\lambda^2 \sim M^2/Q$ does not contribute to the jettiness. This is also recognized in ref. [29] in a different context of measuring the transverse momentum q_T and the 0-jettiness \mathcal{T}_0 .

We first describe SCET_I in order to set up the elements of the factorization. In order to obtain SCET_{II}, the hard-collinear modes, which are previously collinear modes in SCET_I, are integrated out to reach the collinear modes in SCET_{II}. Note that the scaling of the usoft momentum in SCET_I, and the soft momentum in SCET_{II} remain the same, but the small parameter λ , responsible for the power counting, is rescaled from $\sqrt{\mathcal{T}/Q}$ to \mathcal{T}/Q . We present the results in both cases.

3 Factorization for the N -jettiness

3.1 SCET_I: $\mathcal{T}^2 \sim M^2 \ll p_c^2 \sim Q\mathcal{T} \ll Q^2$

The procedure of obtaining the effective operators by integrating out the degrees of freedom of order Q with their Wilson coefficients was previously studied extensively in constructing the weak effective Hamiltonian with the QCD radiative corrections [30]. We follow the same technique, and the Wilson coefficients D_I for the operators O_I are obtained by matching the full theory onto SCET at any fixed order. The four-lepton operators for the process $e^-e^+ \rightarrow \mu^-\mu^+X$ in SCET are given as³

$$O_I(x) = \bar{\ell}_{L2}(x)T_I\gamma^\mu\ell_{L1}(x) \cdot \bar{\ell}_{L3}(x)T_I\gamma_\mu\ell_{L4}(x), \quad (I = 1, 2), \tag{3.1}$$

³In ref. [24], other four-fermion operators are listed for neutrino scattering $\nu p \rightarrow \ell X$.

at leading order in M/Q . We label the incoming leptons as 1 and 2, and the outgoing leptons as 3 and 4. The index I refers to the weak charge ($T_1 = t^a$ for the nonsinglet and $T_2 = 1$ for the singlet). At tree level, O_1 is obtained by the exchange of a gauge boson, which leads to the matching coefficient

$$D_1^{(0)} = \frac{ig^2}{2p_1 \cdot p_2}, \quad (3.2)$$

where the incoming momenta are p_1 and p_2 for the weak doublets ℓ_{L1} and ℓ_{L2} with $2p_1 \cdot p_2 \sim Q^2$. The matching coefficient D_2 for O_2 begins at order g^4 . Here we can utilize the results of the corresponding four-quark operators in QCD for $q\bar{q} \rightarrow q'\bar{q}'$ at NLO, and the Wilson coefficients can be read off from those in QCD in ref. [31] by adjusting the group theory factors for $SU(2)_W$. In constructing the Wilson coefficients for our process, note that only the left-handed doublets participate in the scattering. The effective Lagrangian for the leptonic high-energy scattering can be written as

$$\mathcal{L}_{\text{eff}} = -i \sum_I D_I O_I + \text{hermitian conjugate}. \quad (3.3)$$

The fields in the operators O_I are now expressed in terms of the collinear fields in SCET. We refer to refs. [1–4] for the detailed formulation of SCET, and here we collect the necessary ingredients to express the operators in SCET. We introduce a lightcone vector n^μ , and its conjugate light-cone vector \bar{n}^μ such that $n^2 = \bar{n}^2 = 0$ and $n \cdot \bar{n} = 2$. A four-vector p^μ can be decomposed as $p^\mu = (p^-, p_\perp, p^+)$, and the n -collinear momentum p_c^μ scales as $p_c^\mu = (p_c^-, p_{c\perp}, p_c^+) \sim p_c^-(1, \lambda, \lambda^2)$, where λ is a small parameter in SCET. The usoft momentum scales as $p_{us}^\mu = (p_{us}^-, p_{us\perp}, p_{us}^+) \sim p_c^-(\lambda^2, \lambda^2, \lambda^2)$.

The collinear operators, which are invariant under collinear gauge transformations, are constructed in terms of the product of the fields and the Wilson lines. The basic building blocks for the lepton and the gauge bosons are defined as

$$\ell_n(x) = W_n^\dagger(x) \xi_n(x), \quad \mathcal{B}_{n\perp}^\mu(x) = \frac{1}{g} [W_n^\dagger(x) iD_{n\perp}^\mu W_n(x)], \quad (3.4)$$

where $iD_{n\perp}^\mu = \mathcal{P}_{n\perp}^\mu + gA_{n\perp}^\mu$ is the covariant derivative. The collinear Wilson line is given as

$$W_n(x) = \text{P exp} \left(ig \int_{-\infty}^0 ds \bar{n} \cdot A_n(x + s\bar{n}) \right) = \sum_{\text{perm.}} \exp \left[-g \frac{\bar{n} \cdot A_n(x)}{\bar{n} \cdot \mathcal{P}} \right], \quad (3.5)$$

where P denotes the path ordering along the integration path.

At leading order in SCET, the interactions of soft gauge bosons with collinear fields exponentiate to form eikonal soft Wilson lines⁴. The soft gauge bosons are decoupled by the field redefinition [4]

$$\ell_n^{(0)}(x) = Y_n^\dagger(x) \ell_n(x), \quad \mathcal{B}_{n\perp}^{\mu(0)}(x) = Y_n^\dagger(x) \mathcal{B}_{n\perp}^\mu(x) Y_n(x). \quad (3.6)$$

⁴When no confusion arises, we refer to the usoft momentum as the soft momentum.

In this paper we use the fields after the decoupling and we drop the superscript (0) for simplicity. Here $Y_n(x)$ is the soft Wilson line in the fundamental representation

$$Y_n(x) = \text{P exp} \left(ig \int_{-\infty}^0 ds n \cdot A_{us}(x + sn) \right) = \sum_{\text{perm.}} \exp \left[-g \frac{n \cdot A_{us}(x)}{n \cdot \mathcal{P}} \right]. \quad (3.7)$$

Employing SCET, the operators O_I in eq. (3.1) are written as

$$O_I = \bar{\ell}_{L2} Y_2^\dagger \gamma^\mu T_I Y_1 \ell_{L1} \cdot \bar{\ell}_{L3} Y_3^\dagger \gamma_\mu T_I Y_4 \ell_{L4}. \quad (3.8)$$

The differential cross section for the 2-jettiness \mathcal{T}_2 is given by [32]

$$\frac{d\sigma}{d\mathcal{T}_2} = \frac{1}{2s} \int d^4x \sum_X \langle I | \mathcal{L}_{\text{eff}}(x) | X \rangle \langle X | \mathcal{L}_{\text{eff}}(0) | I \rangle \delta(\mathcal{T}_2 - g(X)), \quad (3.9)$$

where $|I\rangle$ represents the initial state, $|X\rangle$ denotes the final state, and the sum over X includes a sum over states with the appropriate phase space. The function $g(X)$ computes the value of the jettiness for the final state X . In SCET, the final states $|X\rangle$ consist of the collinear states $|X_i\rangle$ in the n_i directions ($i = 1, 2, 3, 4$) and the soft states $|X_s\rangle$. Since the n_i -collinear particles do not interact with each other, and the soft particles are decoupled from the collinear sectors by the redefinition in eq. (3.6), the final states $|X\rangle$ in the Hilbert space can be expressed in terms of the tensor product of the collinear states $|X_i\rangle$ and the soft states $|X_s\rangle$ as

$$|X\rangle = |X_1\rangle \otimes |X_2\rangle \otimes |X_3\rangle \otimes |X_4\rangle \otimes |X_s\rangle. \quad (3.10)$$

The factorization in SCET is established in the scattering cross section, that is, at the amplitude-squared level, instead of at the amplitude level, as shown in eq. (3.9). Therefore we need to factorize the product of the operators $O_I^\dagger(x) O_J(0)$, which will be reorganized in terms of the collinear operators in each collinear direction along with the soft Wilson lines, and it will be implemented in eq. (3.9) to express the factorized result for the N -jettiness. The product of the operators $O_I^\dagger(x) O_J(0)$ is given as

$$\begin{aligned} O_I^\dagger(x) O_J(0) &= \left(\bar{\ell}_{L1} Y_1^\dagger \gamma^\nu T_I Y_2 \ell_{L2} \cdot \bar{\ell}_{L4} Y_4^\dagger \gamma_\nu T_I Y_3 \ell_{L3} \right)(x) \\ &\quad \times \left(\bar{\ell}_{L2} Y_2^\dagger \gamma^\mu T_J Y_1 \ell_{L1} \cdot \bar{\ell}_{L3} Y_3^\dagger \gamma_\mu T_J Y_4 \ell_{L4} \right)(0). \end{aligned} \quad (3.11)$$

We rewrite the product by grouping the fields in respective collinear directions, and use the relation [24]

$$\begin{aligned} (\bar{\ell}_n)_\alpha^i (\ell_n)_\beta^j &= \frac{1}{2N} \delta^{ij} (\mathcal{P}_L \not{n})_{\beta\alpha} \bar{\not{n}} \ell_n + (t^c)^{ji} (\mathcal{P}_L \not{n})_{\beta\alpha} \bar{\not{n}} t^c \ell_n \\ &\equiv \delta^{ij} (\mathcal{P}_L \not{n})_{\beta\alpha} C_\ell^0 + (t^c)^{ji} (\mathcal{P}_L \not{n})_{\beta\alpha} C_\ell^c, \end{aligned} \quad (3.12)$$

where i, j are the gauge indices, α, β are the Dirac indices, and $\mathcal{P}_L = (1 - \gamma_5)/2$. To make the notation concise, we have extended the index to 0 such that

$$C_\ell^0(x, y) = \frac{1}{2N} \bar{\ell}_{Ln}(x) \frac{\not{n}}{2} T^0 \ell_{Ln}(y), \quad C_\ell^a(x, y) = \bar{\ell}_{Ln}(x) \frac{\not{n}}{2} T^a \ell_{Ln}(y), \quad (3.13)$$

with $T^0 = 1$ and $T^a = t^a$ are the gauge generators for $a = 1, \dots, N^2 - 1$. We keep N as it is for the $SU(N)$ gauge interaction, and the Casimir invariants are denoted by $C_F = (N^2 - 1)/(2N)$ and $C_A = N$. For the $SU(2)_W$ gauge group, we put $N = 2$.

After some manipulation, eq. (3.11) can be written as

$$\begin{aligned}
& 16n_1 \cdot n_4 n_2 \cdot n_3 \left(Y_2^\dagger T_J Y_1(0) \right)^{i_1 k_1} \left(Y_1^\dagger T_I Y_2(x) \right)^{i_2 k_2} \left(Y_3^\dagger T_J Y_4(0) \right)^{i_3 k_3} \left(Y_4^\dagger T_I Y_3(x) \right)^{i_4 k_4} \\
& \times \left[(T^c)^{k_2 i_1} C_{\ell_2}^c(0, x) \right] \left[(T^d)^{k_1 i_2} C_{\ell_1}^d(x, 0) \right] \left[(T^e)^{k_4 i_3} C_{\ell_3}^e(0, x) \right] \left[(T^f)^{k_3 i_4} C_{\ell_4}^f(x, 0) \right] \\
& = 16n_1 \cdot n_4 n_2 \cdot n_3 C_{\ell_2}^c(0, x) C_{\ell_1}^d(x, 0) C_{\ell_3}^e(0, x) C_{\ell_4}^f(x, 0) \\
& \times \text{Tr} \left[T^c Y_2^\dagger T_J Y_1(0) T^d Y_1^\dagger T_I Y_2(x) \right] \cdot \text{Tr} \left[T^e Y_3^\dagger T_J Y_4(0) T^f Y_4^\dagger T_I Y_3(x) \right]. \tag{3.14}
\end{aligned}$$

Here the coefficient $n_1 \cdot n_4 n_2 \cdot n_3$ will be absorbed into the hard function. In order to construct the expression for the jettiness, all the collinear and the soft parts should be organized in such a way that the contribution to the jettiness from each part becomes manifest.

The N -jettiness (the 2-jettiness here) can be expressed in terms of the matrix elements for each collinear part and the soft part, which is schematically expressed as

$$\begin{aligned}
\frac{d\sigma}{d\mathcal{T}_2} &= \frac{1}{2s} \sum_{IJ} H_{JI} \langle e^+ | C_{\ell_2}^c(0, x) | e^+ \rangle \langle e^- | C_{\ell_1}^d(x, 0) | e^- \rangle \langle 0 | C_{\ell_3}^e(0, x) | 0 \rangle \langle 0 | C_{\ell_4}^f(x, 0) | 0 \rangle \\
& \times \langle 0 | \text{Tr} \left[T^c Y_2^\dagger T_J Y_1(0) T^d Y_1^\dagger T_I Y_2(x) \right] \cdot \text{Tr} \left[T^e Y_3^\dagger T_J Y_4(0) T^f Y_4^\dagger T_I Y_3(x) \right] | 0 \rangle \\
& \times \delta(\mathcal{T}_2 - g(X)). \tag{3.15}
\end{aligned}$$

Eq. (3.15) is unavoidably complicated due to the presence of the gauge indices, compared to the corresponding expression in QCD, in which there are only singlet contributions.

The matrix elements between the corresponding states in the Hilbert space can be obtained because the collinear currents C_ℓ^a in different collinear directions and the soft part are decoupled. For example, $\langle e^- | C_{\ell_1}^d(x, 0) | e^- \rangle$ yields the electron beam function, and when we consider the intermediate states, the projection into the n_1 -collinear states $\sum |X_1\rangle\langle X_1|$ is inserted. The matrix element $\langle 0 | C_{\ell_3}^e(0, x) | 0 \rangle$ describes the final-state jet and the projection $\sum |X_3\rangle\langle X_3|$ is inserted for the intermediate states. The matrix element for the soft Wilson lines yields the soft function, and the intermediate states consist of $\sum |X_s\rangle\langle X_s|$. The treatment of the matrix elements is delineated below.

3.1.1 The beam function

The beam functions are obtained by taking the matrix elements of $C_{\ell_2}^c(0, x)$ and $C_{\ell_1}^d(x, 0)$ in eq. (3.14) between the initial states $|e^-(P_1)\rangle$ or $|e^+(P_2)\rangle$. For the matrix element of $C_{\ell_1}^d(x, 0)$, the coordinate x can be expanded around the lightcone coordinate $n_1 \cdot x$, and the subleading terms can be neglected. Then by writing $p^+ = n_1 \cdot p$, $p^- = \bar{n}_1 \cdot p$, the matrix element can be written as

$$\begin{aligned}
\langle e^- | C_{\ell_1}^d(x, 0) | e^- \rangle &= k_d \langle e^- | \bar{\ell}_{L1} \left(x^+ \frac{\bar{n}_1}{2} \right) \frac{\not{\bar{n}}_1}{2} T^d \ell_{L1}(0) | e^- \rangle \\
&= k_d \int dq^+ dq^- \langle e^- | e^{i\hat{p}^- x^+ / 2} \bar{\ell}_{L1}(0) e^{-i\hat{p}^- x^+ / 2} \frac{\not{\bar{n}}_1}{2} T^d \delta(q^+ + \mathcal{P}^+) \delta(q^- + \mathcal{P}^-) \ell_{L1}(0) | e^- \rangle
\end{aligned}$$

$$= k_d \int dq^+ dq^- e^{i(P_1^- - q^-)x^+/2} \langle e^- | \bar{\ell}_{L1}(0) \frac{\not{n}_1}{2} T^d \delta(q^+ + \mathcal{P}^+) \delta(q^- + \mathcal{P}^-) \ell_{L1}(0) | e^- \rangle, \quad (3.16)$$

where $k_0 = 1/(2N)$ for the singlet and $k_d = 1$ ($d \neq 0$) for the nonsinglets. In the second line, the integration of the delta functions, which is equal to the identity, is inserted. The operators \mathcal{P}^\pm extract the corresponding momenta for the annihilated particles. And $\bar{\ell}_{L1}(x^+ \bar{n}_1/2)$ is translated to the origin using the momentum operator \hat{p}^μ .

The last part in the last eq. (3.16) can be manipulated as

$$\begin{aligned} \delta(q^- + \mathcal{P}^-) \ell_{L1}(0) | e^-(P_1^-) \rangle &= \int \frac{dy}{2\pi} e^{i(\mathcal{P}^- + q^-)y} \ell_{L1}(0) e^{-i\mathcal{P}^- y} e^{i\mathcal{P}^- y} | e^-(P_1^-) \rangle \\ &= \int \frac{dy}{2\pi} e^{-i(P_1^- - q^-)y} e^{i\mathcal{P}^- y} \ell_{L1}(0) e^{-i\mathcal{P}^- y} | e^-(P_1^-) \rangle \\ &= \int \frac{dy}{2\pi} e^{-i(P_1^- - q^-)y} [e^{i\mathcal{P}^- y} \ell_{L1}(0)] | e^-(P_1^-) \rangle = [\delta(P_1^- - q^- - \mathcal{P}^-) \ell_{L1}(0)] | e^-(P_1^-) \rangle, \end{aligned} \quad (3.17)$$

using the relation $e^{i\mathcal{P}^- y} \ell_{L1}(0) e^{-i\mathcal{P}^- y} = [e^{i\mathcal{P}^- y} \ell_{L1}(0)]$, where the operator \mathcal{P}^- in the bracket acts only inside the bracket.

Now we change the variables to $q^- = (1 - z_1) \bar{n}_1 \cdot P_1$, $q^+ = t_1/\omega_1$ with $\omega_1 = z_1 \bar{n}_1 \cdot P_1$. Then eq. (3.16) is written as

$$\begin{aligned} \langle e^- | C_{\ell_1}^d(x, 0) | e^- \rangle &= k_d \int \frac{dz_1}{z_1} \int dt_1 \omega_1 e^{i\omega_1 n_1 \cdot x/2} \\ &\times \langle e^- | \bar{\ell}_{L1}(0) \frac{\not{n}_1}{2} T^d \delta(t_1 + \omega_1 n_1 \cdot \mathcal{P}) [\delta(\omega_1 - \bar{n}_1 \cdot \mathcal{P}) \ell_{L1}(0)] | e^- \rangle \\ &= k_d \int \frac{dz_1}{z_1} \int dt_1 \omega_1 e^{i\omega_1 n_1 \cdot x/2} B_e^d(t_1, z_1, M, \mu), \end{aligned} \quad (3.18)$$

where the electron beam function $B_e^d(t_1, z_1, M, \mu)$ is defined as

$$B_e^d(t_1, z_1, M, \mu) = \langle e^- | \bar{\ell}_{L1}(0) \frac{\not{n}_1}{2} T^d \delta(t_1 + \omega_1 n_1 \cdot \mathcal{P}) [\delta(\omega_1 - \bar{n}_1 \cdot \mathcal{P}) \ell_{L1}(0)] | e^- \rangle. \quad (3.19)$$

Note that the quantity t_1/ω_1 is the contribution to the jettiness. Similarly, the matrix element for $C_{\ell_2}^c(0, x)$ can be written as

$$\langle e^+ | C_{\ell_2}^c(0, x) | e^+ \rangle = k_c \int \frac{dz_2}{z_2} dt_2 \omega_2 e^{i\omega_2 n_2 \cdot x/2} B_e^c(t_2, z_2, M, \mu), \quad (3.20)$$

where the anti-electron (positron) beam function $B_e^c(t_2, z_2, M, \mu)$ is defined as

$$B_e^c(t_2, z_2, M, \mu) = \text{Tr} \langle e^+ | \ell_{L2}(0) \delta(t_2 + \omega_2 n_2 \cdot \mathcal{P}) [\delta(\omega_2 - \bar{n}_2 \cdot \mathcal{P}) \bar{\ell}_{L2}(0) \frac{\not{n}_2}{2} T^c] | e^+ \rangle. \quad (3.21)$$

3.1.2 The jet function and the semi-inclusive jet function

The matrix element for $C_{\ell_3}^e(0, x)$ can be written, by inserting the identity $\int d^4 p_3 \delta^{(4)}(p_3 + \mathcal{P})$, and translating $\ell_{L3}(n_3 \cdot x \bar{n}_3/2)$ to the origin, as

$$\begin{aligned} \langle 0 | C_{\ell_3}^e(0, x) | 0 \rangle &= k_e \int d^4 p_3 e^{-i\omega_3 n_3 \cdot x/2} \text{Tr} \langle 0 | \ell_{L3}(0) \delta^{(4)}(p_3 + \mathcal{P}) \bar{\ell}_{L3}(0) \frac{\not{n}_3}{2} T^e | 0 \rangle \\ &= k_e \int \frac{d^4 p_3}{(2\pi)^3} e^{-i\omega_3 n_3 \cdot x/2} \omega_3 J^e(p_3^2, M, \mu), \end{aligned} \quad (3.22)$$

where $\omega_3 = \bar{n}_3 \cdot p_3$, and the lepton jet function $J^e(p_3^2, M, \mu)$ is defined as

$$J^e(p_3^2, M, \mu) = \frac{2(2\pi)^3}{\omega_3} \text{Tr} \langle 0 | \ell_{L3}(0) \delta(n_3 \cdot p_3 + n_3 \cdot \mathcal{P}) \delta^{(2)}(p_{3\perp} + \mathcal{P}_\perp) \times [\delta(\omega_3 + \bar{n}_3 \cdot \mathcal{P}) \bar{\ell}_{L3}(0)] \frac{\not{n}_3}{2} T^e | 0 \rangle. \quad (3.23)$$

The quantity p_3^2/ω_3 contributes to the jettiness from the jet function. Here the trace refers to the sum over the Dirac indices and the weak charge indices. The definition of the jet function in eq. (3.23) may look different from the conventional one, but it turns out to be the same. Eq. (3.23) can be written as

$$\begin{aligned} J^e(p_3^2, M, \mu) &= (2\pi)^2 \int \frac{d\bar{n}_3 \cdot y}{\omega_3} e^{in_3 \cdot p_3 \bar{n}_3 \cdot y/2} \\ &\times \text{Tr} \langle 0 | \ell_{L3}(0) e^{in_3 \cdot \mathcal{P} \bar{n}_3 \cdot y/2} \delta(\omega_3 + \bar{n}_3 \cdot \mathcal{P}) \delta^{(2)}(p_{3\perp} + \mathcal{P}_\perp) \bar{\ell}_{L3}(0) \frac{\not{n}_3}{2} T^e | 0 \rangle \\ &= (2\pi)^2 \int \frac{d\bar{n}_3 \cdot y}{\omega_3} e^{in_3 \cdot p_3 \bar{n}_3 \cdot y/2} \\ &\times \text{Tr} \langle 0 | \ell_{L3} \left(\bar{n}_3 \cdot y \frac{n_3}{2} \right) \delta(\omega_3 + \bar{n}_3 \cdot \mathcal{P}) \delta^{(2)}(p_{3\perp} + \mathcal{P}_\perp) \bar{\ell}_{L3}(0) \frac{\not{n}_3}{2} T^e | 0 \rangle, \end{aligned} \quad (3.24)$$

which is the same as eq. (2.30) in ref. [33] except the factor $1/(2N_c)$. Note that the QCD jet functions single out the color singlet components by taking the color and spin averages. However, since we are dealing with the left-handed fields with a given weak charge, we do not average over spin and color.

Note that $J^e(p_3^2, M, \mu)$ is the inclusive jet function, and the nonsinglet part is zero, because the weak doublets with the opposite weak charges contribute with the opposite sign. It is the reason why there is only the color singlet contribution in QCD. Here we can extend the definition of the jet functions such that the individual nonsinglet contribution can be extracted. And it can be probed by observing a muon and an antimuon in each final jet experimentally. If we are interested in the jet in which, say, a lepton l (a muon) is observed, we can define the semi-inclusive jet function as

$$\begin{aligned} J_l^a(p_3^2, M, \mu) &= \int \frac{d\bar{n}_3 \cdot p_l}{\bar{n}_3 \cdot p_l} \int \frac{d^2 \mathbf{p}_l^\perp}{\omega_3} \sum_X \text{Tr} \langle 0 | \ell_{L3}(0) \delta(n_3 \cdot p_3 + n_3 \cdot \mathcal{P}) \delta^{(2)}(p_{3\perp} + \mathcal{P}_\perp) | l X \rangle \\ &\times \langle l X | [\delta(\omega_3 + \bar{n}_3 \cdot \mathcal{P}) \bar{\ell}_{L3}(0)] \frac{\not{n}_3}{2} T^a | 0 \rangle, \end{aligned} \quad (3.25)$$

where the lepton l is specified in the final state, noting that the phase space for l can be written as

$$\int \frac{d^3 \mathbf{p}_l}{(2\pi)^3 2E_l} = \int \frac{d^4 p_l}{(2\pi)^3} \delta(n_3 \cdot p_l \bar{n}_3 \cdot p_l - \mathbf{p}_l^{\perp 2}) = \frac{1}{2(2\pi)^3} \int \frac{d\bar{n}_3 \cdot p_l}{\bar{n}_3 \cdot p_l} \int d^2 \mathbf{p}_l^\perp. \quad (3.26)$$

Then the semi-inclusive jet function at tree level is normalized as $J_l^{a(0)}(p^2) = \delta(p^2) \text{Tr}(T^a P_l)$, where P_l is the projection operator to the given lepton l . For example, the projection operator for the muon is given by $P_\mu = (1 - t^3)/2$ in the $SU(2)$ weak interaction, and $P_{\nu_\mu} = (1 + t^3)/2$ for the muon neutrino.

The terminology ‘semi-inclusive jet function’ was used in ref. [34], but it is different from ours. Their definition corresponds to our fragmentation function with the final jet instead of a final lepton. It is called the fragmentation function to a jet (FFJ) in ref. [35]. The relation among the FJF, the semi-inclusive jet function and the fragmentation function will be discussed in section 5.3.

In terms of the semi-inclusive lepton jet function, $\langle 0|C_{\ell_3}^e(0, x)|0\rangle_l$, with the lepton l in the final state, can be written as

$$\langle 0|C_{\ell_3}^e(0, x)|0\rangle_l = k_e \int \frac{d^4 p_3}{(2\pi)^3} e^{-i\omega_3 n_3 \cdot x/2} \omega_3 J_l^e(p_3^2, M, \mu). \quad (3.27)$$

In a similar way, the collinear matrix element, $\langle 0|C_{\ell_4}^f(x, 0)|0\rangle_l$ can be written as

$$\langle 0|C_{\ell_4}^f(x, 0)|0\rangle_l = k_f \int \frac{d^4 p_4}{(2\pi)^3} e^{-i\omega_4 n_4 \cdot x/2} \omega_4 J_l^f(p_4^2, M, \mu), \quad (3.28)$$

where the semi-inclusive antilepton jet function $J_l^f(p_4^2, M, \mu)$ is given as

$$\begin{aligned} J_l^f(p_4^2, M, \mu) &= \int \frac{d\bar{n}_4 \cdot p_l}{\bar{n}_4 \cdot p_l} \int \frac{d^2 \mathbf{p}_l^\perp}{\omega_4} \sum_X \langle 0|\bar{\ell}_{L4}(0)\delta(n_4 \cdot p_4 + n_4 \cdot \mathcal{P})\delta^{(2)}(p_{4\perp} + \mathcal{P}_\perp)|lX\rangle \\ &\times \langle lX|\frac{\bar{m}_4}{2}T^f[\delta(\omega_4 + \bar{n}_4 \cdot \mathcal{P})\ell_{L4}(0)]|0\rangle. \end{aligned} \quad (3.29)$$

The fragmentation function or the FJF will be discussed later.

3.1.3 The soft function

The soft matrix elements from eq. (3.14) are written as

$$\begin{aligned} &\langle 0|\text{Tr}\left(T^c Y_2^\dagger T_J Y_1(0)T^d Y_1^\dagger T_I Y_2(x)\right)\text{Tr}\left(T^e Y_3^\dagger T_J Y_4(0)T^f Y_4^\dagger T_I Y_3(x)\right)|0\rangle \\ &= \langle 0|\left(Y_1^\dagger T_I Y_2(x)T^c\right)^{ij}\left(Y_4^\dagger T_I Y_3(x)T^e\right)^{kl}\left(Y_2^\dagger T_J Y_1(0)T^d\right)^{ji}\left(Y_3^\dagger T_J Y_4(0)T^f\right)^{lk}|0\rangle \\ &= \int d\mathcal{T}_S \int d^4 p_s e^{-ip_s \cdot x} \mathcal{S}_{IJ}^{cdef}(\mathcal{T}_S, M, \mu, p_s), \end{aligned} \quad (3.30)$$

where $\mathcal{S}_{IJ}^{cdef}(\mathcal{T}_S, M, \mu, p_s)$ is given by

$$\begin{aligned} \mathcal{S}_{IJ}^{cdef}(\mathcal{T}_S, M, \mu, p_s) &= \langle 0|\left(Y_1^\dagger T_I Y_2(0)T^c\right)^{ij}\left(Y_4^\dagger T_I Y_3(0)T^e\right)^{kl}\delta^{(4)}(p_s + \mathcal{P}) \\ &\times \delta\left(\mathcal{T}_S - \sum_{X_s} \min(\{n_i \cdot p_{X_s}\})\right)\left(Y_2^\dagger T_J Y_1(0)T^d\right)^{ji}\left(Y_3^\dagger T_J Y_4(0)T^f\right)^{lk}|0\rangle. \end{aligned} \quad (3.31)$$

Note that we have reshuffled the Wilson lines such that those with the coordinate x are moved to the left.

The exponential factor $e^{-ip_s \cdot x}$ in eq. (3.30) disappears by appropriate reparameterization transformations [36], and eq. (3.30) can be written as $\int d\mathcal{T}_S \mathcal{S}_{IJ}^{cdef}(\mathcal{T}_S, M, \mu)$, where the

soft function for the 2-jettiness is defined as

$$S_{IJ}^{cdef}(\mathcal{T}_S, M, \mu) = \langle 0 | \left(Y_1^\dagger T_I Y_2 T^c \right)^{ij} \left(Y_4^\dagger T_I Y_3 T^e \right)^{kl} \\ \times \delta \left(\mathcal{T}_S - \sum_{X_s} \min(\{n_i \cdot p_{X_s}\}) \right) \left(Y_2^\dagger T_J Y_1 T^d \right)^{ji} \left(Y_3^\dagger T_J Y_4 T^f \right)^{lk} | 0 \rangle. \quad (3.32)$$

In this form, the virtual contribution comes from the contraction of the soft Wilson lines to the left-hand side or to the right-hand side of the delta function. The real contribution can be obtained by contracting the Wilson lines across the delta function.

3.1.4 Factorized N -jettiness in SCET_I

Combining all these components, the factorized cross section for the 2-jettiness, according to eq. (3.9), can be written as

$$\begin{aligned} \frac{d\sigma}{d\mathcal{T}_2} &= \frac{8}{Q^2} \sum_{IJ} \int \frac{dz_1}{z_1} \int \frac{dz_2}{z_2} \int \frac{d^4 p_3}{(2\pi)^3} \frac{d^4 p_4}{(2\pi)^3} (2\pi)^4 \delta^{(4)} \left(\frac{\omega_1 n_1}{2} + \frac{\omega_2 n_2}{2} - \frac{\omega_3 n_3}{2} - \frac{\omega_4 n_4}{2} \right) \\ &\times \left(\omega_1 \omega_2 \omega_3 \omega_4 n_1 \cdot n_4 n_2 \cdot n_3 D_I^* D_J \right) \int d\mathcal{T}_S \delta \left(\mathcal{T}_2 - \frac{t_1}{\omega_1} - \frac{t_2}{\omega_2} - \frac{p_3^2}{\omega_3} - \frac{p_4^2}{\omega_4} - \mathcal{T}_S \right) \sum_{cdef} k_c k_d k_e k_f \\ &\times \int dt_1 B_e^d(t_1, z_1, M, \mu) \int dt_2 B_e^c(t_2, z_2, M, \mu) J_\mu^e(p_3^2, M, \mu) J_\mu^f(p_4^2, M, \mu) S_{IJ}^{cdef}(\mathcal{T}_S, M, \mu) \\ &= \frac{8}{Q^2} \int \frac{dz_1}{z_1} \int \frac{dz_2}{z_2} \int d\Phi(\{p_J\}) (2\pi)^4 \delta^{(4)} \left(\frac{\omega_1 n_1}{2} + \frac{\omega_2 n_2}{2} - \frac{\omega_3 n_3}{2} - \frac{\omega_4 n_4}{2} \right) \int d\mathcal{T}_S \\ &\times \sum_{cdef} k_c k_d k_e k_f \int dt_1 B_e^d(t_1, z_1, M, \mu) \int dt_2 B_e^c(t_2, z_2, M, \mu) J_\mu^e(p_3^2, M, \mu) J_\mu^f(p_4^2, M, \mu) \\ &\times \sum_{IJ} H_{JI} S_{IJ}^{cdef}(\mathcal{T}_S, M, \mu) \delta \left(\mathcal{T}_2 - \frac{t_1}{\omega_1} - \frac{t_2}{\omega_2} - \frac{p_3^2}{\omega_3} - \frac{p_4^2}{\omega_4} - \mathcal{T}_S \right). \end{aligned} \quad (3.33)$$

After integrating over the coordinate x , the exponential factors in eqs. (3.18), (3.20), (3.27) and (3.28) yield the delta function, responsible for the momentum conservation. Note that the last delta function in eq. (3.33) corresponds to $\delta(\mathcal{T}_2 - g(X))$ in eq. (3.9). The corresponding factorization formula for the N -jettiness in QCD in the framework of SCET is presented in refs. [25, 37], and this result is an extension including the nonsinglet contributions.

The Mandelstam variables s, t, u are given by $s = (p_1 + p_2)^2 = (p_3 + p_4)^2$, $t = (p_1 - p_3)^2 = (p_2 - p_4)^2$, $u = (p_1 - p_4)^2 = (p_2 - p_3)^2$, where p_i are the partonic momenta. In terms of ω_i , u is given by $u = \omega_1 \omega_4 n_1 \cdot n_4 / 2 = \omega_2 \omega_3 n_2 \cdot n_3 / 2$. We set the hard coefficients H_{JI} as

$$H_{JI} = 4u^2 D_I^* D_J = \omega_1 \omega_2 \omega_3 \omega_4 n_1 \cdot n_4 n_2 \cdot n_3 D_I^* D_J \equiv C_I^* C_J, \quad (3.34)$$

where the Wilson coefficients C_I are defined as $C_I = 2u D_I$. The phase space is denoted as $d\Phi(\{p_J\})$, which is given by

$$d\Phi(\{p_J\}) = \prod_J \frac{d^4 p_J}{(2\pi)^3}. \quad (3.35)$$

At tree level, the jet function is proportional to $\delta(p_J^2)$, and when combined with $d^4 p_J/(2\pi)^3$, it gives $\delta(p_J^2)d^4 p_J/(2\pi)^3 = d^3 \mathbf{p}_J/[2E_J(2\pi)^3]$, which is the phase space for the final-state particle J .

3.2 SCET_{II}: $\mathcal{T}^2 \sim M^2 \sim p_c^2 \ll Q\mathcal{T} \ll Q^2$

In SCET_{II}, the soft momentum scales as $p_s^\mu \sim (\mathcal{T}, \mathcal{T}, \mathcal{T})$, while the n -collinear momentum scales as $p_n^\mu \sim (Q, \mathcal{T}, \mathcal{T}^2/Q)$. Therefore the small component p_n^+ does not contribute to the jettiness, and the factorized form of the 2-jettiness in Eq. (3.33) should be changed. If we naively employed the PDFs f_i^a and the fragmentation functions D_i^a instead of the beam functions and the jet functions, there would be no contribution to the jettiness from these collinear functions [29]. Schematically, the 2-jettiness in SCET_{II} might be written as

$$\frac{d\sigma}{d\mathcal{T}_2} \sim f_e^d(z_1, \mu) \otimes f_e^c(z_2, \mu) D_\mu^e(z_3, \mu) D_\mu^f(z_4, \mu) \int d\mathcal{T}_S \sum_{IJ} H_{JI} S_{IJ}^{cdef}(\mathcal{T}_S, \mu) \delta(\mathcal{T}_2 - \mathcal{T}_S), \quad (3.36)$$

where the phase space and the integration with respect to other variables are omitted. The imminent problem in this formulation is that the sum of the anomalous dimensions does not cancel. Here the soft anomalous dimension depends on the jettiness \mathcal{T}_S . (This will be explicitly shown later.) But, if we use the factorization of the form in eq. (3.36), there is no dependence of the anomalous dimensions on the jettiness in collinear functions. As a result, the total sum of the anomalous dimensions does not cancel.

Therefore, care must be taken in obtaining SCET_{II} from SCET_I. In fact, the collinear modes in SCET_I, scaling as $p_c^\mu \sim (Q, \sqrt{Q\mathcal{T}}, \mathcal{T})$, are integrated out to obtain SCET_{II}. We call the collinear modes in SCET_I as the hard-collinear modes in SCET_{II}. In fig. 1, the hyperbolas for the collinear and soft modes and for the hard-collinear modes are shown. By integrating out the hard-collinear modes, we obtain the corresponding matching coefficients between SCET_I and SCET_{II}.

The relation between the beam function and the PDF can be obtained by the operator product expansion (OPE) of the relevant operators. Let us consider the operators

$$\mathcal{O}_\ell^a(t, \omega, M, \mu) = \bar{\ell}_L(0) \frac{\not{n}}{2} T^a \delta(t + \omega n \cdot \mathcal{P}) [\delta(\omega - \bar{n} \cdot \mathcal{P}) \ell_L(0)], \quad (3.37)$$

of which the matrix elements yield the beam function in eq. (3.19), and

$$\begin{aligned} \mathcal{Q}_\ell^a(\omega, M, \mu) &= \bar{\ell}_L(0) \frac{\not{n}}{2} T^a [\delta(\omega - \bar{n} \cdot \mathcal{P}) \ell_L(0)], \\ \mathcal{Q}_{\bar{\ell}}^a(\omega, M, \mu) &= \text{Tr} \left(\frac{\not{n}}{2} T^a \ell_L(0) [\delta(\omega - \bar{n} \cdot \mathcal{P}) \bar{\ell}_L(0)] \right), \\ \mathcal{Q}_W(\omega, M, \mu) &= -\omega \delta_{bc} \mathcal{B}_{n\perp\mu}^b(0) [\delta(\omega - \bar{n} \cdot \mathcal{P}) \mathcal{B}_{n\perp}^{\mu c}(0)], \end{aligned} \quad (3.38)$$

of which the matrix elements yield the PDFs⁵. [See eq. (5.20) below.]

⁵For SU(N) with $N > 2$, there should be an additional nonsinglet gauge boson operator \mathcal{O}_W^a , where δ_{ab} is replaced by the structure constant d_{abc} . It is also true in eq. (3.42) below.

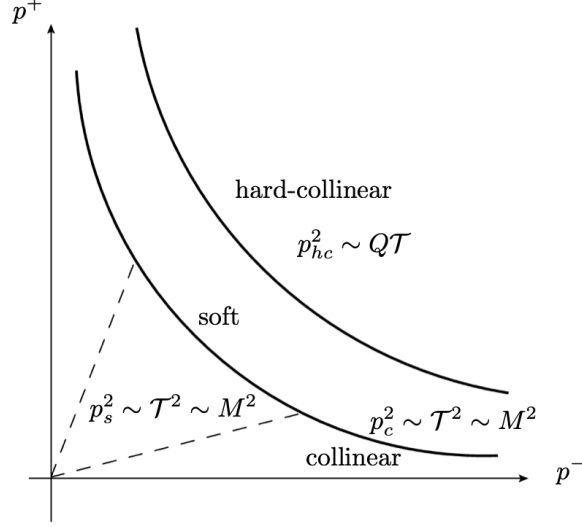


Figure 1. In SCET_{II}, the collinear and soft modes lie on the same mass shell $p_c^2 \sim p_s^2 \sim M^2 \sim \mathcal{T}^2$. The hard-collinear modes with $p_{hc}^2 \sim Q\mathcal{T}$ are integrated out to obtain SCET_{II} from SCET_I.

Using the OPE in the limit $M^2/t \rightarrow 0$, we can expand the operators \mathcal{O}_ℓ^a in terms of a sum of the operators \mathcal{Q}_ℓ^a [33]

$$\mathcal{O}_i^a(t, \omega, M, \mu) = \sum_{j,b} \int \frac{d\omega'}{\omega'} \mathcal{I}_{ij}^{ab} \left(t, \frac{\omega}{\omega'}, \mu \right) \mathcal{Q}_j^b(\omega', M, \mu) + O(M^2/t). \quad (3.39)$$

Eq. (3.39) shows the matching relation between the operators \mathcal{O}_ℓ^a in SCET_I, and the operators \mathcal{Q}_ℓ^b in SCET_{II}, where \mathcal{I}_{ij}^{ab} are the corresponding Wilson coefficients. When we take the electron matrix element of eq. (3.39), we obtain the OPE for the beam functions, with $z = \omega/\bar{n} \cdot p$,

$$B_i^a(t, z, M, \mu) = \sum_{j,b} \int_z^1 \frac{dz'}{z'} \mathcal{I}_{ij}^{ab}(t, z/z', \mu) f_j^b(z', M, \mu) + O(M^2/t). \quad (3.40)$$

We can establish the relation between the semi-inclusive jet functions in SCET_I, and the fragmentation functions in SCET_{II} in the same way. Let us consider the operators in SCET_I

$$O_\ell^a(p^2, M, \mu) = \text{Tr} \left(\ell_L(0) \delta(p^2 + \omega n \cdot \mathcal{P}) \delta^{(2)}(\mathcal{P}_\perp) [\delta(\omega + \bar{n} \cdot \mathcal{P}) \bar{\ell}_L(0)] \frac{\not{n}}{2} T^a \right), \quad (3.41)$$

which yield the semi-inclusive jet functions, and the operators in SCET_{II}

$$\begin{aligned} Q_\ell^a(M, \mu) &= \text{Tr} \left(\ell_L(0) \delta^{(2)}(\mathcal{P}_\perp) [\delta(\omega + \bar{n} \cdot \mathcal{P}) \bar{\ell}_L(0)] \frac{\not{n}}{2} T^a \right), \\ Q_{\bar{\ell}}^a(M, \mu) &= \bar{\ell}_L(0) \frac{\not{n}}{2} T^a \delta^{(2)}(\mathcal{P}_\perp) [\delta(\omega + \bar{n} \cdot \mathcal{P}) \ell_L(0)], \\ Q_W(M, \mu) &= -\omega \delta_{bc} \mathcal{B}_{n\perp\mu}^b(0) \delta^{(2)}(\mathcal{P}_\perp) [\delta(\omega + \bar{n} \cdot \mathcal{P}) \mathcal{B}_{n\perp}^{\mu c}(0)], \end{aligned} \quad (3.42)$$

where we will choose the frame such that the transverse momentum is zero in taking the matrix elements. We employ the OPE in the limit $M^2/p^2 \rightarrow 0$ to expand the operators O_ℓ^a in terms of the operators Q_ℓ^a as

$$O_i^a(p^2, M, \mu) = \sum_{j,b} \int \frac{d\omega'}{\omega'} \mathcal{J}_{ij}^{ab}(p^2, \omega/\omega', \mu) Q_j^b(\omega', M, \mu) + O(M^2/p^2). \quad (3.43)$$

This equation shows the matching relation between O_i^a in SCET_I, and Q_j^b in SCET_{II}, where \mathcal{J}_{ij}^{ab} are the corresponding matching coefficients. In order to obtain the relation between the semi-inclusive jet function in SCET_I, and the fragmentation function in SCET_{II}, we take the vacuum expectation values, but with the state i included in the intermediate states. The result is written as

$$J_i^a(p^2, \mu) = \sum_{j,b} \int_0^1 dz \int_z^1 \frac{dz'}{z'} \mathcal{J}_{ij}^{ab}(p^2, z/z', \mu) D_j^b(z', \mu) + O(M^2/p^2). \quad (3.44)$$

In addition, the soft Wilson lines are obtained by integrating out the offshell modes when the soft gauge particles are emitted from the collinear source, which are given by

$$S_i = \sum_{\text{perm.}} \exp \left[-g \frac{n_i \cdot A_s}{n_i \cdot \mathcal{P}} \right], \quad (3.45)$$

where A_s is the soft gauge field. As a result, the soft Wilson line Y_i in SCET_I is replaced by S_i , which is the rescaled version in SCET_{II}.

With these ingredients, the cross section for the 2-jettiness in SCET_{II} is written as

$$\begin{aligned} \frac{d\sigma}{d\mathcal{T}_2} &= \frac{8}{Q^2} \int \frac{dz_1 dz_2}{z_1 z_2} \int d\Phi(\{p_J\}) (2\pi)^4 \delta^{(4)} \left(\frac{\omega_1 n_1}{2} + \frac{\omega_2 n_2}{2} - \frac{\omega_3 n_3}{2} - \frac{\omega_4 n_4}{2} \right) \sum_{cdef} k_c k_d k_e k_f \\ &\times \int d\mathcal{T}_S \sum_{ij,ab} \int dt_1 \int_{z_1}^1 \frac{dz'_1}{z'_1} \mathcal{I}_{ei}^{da} \left(t_1, \frac{z_1}{z'_1}, \mu \right) f_i^a(z'_1, \mu) \int dt_2 \frac{dz'_2}{z'_2} \mathcal{I}_{\bar{e}j}^{cb} \left(t_2, \frac{z_2}{z'_2}, \mu \right) f_j^b(z'_2, \mu) \\ &\times \sum_{kl,pq} \int dz_3 \int_{z_3}^1 \frac{dz'_3}{z'_3} \mathcal{J}_{\mu k}^{ep} \left(p_3^2, \frac{z_3}{z'_3}, \mu \right) D_k^p(z'_3, \mu) \int dz_4 \int_{z_4}^1 \frac{dz'_4}{z'_4} \mathcal{J}_{\bar{\mu} l}^{fq} \left(p_4^2, \frac{z_4}{z'_4}, \mu \right) D_l^q(z'_4, \mu) \\ &\times \sum_{IJ} H_{JI} S_{IJ}^{cdef}(\mathcal{T}_S, \mu) \delta \left(\mathcal{T}_2 - \frac{t_1}{\omega_1} - \frac{t_2}{\omega_2} - \frac{p_3^2}{\omega_3} - \frac{p_4^2}{\omega_4} - \mathcal{T}_S \right). \end{aligned} \quad (3.46)$$

In addition to the contribution of the soft function to the 2-jettiness, note that there are contributions from the hard-collinear contributions. The expression in eq. (3.46) also conforms to the consistent RG behavior of the 2-jettiness. That is, the sum of the anomalous dimensions of all the factorized parts should be zero so that the 2-jettiness is independent of the factorization scale. It cancels only when we use eq. (3.46).

We will present the matching coefficients \mathcal{I}_{ij}^{ab} and \mathcal{J}_{ij}^{ab} explicitly, but a practical way to calculate the collinear parts in SCET_{II} is to compute the beam functions and the jet functions using the power counting in SCET_I, and perform the soft zero-bin subtraction. That is, we compute the combination of the matching coefficients and the PDF or the

fragmentation functions together in SCET_{II}, which are equivalent to the computation of the beam functions and the FJF in SCET_I.

The factorization for the N -jettiness is established both in SCET_I and SCET_{II}. However, there is an important caveat that Glauber exchange between spectator partons may violate factorization when the weak charges of the final states are specified [38]. The possible breakdown of the factorization may start at order α^4 of the magnitude $\sim \alpha^4 \ln^4(M^2/Q^2)$, and it is due to the fact that the group-theory factors for the exchange of two Glauber gauge bosons in different configurations across the unitarity cuts are different and the overall effects do not cancel. This should be considered seriously in ascertaining the factorization in electroweak interaction, but it is beyond the scope of this paper, and will not be considered here.

4 Treatment of rapidity divergence

In SCET, the rapidity divergence shows up because the collinear and the soft modes reside in disparate phase spaces. When these modes have the same invariant mass, they are distinguished by their rapidities. The rapidity divergence appears without regard to the UV and IR divergences, hence it has to be regulated independently. As mentioned in section 1, there are various methods to regulate the rapidity divergence [9–16]. In ref. [17], one of the authors has constructed consistent rapidity regulators both for the collinear and the soft sectors, and we use this prescription here.

The essential idea is to attach a regulator of the form $(\nu/\bar{n} \cdot k)^\eta$ for the n -collinear field, where the rapidity divergence arises. And the rapidity regulator in the soft sector should have the same form as that of the collinear rapidity regulator because we track the same source of the radiation, which causes the rapidity divergence, as in the collinear sector. However, it can be written in such a way to conform to the expression of the soft Wilson line. As an example, let us specify the rapidity regulator for the collinear current $\bar{\xi}_{n_1} W_{n_1} S_{n_1}^\dagger \Gamma S_{n_2} W_{n_2}^\dagger \xi_{n_2}$ with $n_1 \cdot n_2 \sim \mathcal{O}(1)$, which is not necessarily back-to-back. The collinear and soft Wilson lines W_{n_i} and S_{n_i} are inserted to make the current collinear and soft gauge invariant. For the collinear Wilson line W_{n_1} and the soft Wilson line S_{n_2} , the modified Wilson lines with the rapidity regulator are given as

$$\begin{aligned} W_{n_1} &= \sum_{\text{perm.}} \exp\left[-\frac{g}{\bar{n}_1 \cdot \mathcal{P}} \left(\frac{\nu}{|\bar{n}_1 \cdot \mathcal{P}|}\right)^\eta \bar{n}_1 \cdot A_{n_1}\right], \\ S_{n_2} &= \sum_{\text{perm.}} \exp\left[-\frac{g}{n_2 \cdot \mathcal{P}} \left(\frac{\nu}{|n_2 \cdot \mathcal{P}|} \frac{n_1 \cdot n_2}{2}\right)^\eta n_2 \cdot A_s\right], \end{aligned} \quad (4.1)$$

where \mathcal{P} is the operator extracting the momentum. The remaining Wilson lines W_{n_2} and S_{n_1} can be obtained by switching n_1 and n_2 . The point in selecting the rapidity regulator is to trace the same emitted gauge bosons both in the collinear and the soft sectors, which are eikonalized to produce the Wilson lines. Note that the rapidity divergences from W_{n_1} and S_{n_2} have the same origin because the collinear and soft gauge bosons are emitted from the n_2 -collinear quark for both of the Wilson lines. For the soft momentum k , in

the limit $\bar{n}_1 \cdot k \rightarrow \infty$ where the rapidity divergence occurs in the soft sector, it becomes $k^\mu \approx (\bar{n}_1 \cdot k)n_1^\mu/2$ and the soft rapidity regulator approaches

$$\left(\frac{\nu}{n_2 \cdot k} \frac{n_1 \cdot n_2}{2}\right)^\eta \xrightarrow{\bar{n}_1 \cdot k \rightarrow \infty} \left(\frac{\nu}{\bar{n}_1 \cdot k}\right)^\eta, \quad (4.2)$$

which has the same form as the collinear rapidity regulator for W_{n_1} . Another pair possessing the same source of rapidity divergence is $W_{n_2}^\dagger$ and $S_{n_1}^\dagger$. Tracking the same source of the emission of gauge bosons in the soft sector gives the correct directional dependence in the soft anomalous dimensions, in the sense that they cancel the total anomalous dimensions when combined with other factorized parts [28].

The source of the rapidity divergence can be understood as follows: For the soft modes with small rapidities, they cannot recognize the region with large rapidity, in which the collinear modes reside. But these collinear modes are obtained by traversing the boundary from the soft sector to the collinear sector. Technically, with the momentum $k^\mu = (k^-, k_\perp, k^+)$, the rapidity divergence arises when k^+ or k^- approaches infinity while \mathbf{k}_\perp^2 is fixed. Therefore we modify the region with large rapidity such that the rapidity divergence can be extracted.

On the other hand, for the n -collinear modes, k^- cannot approach infinity in the real contribution because it cannot exceed the large scale Q . Therefore, in our choice of the rapidity regulators, there is no rapidity divergence in the naive collinear contribution, though there appears the divergence associated with the region $k^- \rightarrow 0$. However, the true collinear contribution is obtained by performing the zero-bin subtraction [13, 14] in which the collinear contribution in the soft limit is removed to avoid double counting. The zero-bin subtraction can be regarded as the matching between the collinear part with large rapidity and the soft part with small rapidity when the soft part is obtained by integrating out the region with large rapidity.

The divergence in the collinear part as $k^- \rightarrow 0$ with fixed \mathbf{k}_\perp^2 is cancelled by the zero-bin subtraction in analogy to the cancellation of the IR divergence in matching. Note that the rapidity divergence from the collinear sector has the opposite sign compared to the rapidity divergence in the soft sector. It is the reason why the rapidity divergences cancel when the collinear and the soft sectors are combined. It is consistent with the fact that the full QCD does not have any rapidity divergence since there is no such kinematic constraint, separating the collinear and the soft modes. However, the structure of rapidity divergence and its evolution in each sector sheds light on the intricate nature of the theory.

In electroweak interaction, in which the weak nonsinglets can appear in each factorized part, the behavior of the rapidity divergence is strikingly different from QCD. In collinear quantities such as the jet function, and the FJF, etc., the rapidity divergence cancels for the gauge singlets in each function. Technically, this happens due to the fact that the real and virtual contributions to the rapidity divergence are equal, but with the opposite sign. For gauge nonsinglets, the group theory factors are different for real and virtual contributions, hence producing nontrivial rapidity divergence in each sector. We will present the resummed result at next-to-leading logarithmic (NLL) order for the 2-jettiness in $e^-e^+ \rightarrow \mu^- \text{ jet } \mu^+ \text{ jet } + X$, evolving both under the renormalization scale and

the rapidity scale. The cancellation of the rapidity divergence when all the contributions are added becomes more sophisticated. But the non-cancellation of the rapidity divergence in each sector for the gauge singlets induces the additional evolution with respect to the rapidity scale in the process of resummation.

5 Collinear functions

5.1 Beam function and PDF

The beam functions for QCD are defined in refs. [33, 37], and they describe the initial-state radiations from the incoming particles. We can extend them to those for the weak interaction. The singlet and nonsinglet beam functions are defined as the matrix elements with a target electron e in our case, which are given as [See eq. (3.21).]

$$B_e^a(t, z = \omega/P^-, M, \mu) = \langle e(P) | \theta(\omega) \bar{\ell}_n(0) \delta(t + \omega n \cdot \mathcal{P}) \frac{\overline{\not{n}}}{2} T^a \left[\delta(\omega - \bar{n} \cdot \mathcal{P}) \ell_n(0) \right] | e(P) \rangle, \quad (5.1)$$

where $T^0 = 1$ and $T^a = t^a$ are the weak generators. The beam functions at tree level are given as

$$B_e^{\alpha(0)}(t, z, M, \mu) = \delta(t) \delta(1 - z) \text{Tr}(T^a P_e), \quad (5.2)$$

where P_e is the projection operator in the weak charge space to project out the electron e , because the beam function is initiated by the incoming electron. Otherwise, the nonsinglet beam function vanishes because the contributions from the electron and the electron neutrino cancel. In QCD, since the initial state consists of a color singlet, say, a proton, the color average is performed in the beam function. However it is not true in this case. If we consider the imaginary situation in which the color can be measured in QCD, we should define the beam function with fixed color charges. The beam functions for antileptons can be defined accordingly as

$$B_e^a(t, z, M, \mu) = \text{Tr} \langle e^+ | \theta(\omega) \ell_L(0) \delta(t + \omega n \cdot \mathcal{P}) [\delta(\omega - \bar{n} \cdot \mathcal{P}) \bar{\ell}_L(0) \frac{\overline{\not{n}}}{2} T^a] | e^+ \rangle. \quad (5.3)$$

The Feynman diagrams for the beam function at order α are shown in figure 2. We choose the reference frame in which the transverse momentum of the incoming particle is zero. Our computational method is different from what was performed in ref. [33]. Here all the massless fermions are on the mass shell with the nonzero gauge boson mass M . In our computation, we express the beam functions and the PDFs in terms of the variables t and $z = \omega/p^-$, while we put $t' = -\omega p^+ = -z p^+ p^- = 0$. Nonzero t' plays the role of an IR regulator in ref. [33]. In our calculation, the massless fermions are on the mass shell and there is no IR divergence because of the physical nonzero gauge boson mass M .

The radiative correction of the singlet beam function at order α is different in finite terms from the result in ref. [33], but the matching coefficients between the beam functions and the PDFs turn out to be the same. However, what is new here is that we include the nonsinglet contributions which show distinct behavior, compared to the singlet contributions. In SCET_I, since $t \gg M^2$, we take the limit of small M in the final result. In

SCET_{II}, the hard-collinear contribution from the matching coefficients \mathcal{I} contains t , and we also take the small M limit.

The contribution of figure 2 (a) apart from the group theory factor is given by

$$\begin{aligned}
M_a &= 2\pi g^2 \mu_{\overline{\text{MS}}}^{2\epsilon} \int \frac{d^D \ell}{(2\pi)^D} \frac{2(2-2\epsilon)p^- \ell_{\perp}^2}{(p-\ell)^2} \delta(t-\omega\ell^+) \delta(\omega-p^-+\ell^-) \\
&\quad \times \delta(\ell^2-M^2) \theta(\ell^-) \theta(p^--\ell^-) \\
&= \frac{\alpha}{2\pi} \theta\left((1-z)t-zM^2\right) \theta(z) \theta(1-z) \frac{(1-z)t-zM^2}{(t-zM^2)^2} \\
&\rightarrow (1-z) \theta(z) \theta(1-z) \left[\left(-1 + \ln \frac{(1-z)\mu^2}{z^2 M^2}\right) \delta(t) + \frac{1}{\mu^2} \mathcal{L}_0\left(\frac{t}{\mu^2}\right) \right]. \quad (5.4)
\end{aligned}$$

The last result is obtained by taking the small M limit. The detailed calculation taking this limit is presented in appendix B. There is no zero-bin contribution for M_a at leading order.

The naive collinear contribution in figure 2 (b), with the momentum ℓ of the gauge boson, yields

$$\begin{aligned}
\tilde{M}_b &= -4\pi g^2 \mu_{\overline{\text{MS}}}^{2\epsilon} \theta(t) \int \frac{d^D \ell}{(2\pi)^D} \frac{p^-(p^--\ell^-)}{\ell^-(p-\ell)^2} \left(\frac{\nu}{\ell^-}\right)^\eta \delta(t-\omega\ell^+) \delta(\omega-p^-+\ell^-) \\
&\quad \times \delta(\ell^2-M^2) \theta(\ell^-) \theta(p^--\ell^-) \\
&= \frac{\alpha}{2\pi} \frac{(\mu^2 e^{\gamma_E})^\epsilon}{\Gamma(1-\epsilon)} \left(\frac{\nu}{p^-}\right)^\eta \theta(z) \theta(1-z) \theta(t) \left(\frac{(1-z)t}{z} - M^2\right)^{-\epsilon} \frac{z}{(1-z)^{1+\eta}} \frac{1}{t-zM^2} \\
&= \frac{\alpha}{2\pi} \frac{z}{1-z} \frac{1}{t-zM^2} \theta\left((1-z)t-zM^2\right) \theta(z) \theta(1-z) \\
&\rightarrow \frac{\alpha}{2\pi} \left[\delta(t) \delta(1-z) \frac{1}{2} \ln^2 \frac{\mu^2}{M^2} + \delta(t) z \left(\ln \frac{\mu^2}{z^2 M^2} \mathcal{L}_0(1-z) + \mathcal{L}_1(1-z) \right) \right. \\
&\quad \left. + \delta(1-z) \left(\frac{1}{\mu^2} \mathcal{L}_0\left(\frac{t}{\mu^2}\right) \ln \frac{\mu^2}{M^2} + \frac{1}{\mu^2} \mathcal{L}_1\left(\frac{t}{\mu^2}\right) \right) + \frac{z}{\mu^2} \mathcal{L}_0\left(\frac{t}{\mu^2}\right) \mathcal{L}_0(1-z) \right]. \quad (5.5)
\end{aligned}$$

We put $\epsilon = \eta = 0$ because there is neither UV nor rapidity divergence.

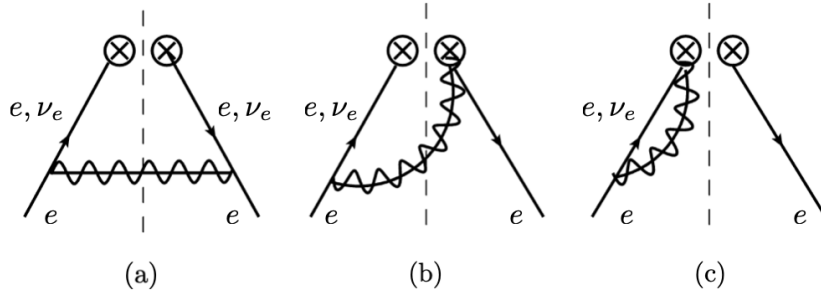


Figure 2. Feynman diagrams for the beam function and the PDF at one loop. The mirror images of (b) and (c) are omitted. The wavy lines with solid lines denote collinear gauge bosons. The dashed lines denote the final cuts. For the beam function, the virtuality t and the longitudinal momentum fraction z are measured, while only the momentum fraction z is measured for the PDF.

The zero-bin contribution from figure 2 (b), in which the rapidity regulator in eq. (4.1) is implemented, is given by

$$\begin{aligned}
M_b^\varnothing &= -4\pi g^2 \mu_{\text{MS}}^{2\epsilon} \theta(t) \int \frac{d^D \ell}{(2\pi)^D} \frac{(p^-)^2}{\ell^- (p-\ell)^2} \left(\frac{\nu}{\ell^-}\right)^\eta \delta(t - \omega \ell^+) \delta(\omega - p^-) \\
&\times \delta(\ell^2 - M^2) \theta(\ell^-) \theta(p^-) \\
&= \frac{\alpha}{2\pi} \frac{(\mu^2 e^{\gamma_E})^\epsilon}{\Gamma(1-\epsilon)} \delta(1-z) \frac{\theta(t)}{t} \int_{\omega M^2/t}^\infty \frac{d\ell^-}{\ell^-} \left(\frac{\nu}{\ell^-}\right)^\eta \left(\frac{t\ell^-}{\omega} - M^2\right)^{-\epsilon} \\
&= \frac{\alpha}{2\pi} \left(\frac{\mu^2 e^{\gamma_E}}{M^2}\right)^\epsilon \left(\frac{\nu \mu^2}{\omega M^2}\right)^\eta \frac{\Gamma(\epsilon + \eta)}{\Gamma(1 + \eta)} \left[\frac{1}{\eta} \delta(t) + \frac{1}{\mu^2} \mathcal{L}_0\left(\frac{t}{\mu^2}\right) \right] \\
&= \frac{\alpha}{2\pi} \left\{ \delta(t) \left[\left(\frac{1}{\eta} + \ln \frac{\nu}{\omega}\right) \left(\frac{1}{\epsilon} + \ln \frac{\mu^2}{M^2}\right) - \frac{1}{\epsilon^2} + \frac{1}{2} \ln^2 \frac{\mu^2}{M^2} + \frac{\pi^2}{12} \right] \right. \\
&\quad \left. + \frac{1}{\mu^2} \mathcal{L}_0\left(\frac{t}{\mu^2}\right) \left(\frac{1}{\epsilon} + \ln \frac{\mu^2}{M^2}\right) \right\} \delta(1-z), \tag{5.6}
\end{aligned}$$

where the following relation is used.

$$\frac{(\mu^2)^{-\eta}}{t^{1-\eta}} = \frac{1}{\eta} \delta(t) + \frac{1}{\mu^2} \mathcal{L}_0\left(\frac{t}{\mu^2}\right) + \mathcal{O}(\eta). \tag{5.7}$$

The distributions $\mathcal{L}_n(z)$ are listed in appendix C.1 [39].

By performing the contour integral in the complex ℓ^+ -plane, the naive collinear contribution of figure 2 (c) is given as

$$\begin{aligned}
\tilde{M}_c &= 2ig^2 \mu_{\text{MS}}^{2\epsilon} \delta(t) \delta(1-z) \int \frac{d^D l}{(2\pi)^D} \frac{p^- - \ell^-}{\ell^- (\ell^2 - M^2 + i0) ((p-\ell)^2 + i0)} \left(\frac{\nu}{\ell^-}\right)^\eta \\
&= -\frac{\alpha}{2\pi} \left(\frac{\mu^2 e^{\gamma_E}}{M^2}\right)^\epsilon \Gamma(\epsilon) \left(\frac{\nu}{\omega}\right)^\eta \delta(t) \delta(1-z) \int_0^1 dx \frac{(1-x)^{1-\epsilon}}{x^{1+\eta}}, \tag{5.8}
\end{aligned}$$

where $x = \ell^-/p^-$. And the zero-bin contribution is given as

$$\begin{aligned}
M_c^\varnothing &= 2ig^2 \mu_{\text{MS}}^{2\epsilon} \delta(t) \delta(1-z) \int \frac{d^D l}{(2\pi)^D} \frac{p^-}{\ell^- (\ell^2 - M^2 + i0) (-p^- \ell^+ + i0)} \left(\frac{\nu}{\ell^-}\right)^\eta \\
&= -\frac{\alpha}{2\pi} \left(\frac{\mu^2 e^{\gamma_E}}{M^2}\right)^\epsilon \Gamma(\epsilon) \left(\frac{\nu}{\omega}\right)^\eta \delta(t) \delta(1-z) \int_0^\infty \frac{dx}{x^{1+\eta}}. \tag{5.9}
\end{aligned}$$

The net contribution with the zero-bin subtraction is given as

$$\begin{aligned}
M_c &= \tilde{M}_c - M_c^\varnothing \\
&= -\frac{\alpha}{2\pi} \left(\frac{\mu^2 e^{\gamma_E}}{M^2}\right)^\epsilon \Gamma(\epsilon) \left(\frac{\nu}{\omega}\right)^\eta \delta(t) \delta(1-z) \left(\int_0^1 dx \frac{(1-x)^{1-\epsilon} - 1}{x^{1+\eta}} - \int_1^\infty \frac{dx}{x^{1+\eta}} \right) \\
&= \frac{\alpha}{2\pi} \delta(t) \delta(1-z) \left[\left(\frac{1}{\epsilon} + \ln \frac{\mu^2}{M^2}\right) \left(\frac{1}{\eta} + \ln \frac{\nu}{\omega} + 1\right) + 1 - \frac{\pi^2}{6} \right], \tag{5.10}
\end{aligned}$$

where the zero-bin contribution is split such that there is no divergence near $x = 0$. Note that the rapidity divergence occurs at large ℓ^- region due to the zero-bin subtraction which

cancels the divergence at small ℓ^- from the naive collinear contribution. The result is consistent with ref. [17]. The zero-bin contributions can be computed for the jet functions, FJF, etc. in the same spirit. The wavefunction renormalization $Z^{(1)}$ and the residue $R^{(1)}$ at one loop are given by

$$Z^{(1)} + R^{(1)} = \frac{\alpha}{2\pi} \left(-\frac{1}{2\epsilon} - \frac{1}{2} \ln \frac{\mu^2}{M^2} + \frac{1}{4} \right). \quad (5.11)$$

We express the singlet and nonsinglet beam functions B^0 and B^a in terms of B_s and B_n by extracting and separating the group theory factors as⁶

$$B_e^0(t, z, M, \mu) = B_s(t, z, M, \mu) \text{Tr}(T^0 P_e), \quad B_e^a(t, z, M, \mu) = B_n(t, z, M, \mu) \text{Tr}(T^a P_e). \quad (5.12)$$

The bare beam functions B_s and B_n are given at NLO as

$$\begin{aligned} B_s^{(1)}(t, z, M, \mu) &= C_F \left(M_a + 2(\tilde{M}_b - M_b^\emptyset) + 2M_c + (Z^{(1)} + R^{(1)})\delta(t)\delta(1-z) \right) \quad (5.13) \\ &= \frac{\alpha C_F}{2\pi} \left\{ \delta(t)\delta(1-z) \left(\frac{2}{\epsilon^2} + \frac{3}{2\epsilon} + \frac{9}{4} - \frac{\pi^2}{2} \right) \right. \\ &\quad + \delta(t) \left[P_{\ell\ell}(z) \ln \frac{\mu^2}{z^2 M^2} + (1+z^2)\mathcal{L}_1(1-z) - (1-z)\theta(z)\theta(1-z) \right] \\ &\quad \left. + \delta(1-z) \left[-\frac{2}{\epsilon} \frac{1}{\mu^2} \mathcal{L}_0\left(\frac{t}{\mu^2}\right) + \frac{2}{\mu^2} \mathcal{L}_1\left(\frac{t}{\mu^2}\right) \right] + (1+z^2)\mathcal{L}_0(1-z) \frac{1}{\mu^2} \mathcal{L}_0\left(\frac{t}{\mu^2}\right) \right\}, \\ B_n^{(1)}(t, z, M, \mu) &= \left[\left(C_F - \frac{C_A}{2} \right) \left(M_a + 2(\tilde{M}_b - M_b^\emptyset) \right) + C_F \left(2M_c + (Z^{(1)} + R^{(1)})\delta(t)\delta(1-z) \right) \right] \\ &= B_s(t, z, M, \mu) \\ &\quad - \frac{\alpha C_A}{4\pi} \left\{ -2\delta(t)\delta(1-z) \left[\left(\frac{1}{\eta} + \ln \frac{\nu}{\omega} \right) \left(\frac{1}{\epsilon} + \ln \frac{\mu^2}{M^2} \right) - \frac{1}{\epsilon^2} + \frac{\pi^2}{12} \right] \right. \\ &\quad + \delta(t) \left[(1+z^2)\mathcal{L}_0(1-z) \ln \frac{\mu^2}{z^2 M^2} + (1+z^2)\mathcal{L}_1(1-z) - (1-z)\theta(z)\theta(1-z) \right] \\ &\quad \left. + \delta(1-z) \left[-\frac{2}{\epsilon} \frac{1}{\mu^2} \mathcal{L}_0\left(\frac{t}{\mu^2}\right) + \frac{2}{\mu^2} \mathcal{L}_1\left(\frac{t}{\mu^2}\right) \right] + (1+z^2)\mathcal{L}_0(1-z) \frac{1}{\mu^2} \mathcal{L}_0\left(\frac{t}{\mu^2}\right) \right\}. \end{aligned}$$

Here the splitting function $P_{\ell\ell}(z)$ for $\ell \rightarrow \ell W$ is the same as the quark splitting function $P_{qq}(z)$, and is given by

$$P_{\ell\ell}(z) = P_{qq}(z) = \mathcal{L}_0(1-z)(1+z^2) + \frac{3}{2}\delta(1-z) = \left[\theta(1-z) \frac{1+z^2}{1-z} \right]_+. \quad (5.14)$$

Note that the group theory factors for the real emission (M_a , M_b) and for the virtual correction (M_c , $Z^{(1)}$ and $R^{(1)}$) are the same for the singlet, while they are different for the nonsinglet. Due to this fact, the rapidity divergence cancels in the singlet, while it does not in the nonsinglet.

⁶We will also separate the group theory factors and express the singlet and nonsinglet functions in a similar way for the PDFs [eq. (5.23)], the matching coefficients between the beam functions and the PDFs [eq. (5.28)], the jet functions [eq. (5.31)], the FJFs [eq. (5.41)], and the matching coefficients between the fragmentation functions and the FJFs [eq. (5.48)].

The μ -anomalous dimensions γ_B^μ and the ν -anomalous dimensions γ_B^ν of the beam functions are given as

$$\begin{aligned}\gamma_{B_s}^\mu &= -2C_F\Gamma_c\frac{1}{\mu^2}\mathcal{L}_0\left(\frac{t}{\mu^2}\right) - 2\gamma_\ell\delta(t), \quad \gamma_{B_s}^\nu = 0 \\ \gamma_{B_n}^\mu &= \gamma_{B_s}^\mu + C_A\Gamma_c\left[\delta(t)\ln\frac{\nu}{\omega} + \frac{1}{\mu^2}\mathcal{L}_0\left(\frac{t}{\mu^2}\right)\right], \quad \gamma_{B_n}^\nu = C_A\Gamma_c\delta(t)\ln\frac{\mu}{M},\end{aligned}\quad (5.15)$$

where $\gamma_\ell^{(1)} = -3C_F/(4\pi)$ at NLO.

The 2-jettiness in eqs. (3.33) and (3.46) is expressed in terms of the convolution of the collinear and the soft functions, but it is convenient to express it in terms of the Laplace transform because the 2-jettiness is expressed in terms of the products. For the beam function, we make a Laplace transform with respect to the jettiness $k = t/\omega$, which is written as

$$\tilde{B}_i\left(\ln\frac{\omega Q_L}{\mu^2}, z, M, \mu\right) = \int_0^\infty dk e^{-sk} B_i(\omega k, z, M, \mu), \quad s = \frac{1}{e^{\gamma_E} Q_L}. \quad (5.16)$$

When we make a Laplace transform of the various collinear functions, each part should contain the same scale, and we choose $s = 1/(Q_L e^{\gamma_E})$. Here Q_L is an arbitrary scale involved in the Laplace transform. Various distributions appearing in eq. (5.15) are expressed as regular functions in the Laplace transforms. (See appendix A.) As we will show later, the evolution of the jettiness is independent of the factorization scale μ_F , as well as Q_L .

The anomalous dimensions of the Laplace-transformed beam functions are given as

$$\begin{aligned}\tilde{\gamma}_{B_s}^\mu &= 2C_F\Gamma_c\ln\frac{\mu^2}{\omega Q_L} - 2\gamma_\ell, \quad \tilde{\gamma}_{B_s}^\nu = 0, \\ \tilde{\gamma}_{B_n}^\mu &= \tilde{\gamma}_{B_s}^\mu - C_A\Gamma_c\ln\frac{\mu^2}{\nu Q_L}, \quad \tilde{\gamma}_{B_n}^\nu = C_A\Gamma_c\ln\frac{\mu}{M}.\end{aligned}\quad (5.17)$$

To be precise, these anomalous dimensions are those of the beam functions in SCET_I, but in SCET_{II}, they are regarded as the anomalous dimensions of the combination of the matching coefficients and the PDFs. Here $\Gamma_c(\alpha)$ is the cusp anomalous dimension [40, 41], which can be expanded as

$$\Gamma_c(\alpha) = \frac{\alpha}{4\pi}\Gamma_c^0 + \left(\frac{\alpha}{4\pi}\right)^2\Gamma_c^1 + \dots, \quad (5.18)$$

with

$$\Gamma_c^0 = 4, \quad \Gamma_c^1 = \left(\frac{268}{9} - \frac{4}{3}\pi^2\right)C_A - \frac{40n_f}{9}. \quad (5.19)$$

To NLL accuracy, the cusp anomalous dimension to two loops is needed.

The PDFs are defined in terms of the matrix elements with a target e as

$$f_e^a(z = \omega/P^-, M, \mu) = \langle e(P) | \theta(\omega) \bar{\ell}_n(0) \frac{\not{n}}{2} T^a \left[\delta(\omega - \bar{n} \cdot \mathcal{P}) \ell_n(0) \right] | e(P) \rangle, \quad (5.20)$$

and it is normalized at tree level as

$$f_e^{a(0)}(z) = \delta(1-z)\text{Tr}(T^a P_e). \quad (5.21)$$

The Feynman diagrams for the PDFs at one loop are shown in figure 2. Note that the Feynman diagrams are the same as those for the beam functions, but the measured quantities are different. Including the zero-bin subtractions, the matrix elements apart from the group theory factors are given as

$$\begin{aligned}
M_a &= \frac{\alpha}{2\pi}(1-z)\left(\frac{1}{\epsilon} - 2 + \ln \frac{\mu^2}{zM^2}\right), \\
M_b &= \frac{\alpha}{2\pi}\left(\frac{1}{\epsilon} + \ln \frac{\mu^2}{zM^2}\right)\left[-\delta(1-z)\left(\frac{1}{\eta} + \ln \frac{\nu}{\omega}\right) + z\mathcal{L}_0(z)\right], \\
M_c &= \frac{\alpha}{2\pi}\delta(1-z)\left[\left(\frac{1}{\epsilon} + \ln \frac{\mu^2}{M^2}\right)\left(\frac{1}{\eta} + \ln \frac{\nu}{\omega} + 1\right) + 1 - \frac{\pi^2}{6}\right].
\end{aligned} \tag{5.22}$$

The singlet and nonsinglet PDFs are expressed in terms of $f_{\ell s}$ and $f_{\ell n}$ as

$$f_{\ell}^0(z, M, \mu) = f_{\ell s}(z, M, \mu)\text{Tr}(T^0 P_{\ell}), \quad f_{\ell}^a(z, M, \mu) = f_{\ell n}(z, M, \mu)\text{Tr}(T^a P_{\ell}), \tag{5.23}$$

where $f_{\ell s}$ and $f_{\ell n}$ at NLO are given as

$$\begin{aligned}
f_{\ell s}^{(1)}(z, M, \mu) &= C_F\left(M_a + 2M_b + 2M_c + (Z^{(1)} + R^{(1)})\delta(1-z)\right) \\
&= \frac{\alpha C_F}{2\pi}\left[\left(\frac{1}{\epsilon} + \ln \frac{\mu^2}{zM^2}\right)P_{\ell\ell}(z) + \left(\frac{9}{4} - \frac{\pi^2}{3}\right)\delta(1-z) - 2(1-z)\theta(1-z)\right], \\
f_{\ell n}^{(1)}(z, M, \mu) &= \left(C_F - \frac{C_A}{2}\right)(M_a + 2M_b) + C_F\left(2M_c + (Z^{(1)} + R^{(1)})\delta(1-z)\right) \\
&= f_{\ell s}(z, M, \mu) + \frac{\alpha C_A}{2\pi}\left[\delta(1-z)\left(\frac{1}{\epsilon} + \ln \frac{\mu^2}{M^2}\right)\left(\frac{1}{\eta} + \ln \frac{\nu}{\omega}\right) + (1-z)\theta(1-z)\right. \\
&\quad \left. - \frac{1}{2}\left(\frac{1}{\epsilon} + \ln \frac{\mu^2}{zM^2}\right)(1+z^2)\mathcal{L}_0(1-z)\right].
\end{aligned} \tag{5.24}$$

Here the rapidity divergence shows up in the nonsinglet PDF for the same reason as in the beam functions. It coincides with the result in ref. [24]. The μ - and ν -anomalous dimensions of the PDFs are given as

$$\begin{aligned}
\gamma_{f_s}^{\mu} &= C_F\Gamma_c P_{\ell\ell}(z), \quad \gamma_{f_s}^{\nu} = 0 \\
\gamma_{f_n}^{\mu} &= \gamma_{f_s}^{\mu} + C_A\Gamma_c\left(\delta(1-z)\ln \frac{\nu}{\omega} - \frac{1}{2}(1+z^2)\mathcal{L}_0(1-z)\right), \quad \gamma_{f_n}^{\nu} = C_A\Gamma_c \ln \frac{\mu}{M}.
\end{aligned} \tag{5.25}$$

It is noteworthy to compare the distinction between QCD and the weak interaction. The results for the singlets correspond to QCD and there is only a single logarithm in the singlet PDF, and it satisfies the usual DGLAP equation

$$\frac{df_{\ell s}(z, M, \mu)}{d \ln \mu} = \frac{\alpha}{\pi} \int \frac{dz'}{z'} \sum_{i=\ell, W} P_{\ell i}\left(\frac{z}{z'}\right) f_{is}(z', M, \mu), \tag{5.26}$$

where $P_{\ell W}(z)$ is the analog of the splitting function $P_{qg}(z)$ in QCD. On the other hand, the nonsinglet PDF shows the double logarithms due to the mismatch of the real and virtual contributions, along with the rapidity divergence. Due to the double logarithms, the nonsinglet PDF satisfies more complicated RG equations. It happens to all the collinear functions and the soft function, which necessitates the introduction of SCET_{II}.

The beam functions are related to the PDFs as

$$B_i^a(t, z, M, \mu) = \sum_{j,b} \int_z^1 \frac{d\xi}{\xi} \mathcal{I}_{ij}^{ab} \left(t, \frac{z}{\xi}, \mu \right) f_j^b(\xi, M, \mu), \quad (5.27)$$

where \mathcal{I}_{ij}^{ab} are the matching coefficients, which describe the collinear initial-state radiation and can be computed perturbatively. Here i, j are the indices for particle species, and a, b are the weak indices. The only nonzero matching coefficients are those which are diagonal in weak-charge space, from which the singlet and nonsinglet matching coefficients $\mathcal{I}_{\ell\ell}^s$ and $\mathcal{I}_{\ell\ell}^n$ are defined as

$$\mathcal{I}_{\ell\ell}^s(t, z, \mu) = \mathcal{I}_{\ell\ell}^{00}(t, z, \mu), \quad \mathcal{I}_{\ell\ell}^n(t, z, \mu) = \mathcal{I}_{\ell\ell}^{aa}(t, z, \mu), \quad \mathcal{I}_{\ell\ell}^{a0}(t, z, \mu) = 0. \quad (5.28)$$

The matching coefficients $\mathcal{I}_{\ell\ell}^s$ for the singlet and $\mathcal{I}_{\ell\ell}^n$ for the nonsinglet at NLO are given as

$$\begin{aligned} \mathcal{I}_{\ell\ell}^{s(1)}(t, z, \mu) &= B_{\ell s}^{(1)}(t, z, M, \mu) - f_{\ell s}^{(1)}(z, M, \mu)\delta(t) \\ &= \frac{\alpha C_F}{2\pi} \left\{ -\frac{\pi^2}{6} \delta(t)\delta(1-z) + \delta(t) \left[(1+z^2)\mathcal{L}_1(1-z) + \theta(1-z) \left(1-z - \frac{1+z^2}{1-z} \ln z \right) \right] \right. \\ &\quad \left. + \left(P_{\ell\ell}(z) - \frac{3}{2}\delta(1-z) \right) \frac{1}{\mu^2} \mathcal{L}_0\left(\frac{t}{\mu^2}\right) + \frac{2}{\mu^2} \mathcal{L}_1\left(\frac{t}{\mu^2}\right) \delta(1-z) \right\}, \\ \mathcal{I}_{\ell\ell}^{n(1)}(t, z, \mu) &= B_{\ell n}^{(1)}(t, z, M, \mu) - f_{\ell n}^{(1)}(z, M, \mu)\delta(t) = \frac{C_F - C_A/2}{C_F} \mathcal{I}_{\ell\ell s}^{(1)}. \end{aligned} \quad (5.29)$$

The finite terms in the beam functions and PDFs are different compared to the result in ref. [33] due to the presence of the gauge boson mass M , but the matching coefficient $\mathcal{I}_{\ell\ell}^{s(1)}$ is the same. Note that there is no dependence on M in the matching coefficients, because they should be independent of the low-energy physics. The matching coefficient $\mathcal{I}_{\ell\ell}^{n(1)}$ for the nonsinglet is new, but interestingly enough, it is proportional to $\mathcal{I}_{\ell\ell}^{s(1)}$ for the singlet.

5.2 Semi-inclusive jet functions

The semi-inclusive jet functions are defined in eq. (3.25). The Feynman diagrams at order α are shown in Fig. 3. As in computing the beam functions, the final result is obtained by taking the limit of small M . All the contributions including the zero-bin contributions without the group theory factors at NLO are given as (See appendix C.1.)

$$\begin{aligned} M_a &= \frac{\alpha}{2\pi} \frac{\theta(p^2 - M^2)}{p^2} \left[\frac{1}{2} - \frac{M^2}{p^2} + \frac{1}{2} \left(\frac{M^2}{p^2} \right)^2 \right] \longrightarrow \frac{\alpha}{2\pi} \left[\delta(p^2) \left(-\frac{3}{4} + \frac{1}{2} \ln \frac{\mu^2}{M^2} \right) + \frac{1}{2\mu^2} \mathcal{L}_0\left(\frac{p^2}{\mu^2}\right) \right], \\ \tilde{M}_b &= \frac{\alpha}{2\pi} \theta(p^2 - M^2) \frac{1}{p^2} \left[-1 + \frac{M^2}{p^2} - \ln \frac{M^2}{p^2} \right] \\ &\longrightarrow \frac{\alpha}{2\pi} \left[\delta(p^2) \left(1 - \ln \frac{\mu^2}{M^2} + \frac{1}{2} \ln^2 \frac{\mu^2}{M^2} \right) - \frac{1}{\mu^2} \mathcal{L}_0\left(\frac{p^2}{\mu^2}\right) \left(1 - \ln \frac{\mu^2}{M^2} \right) + \frac{1}{\mu^2} \mathcal{L}_1\left(\frac{p^2}{\mu^2}\right) \right], \\ M_b^\emptyset &= \frac{\alpha}{2\pi} \left\{ \delta(p^2) \left[\left(\frac{1}{\eta} + \ln \frac{\nu}{\omega} \right) \left(\frac{1}{\epsilon} + \ln \frac{\mu^2}{M^2} \right) - \frac{1}{\epsilon^2} + \frac{1}{2} \ln^2 \frac{\mu^2}{M^2} + \frac{\pi^2}{12} \right] \right. \\ &\quad \left. + \left(\frac{1}{\epsilon} + \ln \frac{\mu^2}{M^2} \right) \frac{1}{\mu^2} \mathcal{L}_0\left(\frac{p^2}{\mu^2}\right) \right\}, \\ M_c &= \frac{\alpha}{2\pi} \delta(p^2) \left[\left(\frac{1}{\eta} + \ln \frac{\nu}{\omega} \right) \left(\frac{1}{\epsilon} + \ln \frac{\mu^2}{M^2} \right) + \frac{1}{\epsilon} + \ln \frac{\mu^2}{M^2} + 1 - \frac{\pi^2}{6} \right], \end{aligned} \quad (5.30)$$

and the wavefunction renormalization and the residue are given by eq. (5.11). We put $p^2 = \omega p^+$, where $\omega = \bar{n} \cdot p$, and p^+ is the jettiness from the jet.

The bare singlet and nonsinglet semi-inclusive jet functions J_l^0 and J_l^a , which include the lepton l in the final state, are given as

$$J_l^0(p^2, M, \mu) = J_s(p^2, M, \mu) \text{Tr}(P_l T^0), \quad J_l^a(p^2, M, \mu) = J_n(p^2, M, \mu) \text{Tr}(P_l T^a), \quad (5.31)$$

where P_l is the projection operator to the lepton l ($l = \mu, \nu_\mu$). With the appropriate group theory factors, the bare singlet and the nonsinglet jet functions at NLO are given as

$$\begin{aligned} J_s^{(1)}(p^2, M, \mu) &= C_F \left(M_a + 2(\tilde{M}_b - M_b^\emptyset) + 2M_c + (Z^{(1)} + R^{(1)})\delta(p^2) \right) \\ &= \frac{\alpha C_F}{2\pi} \left[\delta(p^2) \left(\frac{2}{\epsilon^2} + \frac{3}{2\epsilon} + \frac{7}{2} - \frac{\pi^2}{2} \right) - \left(\frac{2}{\epsilon} + \frac{3}{2} \right) \frac{1}{\mu^2} \mathcal{L}_0 \left(\frac{p^2}{\mu^2} \right) + \frac{2}{\mu^2} \mathcal{L}_1 \left(\frac{p^2}{\mu^2} \right) \right], \\ J_n^{(1)}(p^2, M, \mu) &= \left(C_F - \frac{C_A}{2} \right) \left(M_a + 2(\tilde{M}_b - M_b^\emptyset) \right) + C_F \left(2M_c + (Z^{(1)} + R^{(1)})\delta(p^2) \right) \\ &= J_s(p^2, M, \mu) + \frac{\alpha C_A}{2\pi} \left\{ \delta(p^2) \left[\frac{1}{\eta} \left(\frac{1}{\epsilon} + \ln \frac{\mu^2}{M^2} \right) - \frac{1}{\epsilon^2} + \frac{1}{\epsilon} \ln \frac{\nu}{\omega} + \ln \frac{\mu^2}{M^2} \ln \frac{\nu}{\omega} \right. \right. \\ &\quad \left. \left. + \frac{3}{4} \ln \frac{\mu^2}{M^2} - \frac{5}{8} + \frac{\pi^2}{12} \right] + \left(\frac{1}{\epsilon} + \frac{3}{4} \right) \frac{1}{\mu^2} \mathcal{L}_0 \left(\frac{p^2}{\mu^2} \right) - \frac{1}{\mu^2} \mathcal{L}_1 \left(\frac{p^2}{\mu^2} \right) \right\}. \end{aligned} \quad (5.32)$$

Here again the nonsinglet jet function develops the rapidity divergence.

The anomalous dimensions are given as

$$\begin{aligned} \gamma_{J_s}^\mu &= -2C_F \Gamma_c \frac{1}{\mu^2} \mathcal{L}_0 \left(\frac{p^2}{\mu^2} \right) - 2\gamma_\ell \delta(p^2), \quad \gamma_{J_s}^\nu = 0, \\ \gamma_{J_n}^\mu &= \gamma_{J_s}^\mu + C_A \Gamma_c \left[\delta(p^2) \ln \frac{\nu}{\omega} + \frac{1}{\mu^2} \mathcal{L}_0 \left(\frac{p^2}{\mu^2} \right) \right], \quad \gamma_{J_n}^\nu = C_A \Gamma_c \delta(p^2) \ln \frac{\mu}{M}. \end{aligned} \quad (5.33)$$

The Laplace transforms of the anomalous dimensions with $s = 1/(Q_L e^{\gamma_E})$ conjugate to the jettiness p^+ are given by

$$\begin{aligned} \tilde{\gamma}_{J_s}^\mu &= 2C_F \Gamma_c \ln \frac{\mu^2}{\omega Q_L} - 2\gamma_\ell, \quad \tilde{\gamma}_{J_s}^\nu = 0, \\ \tilde{\gamma}_{J_n}^\mu &= \tilde{\gamma}_{J_s}^\mu - C_A \Gamma_c \ln \frac{\mu^2}{\nu Q_L}, \quad \tilde{\gamma}_{J_n}^\nu = C_A \Gamma_c \ln \frac{\mu}{M}, \end{aligned} \quad (5.34)$$

which are the same as the anomalous dimensions of the beam functions in eq. (5.17).

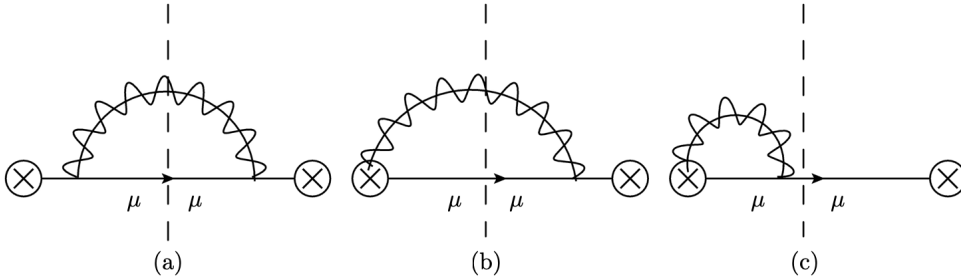


Figure 3. Feynman diagrams for the semi-inclusive jet function at one loop. The dotted lines denote the cut. Mirror images for (b) and (c) are omitted. For the muon semi-inclusive jet functions, the fermions cut by the dotted lines are muons.

5.3 Fragmentation functions and fragmenting jet functions

The collinear parts pertaining to the final states are described either by the fragmentation functions or by the FJFs. The fragmentation function is used when a single particle is observed with no properties of the jet to be probed. The FJF describes the fragmentation of a parton i to another parton j within a jet originating from i with the measurement of the momentum fraction and the invariant mass of the jet.

The fragmentation function from ℓ to the lepton l is extended from the definition in QCD [42, 43] to

$$D_l^a(z, M, \mu) = \int \frac{d^2 p_l^\perp}{z} \sum_X \text{Tr} \langle 0 | T^a \frac{\not{\bar{h}}}{2} [\delta(\omega + \bar{n} \cdot \mathcal{P}) \delta^{(2)}(\mathcal{P}_\perp) \ell_L(0)] | lX \rangle \langle lX | \bar{\ell}_L(0) | 0 \rangle, \quad (5.35)$$

where $z = p_l^- / p_\ell^- = p_l^- / \omega$ is the fraction of the largest lightcone components of the observed lepton l originating from ℓ . At tree level, the fragmentation functions are normalized as

$$D_l^{a(0)}(z, M, \mu) = \delta(1 - z) \text{Tr}(P_l T^a). \quad (5.36)$$

The matrix elements for the fragmentation functions are the same as those for the PDFs in eq. (5.22), and we will not present them here.

The FJF is defined as

$$\begin{aligned} \mathcal{G}_l^a(p^2, z, M, \mu) &= \frac{2(2\pi)^3}{\omega z} \int d^2 \mathbf{p}_{l\perp} \sum_X \quad (5.37) \\ &\times \text{Tr} \langle 0 | T^a \frac{\not{\bar{h}}}{2} \ell_L(0) | lX \rangle \langle lX | \delta(\omega + \bar{n} \cdot \mathcal{P}) \delta^{(2)}(\mathcal{P}_\perp) \delta(p^+ + n \cdot \mathcal{P}) \bar{\ell}_L(0) | 0 \rangle, \end{aligned}$$

where $p^2 = \omega p^+$ is the invariant mass of the collinear jet. The small component p^+ is the jettiness from the fragmented lepton. The FJF is normalized at tree level as

$$\mathcal{G}_l^{a(0)}(p^2, z, M, \mu) = 2(2\pi)^3 \delta(p^2) \delta(1 - z) \text{Tr}(P_l T^a). \quad (5.38)$$

The relations between the FJF, the semi-inclusive jet functions, and the fragmentation functions can be found by comparing eqs. (3.25), (5.35) and (5.37). The FJF probes the

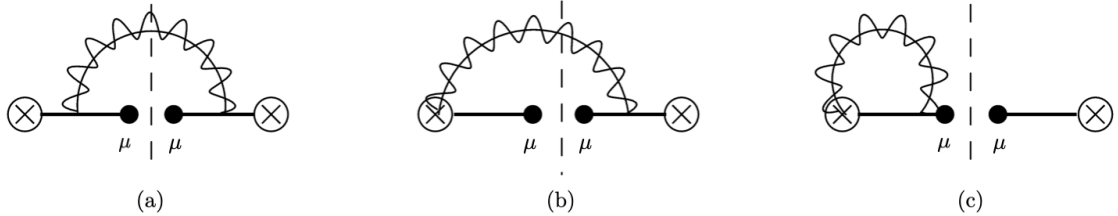


Figure 4. Feynman diagrams for the fragmentation functions and the FJFs at one loop. The dotted lines denote the cut. The mirror images of (b) and (c) are omitted. The dots represent the observed particles in the final state. Note that ω is measured for the fragmentation function, while ω and p^+ are measured for the FJF.

differential distributions with respect to the invariant mass p^2 and the momentum fraction z . If we integrate the FJF over all the possible invariant masses, it yields the fragmentation functions which shows the distributions of the momentum fraction of the observed lepton. On the other hand, if we integrate the FJF over the momentum fraction z , it yields the semi-inclusive jet function for the lepton l in the final state. Therefore the relations can be expressed as

$$D_l^a(z, M, \mu) = \int_0^\infty dp^2 \frac{\mathcal{G}_l^a(p^2, z, M, \mu)}{2(2\pi)^3}, \quad J_l^a(p^2, M, \mu) = \int_0^1 dz \frac{\mathcal{G}_l^a(p^2, z, M, \mu)}{2(2\pi)^3}, \quad (5.39)$$

and it is confirmed at order α . Our definition of the semi-inclusive (singlet) jet function is different from that in ref. [34]. As explained by the authors in ref. [34], their semi-inclusive jet function is similar to the fragmentation function. To be exact, it is the fragmentation function, in which the final-state hadron forms a jet. Our semi-inclusive jet function describes the jet mass distribution with the lepton l (or the leptonic jet which includes l) in the final state.

In ref. [43], integrating the FJF with an additional factor z yields the inclusive jet function $J_i(p^2, \mu)$. The additional factor of z is due to the symmetrization of the final states when all the hadrons in the final state are summed over. However, we refer to the semi-inclusive jet function for the lepton l specified in the final state in eq. (5.39). If we sum over all the final leptons to yield the inclusive jet functions, the additional factor of z should be included.

The Feynman diagrams for the fragmentation functions and the FJFs are shown in figure 4. Though we present the same Feynman diagrams for both functions, note that the observed quantities are different. The matrix elements for the FJF without the group theory factors are given at NLO as

$$\begin{aligned} M_a &= \frac{\alpha}{2\pi} \theta(z) \theta(1-z) \theta\left(p^2 - \frac{M^2}{1-z}\right) \frac{1}{p^2} \left(1 - z - \frac{M^2}{p^2}\right) \\ &\rightarrow \frac{\alpha}{2\pi} \theta(z) \theta(1-z) (1-z) \left[\delta(p^2) \left(\ln \frac{(1-z)\mu^2}{M^2} - 1 \right) + \frac{1}{\mu^2} \mathcal{L}_0\left(\frac{p^2}{\mu^2}\right) \right], \\ \tilde{M}_b &= \frac{\alpha}{2\pi} \theta(z) \theta(1-z) \theta\left(p^2 - \frac{M^2}{1-z}\right) \frac{1}{p^2} \frac{z}{1-z}, \\ &\rightarrow \frac{\alpha}{2\pi} \left[\delta(p^2) \delta(1-z) \frac{1}{2} \ln^2 \frac{\mu^2}{M^2} + \delta(p^2) \left(z \ln \frac{\mu^2}{M^2} \mathcal{L}_0(1-z) + z \mathcal{L}_1(1-z) \right) \right. \\ &\quad \left. + \delta(1-z) \left(\frac{1}{\mu^2} \mathcal{L}_0\left(\frac{p^2}{\mu^2}\right) \ln \frac{\mu^2}{M^2} + \frac{1}{\mu^2} \mathcal{L}_1\left(\frac{p^2}{\mu^2}\right) \right) + \frac{z}{\mu^2} \mathcal{L}_0\left(\frac{p^2}{\mu^2}\right) \mathcal{L}_0(1-z) \right], \\ M_b^\emptyset &= \frac{\alpha}{2\pi} \delta(1-z) \left\{ \left(\frac{1}{\epsilon} + \ln \frac{\mu^2}{M^2} \right) \left[\delta(p^2) \left(\frac{1}{\eta} + \ln \frac{\nu}{\omega} \right) + \frac{1}{\mu^2} \mathcal{L}_0\left(\frac{p^2}{\mu^2}\right) \right] \right. \\ &\quad \left. + \delta(p^2) \left(-\frac{1}{\epsilon^2} + \frac{1}{2} \ln^2 \frac{\mu^2}{M^2} + \frac{\pi^2}{12} \right) \right\} \\ M_c &= \frac{\alpha}{2\pi} \delta(p^2) \delta(1-z) \left[\left(\frac{1}{\epsilon} + \ln \frac{\mu^2}{M^2} \right) \left(\frac{1}{\eta} + \ln \frac{\nu}{\omega} + 1 \right) + 1 - \frac{\pi^2}{6} \right]. \end{aligned} \quad (5.40)$$

Here we also express the matrix elements in the limit of small mass M . The detailed derivation of taking the limit is presented in appendix C.2.

The singlet and nonsinglet FJFs are written as

$$\begin{aligned}\mathcal{G}_l^0(p^2, z, M, \mu) &= \mathcal{G}_{ls}(p^2, z, M, \mu)\text{Tr}(P_l T^0), \\ \mathcal{G}_l^a(p^2, z, M, \mu) &= \mathcal{G}_{ln}(p^2, z, M, \mu)\text{Tr}(P_l T^a).\end{aligned}\quad (5.41)$$

The bare FJFs for the singlet and the nonsinglet at NLO are given as

$$\begin{aligned}\frac{\mathcal{G}_l^{(1)}(p^2, z, M, \mu)}{2(2\pi)^3} &= C_F \left(M_a + 2(\tilde{M}_b - M_b^\emptyset + M_c) + (Z^{(1)} + R^{(1)})\delta(p^2)\delta(1-z) \right) \\ &= \frac{\alpha C_F}{2\pi} \left\{ \delta(p^2)\delta(1-z) \left(\frac{2}{\epsilon^2} + \frac{3}{2\epsilon} + \frac{9}{4} - \frac{\pi^2}{2} \right) \right. \\ &\quad + \delta(p^2) \left[P_{\ell\ell}(z) \ln \frac{\mu^2}{M^2} + (1+z^2)\mathcal{L}_1(1-z) - (1-z)\theta(z)\theta(1-z) \right] \\ &\quad \left. + \delta(1-z) \left[-\frac{2}{\epsilon} \frac{1}{\mu^2} \mathcal{L}_0\left(\frac{p^2}{\mu^2}\right) + \frac{2}{\mu^2} \mathcal{L}_1\left(\frac{p^2}{\mu^2}\right) \right] + (1+z^2)\mathcal{L}_0(1-z) \frac{1}{\mu^2} \mathcal{L}_0\left(\frac{p^2}{\mu^2}\right) \right\},\end{aligned}\quad (5.42)$$

$$\begin{aligned}\frac{\mathcal{G}_{ln}^{(1)}(p^2, z, M, \mu)}{2(2\pi)^3} &= (C_F - C_A/2) \left(M_a + 2(\tilde{M}_b - M_b^\emptyset) \right) \\ &\quad + C_F \left(2M_c + (Z^{(1)} + R^{(1)})\delta(p^2)\delta(1-z) \right) \\ &= \frac{\mathcal{G}_{ls}^{(1)}(p^2, z, M, \mu)}{2(2\pi)^3} \\ &\quad - \frac{\alpha C_A}{4\pi} \left\{ \delta(p^2)\delta(1-z) \left[\frac{2}{\epsilon^2} - 2 \left(\frac{1}{\epsilon} + \ln \frac{\mu^2}{M^2} \right) \left(\frac{1}{\eta} + \ln \frac{\nu}{\omega} \right) - \frac{\pi^2}{6} \right] \right. \\ &\quad + \delta(p^2) \left[(1+z^2)\mathcal{L}_0(1-z) \ln \frac{\mu^2}{M^2} + (1+z^2)\mathcal{L}_1(1-z) - (1-z)\theta(z)\theta(1-z) \right] \\ &\quad \left. + \delta(1-z) \left[-\frac{2}{\epsilon} \frac{1}{\mu^2} \mathcal{L}_0\left(\frac{p^2}{\mu^2}\right) + \frac{2}{\mu^2} \mathcal{L}_1\left(\frac{p^2}{\mu^2}\right) \right] + (1+z^2)\mathcal{L}_0(1-z) \frac{1}{\mu^2} \mathcal{L}_0\left(\frac{p^2}{\mu^2}\right) \right\}.\end{aligned}\quad (5.43)$$

The singlet FJF in eq. (5.42) is the same as the result in ref. [43] though the individual contributions are different. However, the result for the nonsinglet FJFs is new, and note that the dependence on the rapidity scale remains in the nonsinglet FJFs, while there is none for the singlet FJFs.

The anomalous dimensions are given as

$$\begin{aligned}\gamma_{Fs}^\mu &= -2C_F\Gamma_c \frac{1}{\mu^2} \mathcal{L}_0\left(\frac{p^2}{\mu^2}\right) - 2\gamma_\ell\delta(p^2), \quad \gamma_{Fs}^\nu = 0, \\ \gamma_{Fn}^\mu &= \gamma_{Fs}^\mu + C_A\Gamma_c \left[\delta(p^2) \ln \frac{\nu}{\omega} + \frac{1}{\mu^2} \mathcal{L}_0\left(\frac{p^2}{\mu^2}\right) \right], \quad \gamma_{Fn}^\nu = C_A\Gamma_c \delta(p^2) \ln \frac{\mu}{M},\end{aligned}\quad (5.44)$$

and their Laplace transforms are given by

$$\begin{aligned}\tilde{\gamma}_{Fs}^\mu &= 2C_F\Gamma_c \ln \frac{\mu^2}{\omega Q_L} - 2\gamma_\ell, \quad \tilde{\gamma}_{Fs}^\nu = 0, \\ \tilde{\gamma}_{Fn}^\mu &= \tilde{\gamma}_{Fs}^\mu - C_A\Gamma_c \ln \frac{\mu^2}{\nu Q_L}, \quad \tilde{\gamma}_{Fn}^\nu = C_A\Gamma_c \ln \frac{\mu}{M}.\end{aligned}\quad (5.45)$$

Because there is a relation between the semi-inclusive jet function and the FJF in eq. (5.39), the anomalous dimensions of the jet functions and the FJFs are the same. [See eqs. (5.33) and (5.34).]

The matching between the fragmentation function and the FJF are written as

$$\mathcal{G}_i^a(p^2, z, M, \mu) = \sum_j \int_z^1 \frac{dz'}{z'} \mathcal{J}_{ij}^{ab}(p^2, \frac{z}{z'}, \mu) D_j^b(z', M, \mu) \quad (5.46)$$

at leading power, where \mathcal{J}_{ij}^{ab} are the matching coefficients. At tree-level, it is given by

$$\mathcal{J}_{ij}^{ab(0)}(p^2, z, \mu) = 2(2\pi)^3 \delta_{ij} \delta^{ab} \delta(p^2) \delta(1-z). \quad (5.47)$$

If we write

$$\mathcal{J}_{\ell\ell}^{00}(p^2, z, \mu) = \mathcal{J}_{\ell\ell}^s(p^2, z, \mu), \quad \mathcal{J}_{\ell\ell}^{ab}(p^2, z, \mu) = \delta^{ab} \mathcal{J}_{\ell\ell}^n(p^2, z, \mu), \quad \mathcal{J}_{\ell\ell}^{a0}(p^2, z, \mu) = 0, \quad (5.48)$$

the singlet matching coefficient $\mathcal{J}_{\ell\ell}^s$ and the nonsinglet matching coefficient $\mathcal{J}_{\ell\ell}^n$ at order α are given as

$$\begin{aligned} \frac{\mathcal{J}_{\ell\ell}^{s(1)}(p^2, z, \mu)}{2(2\pi)^3} &= \frac{\alpha C_F}{2\pi} \left\{ -\frac{\pi^2}{6} \delta(p^2) \delta(1-z) \right. \\ &\quad \left. + \delta(p^2) \left(P_{\ell\ell}(z) \ln z + (1+z^2) \mathcal{L}_1(1-z) + \theta(1-z)(1-z) \right) \right. \\ &\quad \left. + \delta(1-z) \frac{2}{\mu^2} \mathcal{L}_1\left(\frac{p^2}{\mu^2}\right) + (1+z^2) \mathcal{L}_0(1-z) \frac{1}{\mu^2} \mathcal{L}_0\left(\frac{p^2}{\mu^2}\right) \right\}, \\ \frac{\mathcal{J}_{\ell\ell}^{n(1)}(p^2, z, \mu)}{2(2\pi)^3} &= \frac{C_F - C_A/2}{C_F} \frac{\mathcal{J}_{\ell\ell}^{s(1)}(p^2, z, \mu)}{2(2\pi)^3}. \end{aligned} \quad (5.49)$$

The matching coefficients for the singlet $\mathcal{J}_{\ell\ell}^{s(1)}$ are the same as those in QCD [43]. As in the case of the matching coefficients $\mathcal{I}_{\ell\ell}^{s,n}$ for the beam functions and the PDFs, the new nonsinglet matching coefficient is proportional to the singlet matching coefficient. These matching coefficients do not depend on the gauge boson mass M , as in the matching coefficients in eq. (5.29).

6 Hard function

The hard functions are represented by a matrix in the basis of the singlet and nonsinglet operators O_I , so are the soft functions. The hard functions are defined in eq. (3.34) as $H_{JI} = 4u^2 D_I^* D_J = C_I^* C_J$, where D_I is the Wilson coefficient of the operators O_I for the process $\ell_e \bar{\ell}_e \rightarrow \ell_\mu \bar{\ell}_\mu$. Here ℓ_e and ℓ_μ are electron and muon doublets respectively because the relevant hard processes involve lepton doublets at higher orders. The hard coefficients are determined by matching the results of the full theory onto the effective theory.

We can utilize the results of the hard functions in previous literature. The detailed form of the hard function at one loop for $2 \rightarrow 2$ partonic processes can be found in ref. [31] for QCD, and in ref. [44] for electroweak interactions. Since we deal with the left-handed fields, all the right-handed contributions are put to zero.

The Wilson coefficients C_{ILL} to order α are given by [31, 44]

$$\begin{aligned} C_{1LL}(u, s, t) &= 2g^2 \frac{u}{s} \left\{ 1 + \frac{\alpha}{4\pi} \left[-2C_F L(s)^2 + X_1(u, s, t)L(s) + Y \right. \right. \\ &\quad \left. \left. + \left(\frac{C_A}{2} - 2C_F \right) Z(u, s, t) \right] \right\}, \\ C_{2LL}(u, s, t) &= 2g^2 \frac{u}{s} \frac{\alpha}{4\pi} \left[X_2(u, s, t)L(s) - \frac{C_F}{2C_A} Z(u, s, t) \right], \end{aligned} \quad (6.1)$$

where

$$\begin{aligned} X_1(u, s, t) &= 6C_F - \beta_0 + 8C_F[L(u) - L(t)] - 2C_A[2L(u) - L(s) - L(t)], \\ X_2(u, s, t) &= \frac{2C_F}{C_A}[L(u) - L(t)], \\ Z(u, s, t) &= \frac{s}{u} \left(\frac{s+2t}{u} [L(t) - L(s)]^2 + 2[L(t) - L(s)] + \frac{s+2t}{u} \pi^2 \right), \\ Y &= C_A \left(\frac{10}{3} + \pi^2 \right) + C_F \left(\frac{\pi^2}{3} - 16 \right) + \frac{5}{3} \beta_0. \end{aligned} \quad (6.2)$$

The function $L(x)$ as a function of the Mandelstam variables is given by

$$L(t) = \ln \frac{-t}{\mu^2}, \quad L(u) = \ln \frac{-u}{\mu^2}, \quad L(s) = \ln \frac{s}{\mu^2} - i\pi. \quad (6.3)$$

The RG equation for C_I can be written as

$$\frac{d}{d \ln \mu} \begin{pmatrix} C_1 \\ C_2 \end{pmatrix} = \mathbf{\Gamma}_H \begin{pmatrix} C_1 \\ C_2 \end{pmatrix}, \quad (6.4)$$

where $\mathbf{\Gamma}_H$ is the anomalous dimension matrix for the Wilson coefficients. Then the RG equation for the hard function \mathbf{H} is given as

$$\frac{d}{d \ln \mu} \mathbf{H} = \mathbf{\Gamma}_H \mathbf{H} + \mathbf{H} \mathbf{\Gamma}_H^\dagger. \quad (6.5)$$

The anomalous dimension matrix is given by [31, 44]

$$\mathbf{\Gamma}_H(u, s, t) = \left[2C_F \Gamma_c(\alpha) L(s) + 4\gamma_\ell - \frac{\beta(\alpha)}{\alpha} \right] \mathbf{1} + \Gamma_c(\alpha) \mathbf{M}, \quad (6.6)$$

where the β/α term compensates the $g^2(\mu)$ dependence in the leading Wilson coefficients. Here the beta function β is given by

$$\beta(\alpha) = \frac{d\alpha}{d \ln \mu} = -2\alpha \sum_{k=0} \beta_k \left(\frac{\alpha}{4\pi} \right)^{k+1}, \quad \beta_0 = \frac{11}{3} C_A - \frac{2}{3} n_f. \quad (6.7)$$

The matrix \mathbf{M} can be written as

$$\mathbf{M} = - \sum_{i < j} \mathbf{T}_i \cdot \mathbf{T}_j \left[L(s_{ij}) - L(s) \right], \quad (6.8)$$

where $s = s_{12} = s_{34}$, $t = s_{13} = s_{24}$ and $u = s_{14} = s_{23}$. By explicitly computing the color factors $\mathbf{T}_i \cdot \mathbf{T}_j$ [44], the matrix \mathbf{M} is written as

$$\begin{aligned} \mathbf{M}(u, s, t) &= - \sum_{i < j} \mathbf{T}_i \cdot \mathbf{T}_j \left[L(s_{ij}) - L(s) \right] \\ &= \begin{pmatrix} (2C_F - C_A/2) \ln \frac{n_{13}n_{24}}{n_{14}n_{23}} - \frac{C_A}{2} \ln \frac{n_{12}n_{34}}{n_{14}n_{23}} & \ln \frac{n_{13}n_{24}}{n_{14}n_{23}} \\ -C_F(C_F - C_A/2) \ln \frac{n_{13}n_{24}}{n_{14}n_{23}} & 0 \end{pmatrix} + i\pi \begin{pmatrix} C_A & 0 \\ 0 & 0 \end{pmatrix}, \end{aligned} \quad (6.9)$$

with $n_{ij} = n_i \cdot n_j/2$.

7 Soft function

The soft functions for the N -jettiness or more general jet observables have been discussed in refs. [26, 28]. The authors have considered the differential jettiness, that is, the individual jettiness in the N jets. [See eq. (2.3).] Here we consider the total jettiness which corresponds to the sum of the individual jettiness. The soft function for the jettiness is defined in eq. (3.32). Since the calculation was performed in massless cases in these references, they set the virtual contribution to zero since they consist of scaleless integrals. In our scheme with the nonzero gauge boson mass, there is nonzero virtual contribution, and we present the results here.

7.1 Hemisphere soft function

The diagrams for the emission of a gauge boson between the soft Wilson lines S_i and S_j^\dagger (Y_i and Y_j^\dagger in SCET_I) are shown in figure 5, where S_i is the soft Wilson line in the n_i direction. Because $n_i^2 = 0$, the emission from the soft Wilson lines with $i = j$ vanishes. Figure 5 (a) [figure 5 (b)] denotes the virtual contribution (the real contribution). In computing the total soft function, we include all the possible combinations of i and j with the appropriate group theory factors. The following calculations are based on the contractions of a gauge boson from the soft Wilson lines S_i and S_j^\dagger . The additional minus signs when the contractions are performed between S_i and S_j or S_i^\dagger and S_j^\dagger are included in the group theory factors.

The real contribution is decomposed into the hemisphere and the non-hemisphere parts. Only the hemisphere part involves the divergence, and the non-hemisphere parts are finite [26, 28]. Our case is relevant to ref. [26], which corresponds to the case $\beta_i = 2$ in ref. [28]. We concentrate on the hemisphere soft function to extract the anomalous dimensions of the N -jettiness soft function. The virtual contribution is not affected by the process of choosing the hemisphere functions in the real contribution.

The virtual contribution in figure 5 (a) aside from the group theory factor is written as

$$S_{ij,\text{hemi}}^V = -2\pi g^2 \mu_{\overline{\text{MS}}}^{2\epsilon} \delta(k) \int \frac{d^D q}{(2\pi)^D} \delta(q^2 - M^2) \frac{2n_{ij}}{q_i q_j} R(q_i, q_j), \quad (7.1)$$

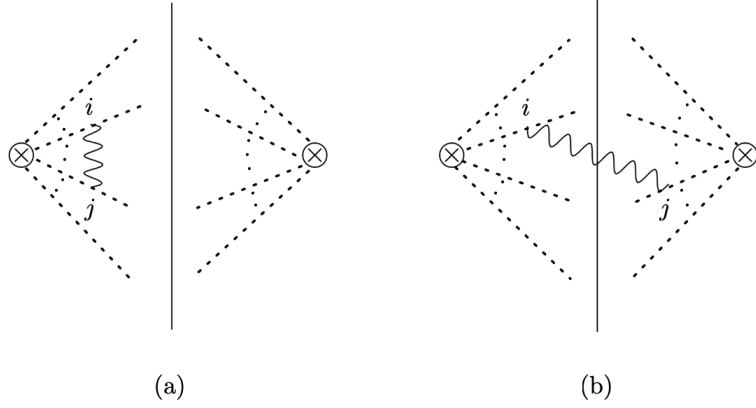


Figure 5. Schematic diagrams for the emission of a soft gauge boson in S_{ij} . The vertical lines are the final-state cut. Diagram (a) denotes the virtual contribution, and diagram (b) denotes the real contribution. The gauge bosons attached to the same i do not contribute. In order to obtain the soft function, all the possible pairs of contractions with different i and j should be included.

where $q_i = n_i \cdot q$ and $q_j = n_j \cdot q$, and $R(q_i, q_j)$ is the rapidity regulator, which can be written at NLO as [17]

$$R(q_i, q_j) = \left(\frac{\nu n_{ij}}{q_j}\right)^\eta \theta(q_j - q_i) + \left(\frac{\nu n_{ij}}{q_i}\right)^\eta \theta(q_i - q_j). \quad (7.2)$$

Since the integrand in eq. (7.1) is symmetric under $i \leftrightarrow j$, the contributions from both terms in the rapidity regulator is the same. Here we pick up the first term in the rapidity regulator and multiply two to get the virtual contribution. It is given as

$$\begin{aligned} S_{ij,\text{hemi}}^V &= -8\pi g^2 \mu_{\overline{\text{MS}}}^{2\epsilon} \delta(k) \int \frac{d^D q}{(2\pi)^D} \delta(q^2 - M^2) \frac{n_{ij}}{q_i q_j} \left(\frac{\nu n_{ij}}{q_j}\right)^\eta \theta(q_j - q_i) \quad (7.3) \\ &= -\frac{\alpha}{\pi} \frac{(\mu^2 e^{\gamma_E})^\epsilon}{\Gamma(1-\epsilon)} \delta(k) \int dq_j dq_i \left(\frac{q_i q_j}{n_{ij}} - M^2\right)^{-\epsilon} \frac{1}{q_i q_j} \left(\frac{\nu n_{ij}}{q_j}\right)^\eta \theta(q_i q_j > n_{ij} M^2) \theta(q_j - q_i) \\ &= -\frac{\alpha}{\pi} \frac{(\mu^2 e^{\gamma_E})^\epsilon}{\Gamma(1-\epsilon)} \delta(k) (\nu n_{ij})^\eta \int_{M^2}^\infty dy_1 \frac{(y_1 - M^2)^{-\epsilon}}{y_1^{1+\eta/2}} \int_1^\infty dy_2 \frac{1}{2y_2^{1+\eta/2}} \\ &= -\frac{\alpha}{\pi} \delta(k) e^{\gamma_E \epsilon} \left(\frac{\mu^2}{M^2}\right)^\epsilon \left(\frac{\nu \sqrt{n_{ij}}}{M}\right)^\eta \frac{1}{\eta} \frac{\Gamma(\epsilon + \eta/2)}{\Gamma(1 + \eta/2)} \\ &= \frac{\alpha}{2\pi} \delta(k) \left[\frac{1}{\epsilon^2} - \frac{2}{\eta} \left(\frac{1}{\epsilon} + \ln \frac{\mu^2}{M^2} \right) - \frac{1}{\epsilon} \ln \frac{n_{ij} \nu^2}{\mu^2} + \frac{1}{2} \ln^2 \frac{\mu^2}{M^2} - \ln \frac{n_{ij} \nu^2}{M^2} \ln \frac{\mu^2}{M^2} - \frac{\pi^2}{12} \right]. \end{aligned}$$

In the third line, we change variables $y_1 = q_i q_j / n_{ij}$, $y_2 = q_j / q_i$. Then q_i and q_j are written as $q_i = \sqrt{n_{ij} y_1 / y_2}$, $q_j = \sqrt{n_{ij} y_1 y_2}$ with $dq_i dq_j = n_{ij} dy_1 dy_2 / (2y_2)$, with $y_1 > M^2$ and $y_2 > 1$.

Here we focus on the real part. The imaginary part can be obtained by implementing the $i\epsilon$ prescription for the soft Wilson lines [45]. The result can be summarized as follows: The logarithmic term can be expressed in the form $\ln(\sigma_{ij} n_{ij} - i\epsilon)$, where $\sigma_{ij} = -1$ when i and j are both incoming or outgoing, and $\sigma_{ij} = 1$ when one is incoming and the other is outgoing. When $\sigma_{ij} = -1$, the imaginary part is induced.

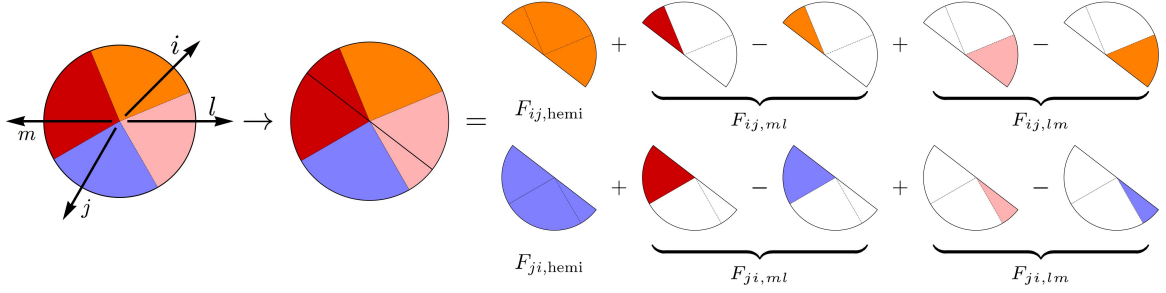


Figure 6. The real soft contribution is decomposed into the hemisphere soft functions $F_{ij,hemi}$ and $F_{ji,hemi}$ and the non-hemisphere soft functions. The hemisphere functions contain all the divergences, while the non-hemisphere functions are finite. Here we focus on the hemisphere soft functions.

The real soft contribution without the group theory factor at order α is given as

$$S_{ij}^{R(1)} = -2\pi g^2 \mu_{\overline{\text{MS}}}^{2\epsilon} \int \frac{d^D q}{(2\pi)^D} \delta(q^2 - M^2) \frac{2n_{ij}}{q_i q_j} R(q_i, q_j) F(k, \{q_i\}), \quad (7.4)$$

where the function F constrains the phase space on the emission of a single gauge boson, from which the hemisphere soft function is to be extracted.

For 2-jettiness, we consider four independent labels i, j, l, m and the constraint function F is given by

$$\begin{aligned} F(k, \{q_i\}) &= \theta(q_j - q_i) \left[\delta(k - q_i) \theta(q_l - q_i) \theta(q_m - q_i) + \delta(k - q_l) \theta(q_i - q_l) \theta(q_m - q_l) \right. \\ &\quad \left. + \delta(k - q_m) \theta(q_i - q_m) \theta(q_l - q_m) \right] + (i \leftrightarrow j) \\ &= \theta(q_j - q_i) \left[\delta(k - q_i) + \theta(q_i - q_m) \theta(q_l - q_m) \left(\delta(k - q_m) - \delta(k - q_i) \right) \right. \\ &\quad \left. + \theta(q_i - q_l) \theta(q_m - q_l) \left(\delta(k - q_l) - \delta(k - q_i) \right) \right] + (i \leftrightarrow j) \\ &\equiv F_{ij,hemi}(k, \{q_i\}) + F_{ij,ml}(k, \{q_i\}) + F_{ij,lm}(k, \{q_i\}) + (i \leftrightarrow j). \end{aligned} \quad (7.5)$$

(See ref. [26] for 1-jettiness.) In obtaining the second relation, the theta functions in the first term is replaced by

$$\theta(q_l - q_i) \theta(q_m - q_i) = \left(1 - \theta(q_i - q_l)\right) \left(1 - \theta(q_i - q_m)\right). \quad (7.6)$$

The hemisphere measurement function for the full hemisphere $q_j > q_i$ is given by

$$F_{ij,hemi}(k, \{q_i\}) = \theta(q_j - q_i) \delta(k - q_i). \quad (7.7)$$

And the non-hemisphere functions are given by

$$\begin{aligned} F_{ij,ml}(k, \{q_i\}) &= \theta(q_j - q_i) \theta(q_i - q_m) \theta(q_l - q_m) \left(\delta(k - q_m) - \delta(k - q_i) \right), \\ F_{ij,lm}(k, \{q_i\}) &= \theta(q_j - q_i) \theta(q_i - q_l) \theta(q_m - q_l) \left(\delta(k - q_l) - \delta(k - q_i) \right), \end{aligned} \quad (7.8)$$

which are the non-hemisphere measurement function for region m and l respectively. Note that the constraint function F is constructed for the gauge boson emitted from the soft

Wilson lines S_i and S_j^\dagger (Y_i and Y_j^\dagger). The hemisphere function for the i and j jet directions contains the collinear and the soft divergences. The contribution to the l and m directions only contains the soft divergence, which is subtracted from the corresponding region of the hemisphere parts. Here we focus on the hemisphere soft functions, from which the anomalous dimensions are obtained. The decomposition of the soft real contribution into the hemisphere functions and the non-hemisphere functions are schematically shown in figure 6. As can be seen in the figure, the soft divergence in the non-hemisphere parts is cancelled by the corresponding subtraction from the hemisphere parts.

The phase space for the real emission is shown in figure 7, and we compute the real contribution in the phase space A , which corresponds to the hemisphere constraint $F_{ij,\text{hemi}}(k, \{q_i\})$. The real contribution from the region A is given by

$$S_{ij,\text{hemi}}^{RA} = -\frac{\alpha}{2\pi} \frac{(\mu^2 e^{\gamma_E})^\epsilon}{\Gamma(1-\epsilon)} (\nu n_{ij})^\eta \int dq_j \frac{1}{k q_j^{1+\eta}} \left(\frac{k q_j}{n_{ij}} - M^2 \right)^{-\epsilon} \theta(q_j - k) \theta(k q_j - n_{ij} M^2). \quad (7.9)$$

We divide the phase space into the region a with $k < \sqrt{n_{ij}} M$ and the region b with $k > \sqrt{n_{ij}} M$, and the integral in the region a is given as

$$\begin{aligned} I_a &= -\frac{\alpha}{2\pi} \frac{(\mu^2 e^{\gamma_E})^\epsilon}{\Gamma(1-\epsilon)} \frac{(\nu n_{ij})^\eta}{k} \int_{n_{ij} M^2/k}^{\infty} dq_j \frac{1}{q_j^{1+\eta}} \left(\frac{k q_j}{n_{ij}} - M^2 \right)^{-\epsilon} \theta(k < \sqrt{n_{ij}} M) \\ &= -\frac{\alpha}{2\pi} e^{\gamma_E \epsilon} \left(\frac{\mu^2}{M^2} \right)^\epsilon \left(\frac{\mu}{\nu} \right)^\eta \left(\frac{\nu^2}{M^2} \right)^\eta \frac{\Gamma(\epsilon + \eta)}{\Gamma(1 + \eta)} \frac{1}{\mu} \left(\frac{\mu}{k} \right)^{1-\eta} \\ &= -\frac{\alpha}{2\pi} \left\{ \delta(k) \left[\frac{1}{\eta} \left(\frac{1}{\epsilon} + \ln \frac{\mu^2}{M^2} \right) - \frac{1}{\epsilon^2} + \frac{1}{\epsilon} \ln \frac{\nu}{\mu} + \ln \frac{\nu}{M} \ln \frac{\mu^2}{M^2} + \frac{\pi^2}{12} \right] \right. \\ &\quad \left. + \left(\frac{1}{\epsilon} + \ln \frac{\mu^2}{M^2} \right) \frac{1}{\mu} \mathcal{L}_0 \left(\frac{k}{\mu} \right) \theta(k < \sqrt{n_{ij}} M) \right\}, \end{aligned} \quad (7.10)$$

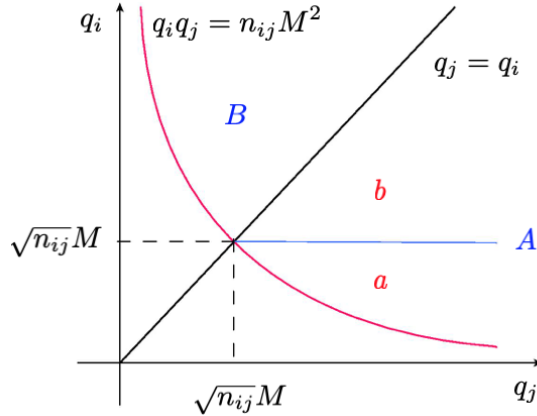


Figure 7. Phase space for a real, soft gauge boson emission. Region A [$F_{ij,\text{hemi}}(k, \{q_i\})$] corresponds to $q_i q_j > n_{ij} M^2$ and $q_j > q_i$. Region B [$F_{ji,\text{hemi}}(k, \{q_i\})$] corresponds to $q_i q_j > n_{ij} M^2$ and $q_i > q_j$. Region A is subdivided into the region a with $k < \sqrt{n_{ij}} M$ and the region b with $k > \sqrt{n_{ij}} M$.

where the following relation is used.

$$\frac{1}{\mu} \left(\frac{\mu}{k} \right)^{1-\eta} = \frac{1}{\eta} \delta(k) + \frac{1}{\mu} \mathcal{L}_0 \left(\frac{k}{\mu} \right) + \mathcal{O}(\eta). \quad (7.11)$$

The integral in the region b is written as

$$\begin{aligned} I_b &= -\frac{\alpha}{2\pi} \frac{(\mu^2 e^{\gamma_E})^\epsilon}{\Gamma(1-\epsilon)} (\nu n_{ij})^\eta \frac{n_{ij}}{k^{1+\epsilon}} \int_k^\infty dq_j \frac{1}{q_j^{1+\eta}} \left(q_j - \frac{n_{ij} M^2}{k} \right)^{-\epsilon} \theta(k > \sqrt{n_{ij}} M) \\ &= -\frac{\alpha}{2\pi} \frac{1}{k} \left(\frac{1}{\epsilon} + \ln \frac{n_{ij} \mu^2}{k^2} \right) \theta(k > \sqrt{n_{ij}} M). \end{aligned} \quad (7.12)$$

Note that $I_a + I_b$ is remains the same when i and j are switched. Therefore the real contribution is twice $S_{ij,\text{hemi}}^{RA}$ because the integration in the region B is the same. The real hemisphere contribution is given by

$$\begin{aligned} S_{ij,\text{hemi}}^R &= -\frac{\alpha}{2\pi} \left\{ \delta(k) \left[\frac{2}{\eta} \left(\frac{1}{\epsilon} + \ln \frac{\mu^2}{M^2} \right) - \frac{2}{\epsilon^2} + \frac{1}{\epsilon} \ln \frac{\nu^2}{\mu^2} + \ln \frac{\nu^2}{M^2} \ln \frac{\mu^2}{M^2} + \frac{\pi^2}{6} \right] \right. \\ &\quad \left. + \left(\frac{1}{\epsilon} + \ln \frac{\mu^2}{M^2} \right) \frac{2}{\mu} \mathcal{L}_0 \left(\frac{k}{\mu} \right) \theta(k < \sqrt{n_{ij}} M) + \frac{2}{k} \left(\frac{1}{\epsilon} + \ln \frac{n_{ij} \mu^2}{k^2} \right) \theta(k > \sqrt{n_{ij}} M) \right\}. \end{aligned} \quad (7.13)$$

With the virtual contribution in eq. (7.3) and the real contribution in eq. (7.13), the hemisphere soft function can be written as

$$\mathbf{S}_{\text{hemi}}(a_1, a_2, a_3, a_4) = \sum_{i \neq j} \left[\mathbf{S}_{ij}^V(a_1, a_2, a_3, a_4) S_{ij,\text{hemi}}^V + \mathbf{S}_{ij}^R(a_1, a_2, a_3, a_4) S_{ij,\text{hemi}}^R \right]. \quad (7.14)$$

Here we represent the color structure of the soft function in the form $\mathbf{S}(a_1, a_2, a_3, a_4)$, in which the indices a_i represent the presence of the nonsinglets from the originating i -th collinear particle ($i = 1, 2$ for the incoming particles, and $i = 3, 4$ for the outgoing particles in our convention). For example, the soft color matrix with all the singlets is given by $\mathbf{S}(0, 0, 0, 0)$ and the soft color matrix with the nonsinglet contributions from 1 and 3 is denoted as $\mathbf{S}(1, 0, 1, 0)$, etc.. For the soft color matrix at tree level, see appendix D.1. With these color matrices, the real soft function for the nonsinglets 1 and 3 is written as $\sum_{i \neq j} \mathbf{S}_{ij}^R(1, 0, 1, 0) S_{ij}^R$, where S_{ij}^R is the soft correction, which is given by eq. (7.13). Using this convention, the hemisphere soft function from $\mathbf{S}_{\text{hemi}}(1, 0, 1, 0)$ incorporates $S_{IJ}^{e_0 e_0}$ by putting the generators T^c and T^e for the first and the third indices respectively, and T^0 in the second and the fourth indices.

The virtual and real contributions to the μ and ν soft anomalous dimensions without the group theory factors are given as

$$\begin{aligned} \frac{dS_{ij,\text{hemi}}^V}{d \ln \mu} &= -\frac{\alpha}{\pi} \delta(k) \ln \frac{n_{ij} \nu^2}{\mu^2}, \quad \frac{dS_{ij,\text{hemi}}^R}{d \ln \mu} = -\frac{\alpha}{\pi} \left[\delta(k) \ln \frac{\nu^2}{\mu^2} + \frac{2}{\mu} \mathcal{L}_0 \left(\frac{k}{\mu} \right) \right], \\ \frac{dS_{ij,\text{hemi}}^V}{d \ln \nu} &= -\frac{\alpha}{\pi} \delta(k) \ln \frac{\mu^2}{M^2}, \quad \frac{dS_{ij,\text{hemi}}^R}{d \ln \nu} = -\frac{\alpha}{\pi} \delta(k) \ln \frac{\mu^2}{M^2}. \end{aligned} \quad (7.15)$$

The derivatives of the Laplace-transformed soft parts are given by

$$\frac{d\tilde{S}_{ij,\text{hemi}}^V}{d\ln\mu} = -\frac{\alpha}{\pi} \ln \frac{n_{ij}\nu^2}{\mu^2}, \quad \frac{d\tilde{S}_{ij,\text{hemi}}^R}{d\ln\mu} = -\frac{\alpha}{\pi} \ln \frac{\nu^2 Q_L^2}{\mu^4}, \quad (7.16)$$

$$\frac{d\tilde{S}_{ij,\text{hemi}}^V}{d\ln\nu} = -\frac{\alpha}{\pi} \ln \frac{\mu^2}{M^2}, \quad \frac{d\tilde{S}_{ij,\text{hemi}}^R}{d\ln\nu} = -\frac{\alpha}{\pi} \ln \frac{\mu^2}{M^2}. \quad (7.17)$$

It is noteworthy to compare eq. (7.16) with the results in ref. [24], in which the soft anomalous dimensions are given in inclusive cross sections. In ref. [24], the virtual and the real contributions at order α are the same except the sign, and the μ -anomalous dimensions depend on n_{ij} . However, in the case of the jettiness in which we give constraints on the phase space in the real emissions, the contribution to the anomalous dimension from the virtual corrections is the same as in ref. [24], but the contribution from the real emission is different, especially it is independent of n_{ij} .

Due to this difference, the N -jettiness soft function with four nonsinglets does not have mixing in contrast to the inclusive soft function, in which the mixing is induced at one loop. The virtual corrections do not cause mixing, while the mixing is cancelled in the sum of the real contributions because the real soft anomalous dimensions in eq. (7.16) is independent of n_{ij} . The proof that there is no mixing in the N -jettiness soft function with four nonsinglets at one loop is presented in detail in appendix D.2.

7.2 Soft anomalous dimensions

The soft functions are written as matrices in the operator basis. The Laplace transform of the soft function is given as

$$\tilde{\mathbf{S}}\left(\ln \frac{Q_L}{\mu}, M, \mu\right) = \int_0^\infty dk e^{-sk} \mathbf{S}(k, M, \mu), \quad s = \frac{1}{e^{\gamma_E} Q_L}. \quad (7.18)$$

The RG equation with respect to the renormalization scale μ for the soft function in Laplace transform is written as

$$\frac{d}{d\ln\mu} \tilde{\mathbf{S}} = \tilde{\mathbf{\Gamma}}_S^{\mu\dagger} \tilde{\mathbf{S}} + \tilde{\mathbf{S}} \tilde{\mathbf{\Gamma}}_S^\mu, \quad (7.19)$$

where $\tilde{\mathbf{\Gamma}}_S^\mu$ is the μ -anomalous dimension matrix. At NLO, eq. (7.19) is written as

$$\frac{d}{d\ln\mu} \tilde{\mathbf{S}}^{(1)} = \tilde{\mathbf{\Gamma}}_S^{\mu\dagger(1)} \tilde{\mathbf{S}}^{(0)} + \tilde{\mathbf{S}}^{(0)} \tilde{\mathbf{\Gamma}}_S^{\mu(1)}, \quad (7.20)$$

where $\mathbf{S}^{(1)}$ is the renormalized soft function. The soft anomalous dimensions can be extracted from the requirement that the sum of the anomalous dimensions from all the factorized parts should cancel. The soft anomalous dimension at one loop is given by

$$\tilde{\mathbf{\Gamma}}_S^{\mu(1)} = -\left(\tilde{\mathbf{\Gamma}}_H^{(1)} + \frac{1}{2}(\tilde{\gamma}_{B_1}^{\mu(1)} + \tilde{\gamma}_{B_2}^{\mu(1)} + \tilde{\gamma}_{J_3}^{\mu(1)} + \tilde{\gamma}_{J_4}^{\mu(1)}) \otimes \mathbf{1}\right), \quad (7.21)$$

where $\tilde{\gamma}_C^\mu$ is the anomalous dimensions of the beam functions or the jet functions. The μ -anomalous dimensions of the soft function with k nonsinglets ($k = 0, 2, 3, 4$) are given as

$$(\tilde{\mathbf{\Gamma}}_S^\mu)_k^{(1)} = -C_F \Gamma_c(\alpha) \left(\ln \frac{\mu^4 n_{12} n_{34}}{Q_L^4} - 2i\pi \right) \times \mathbf{1} - \Gamma_c(\alpha) \mathbf{M} + \frac{C_A \Gamma_c}{2} k \ln \frac{\mu^2}{\nu Q_L} \times \mathbf{1}, \quad (7.22)$$

where \mathbf{M} is the matrix in eq. (6.9) appearing in the hard function. As in the hard function, the imaginary part in the identity matrix does not contribute to the evolution.

The RG equation with respect to the rapidity scale ν is written as

$$\frac{d}{d \ln \nu} \tilde{\mathbf{S}} = \tilde{\Gamma}_S^\nu \tilde{\mathbf{S}}. \quad (7.23)$$

After color algebra [46], the ν -soft anomalous dimensions with k nonsinglets ($k \neq 1$) are given as

$$(\tilde{\Gamma}_S^\nu)_k^{(1)} = -\frac{C_A \Gamma_c}{2} k \ln \frac{\mu^2}{M^2}. \quad (7.24)$$

Note that there is no contribution from those with one nonsinglet $k = 1$ due to charge conservation.

8 Renormalization group evolution

In order to study the RG evolution, it is convenient to make a Laplace transform of the N -jettiness which involves the convolution of the jet, beam and the soft functions in the factorization formulae, eqs. (3.33) and (3.46). The convolution becomes the product of the factorized parts with their Laplace transforms. Here we choose $s = 1/[Q_L \exp(\gamma_E)]$, which is the conjugate variable to the jettiness. Then we can take inverse Laplace transform and express the evolutions accordingly [47].

In order to resum large logarithms, the RG evolutions of the factorized functions start from their own characteristic scales to the common factorization scale μ_F and the rapidity scale ν_F . The characteristic scales are the scales which minimize the logarithms in the factorized functions, and they are give by

$$\mu_H \sim \omega_i, \quad \mu_{C_i} \sim \sqrt{\omega_i M}, \quad \mu_S \sim M, \quad \nu_C \sim \omega_i, \quad \nu_S \sim M, \quad (8.1)$$

where ω_i ($i = 1, \dots, 4$) are the largest collinear components. The characteristic collinear scales (hard-collinear scales in SCET_{II}) μ_{C_i} apply both to the singlets and the nonsinglets of the collinear functions. The collinear rapidity scale ν_C belongs to the nonsinglets. The soft scale μ_S applies to both the singlets and the nonsinglets, while the scale ν_S belongs to the nonsinglet soft functions.

8.1 Hard function

The anomalous dimension of the hard function is given by eq. (6.6). The evolution of the hard function from the high-energy scale μ_H to the factorization scale μ_F is written as

$$\mathbf{H}(\mu_F) = \Pi_H(\mu_F, \mu_H) \mathbf{\Pi}_H(\mu_F, \mu_H) \mathbf{H}(\mu_H) \mathbf{\Pi}_H^\dagger(\mu_F, \mu_H), \quad (8.2)$$

where $\Pi_H(\mu_F, \mu_H)$ is the evolution from the identity matrix of the anomalous dimension, and $\mathbf{\Pi}_H(\mu_F, \mu_H)$ is obtained by the exponentiating the matrix \mathbf{M} . They can be written as

$$\Pi_H(\mu_F, \mu_H) = \exp \left[-8C_F S(\mu_F, \mu_H) - 4C_F a_\Gamma(\mu_F, \mu_H) \ln \frac{\mu_H^2}{s} + 8a_{\gamma_\ell}(\mu_F, \mu_H) \right], \quad (8.3)$$

where

$$\int_{\mu_H}^{\mu_F} \frac{d\mu}{\mu} \Gamma_c(\alpha) \ln \frac{\mu^2}{s} \equiv 2S_\Gamma(\mu_F, \mu_H) + a_\Gamma(\mu_F, \mu_H) \ln \frac{\mu_H^2}{s}, \quad (8.4)$$

and S_Γ and a_f are given as

$$S_\Gamma(\mu, \mu_i) = \int_{\alpha(\mu_i)}^{\alpha(\mu)} d\alpha \frac{\Gamma_c(\alpha)}{\beta(\alpha)} \int_{\alpha(\mu_i)}^{\alpha} \frac{d\alpha'}{\beta(\alpha')}, \quad a_f(\mu, \mu_i) = \int_{\alpha(\mu_i)}^{\alpha(\mu)} \frac{d\alpha}{\beta(\alpha)} f(\alpha), \quad (8.5)$$

for an arbitrary function $f(\alpha)$. The explicit results of S_Γ , a_Γ and a_{γ_ℓ} are presented at next-to-next-to-leading-logarithmic accuracy in ref. [33]. And $\mathbf{\Pi}_H$ is obtained by exponentiating \mathbf{M} as

$$\mathbf{\Pi}_H(\mu_F, \mu_H) = \exp \left[a_\Gamma(\mu_F, \mu_H) \mathbf{M} \right]. \quad (8.6)$$

8.2 Collinear functions

We present the evolution of the beam functions as a representative of the collinear functions. Since the semi-inclusive jet functions and the FJFs have the same anomalous dimensions as the beam functions, their evolutions can be described in a similar way.

The RG equation with respect to μ for the singlet beam function is given by

$$\frac{d}{d \ln \mu} \tilde{B}_s(\mu) = \tilde{\gamma}_{B_s}^\mu \tilde{B}_s(\mu), \quad (8.7)$$

where the μ -anomalous dimension $\tilde{\gamma}_{B_s}^\mu$ for the singlet is given by eq. (5.17). The evolution from the collinear scale μ_C to the factorization scale μ_F is given by

$$\tilde{B}_s(\mu_F) = U_{B_s}(\mu_F, \mu_C) \tilde{B}_s(\mu_C), \quad (8.8)$$

where the evolution kernel U_{B_s} is given by

$$U_{B_s}(\mu_F, \mu_C) = \exp \left[4C_F S_\Gamma(\mu_F, \mu_C) - 2C_F a_\Gamma(\mu_F, \mu_C) \ln \frac{\omega Q_L}{\mu_C^2} - 2a_{\gamma_\ell}(\mu_F, \mu_C) \right]. \quad (8.9)$$

For the nonsinglet, the μ and ν RG equations are given by

$$\frac{d}{d \ln \mu} \tilde{B}_n(\mu, \nu) = \tilde{\gamma}_{B_n}^\mu \tilde{B}_n(\mu, \nu), \quad \frac{d}{d \ln \nu} \tilde{B}_n(\mu, \nu) = \tilde{\gamma}_{B_n}^\nu \tilde{B}_n(\mu, \nu), \quad (8.10)$$

where the μ -anomalous dimensions $\tilde{\gamma}_{B_n}^\mu$ and the ν -anomalous dimensions $\tilde{\gamma}_{B_n}^\nu$ for the nonsinglet are given by eq. (5.17). The order of the evolutions with respect to μ and ν is irrelevant, and here we evolve the beam function with respect to ν first, and then with respect to μ . Since the ν -anomalous dimension contains a large logarithm with $\mu \sim \sqrt{\omega Q_L} \gg M$, we resum this large logarithm first in expressing the evolution with respect to ν [14]. Then the evolution is written as

$$\tilde{B}_n(\mu_F, \nu_F) = U_{B_n}(\mu_F, \mu_C; \nu_F) V_{B_n}(\nu_F, \nu_C; \mu_C) \tilde{B}_n(\mu_C, \nu_C), \quad (8.11)$$

where the μ -evolution kernel U_{Bn} and the ν -evolution kernel V_{Bn} are given by

$$V_{Bn}(\nu_F, \nu_C; \mu_C) = \exp\left[C_A a_\Gamma(\mu_C, M) \ln \frac{\nu_F}{\nu_C}\right], \quad (8.12)$$

$$U_{Bn}(\mu_F, \mu_C; \nu_F) = U_{Bs}(\mu_F, \mu_C) \exp\left[-2C_A S_\Gamma(\mu_F, \mu_C) + C_A a_\Gamma(\mu_F, \mu_C) \ln \frac{\nu_F Q_L}{\mu_C^2}\right].$$

The anomalous dimensions of the semi-inclusive jet functions in eq. (5.34) are the same as those of the beam functions. Therefore the evolution of the semi-inclusive jet functions is the same as the FJF. However, the largest lightcone component in each i -th collinear direction is denoted by ω_i , which determines the characteristic collinear scale in each direction. Let us denote the collinear functions as $C_i(\mu_F, \nu_F)$, where it corresponds to the beam functions for $i = 1, 2$ and to the semi-inclusive jet functions or the FJFs for $i = 3, 4$. Then the evolution of the collinear functions are written as ($i = 1, 2, 3, 4$)

$$\begin{aligned} \tilde{C}_{is}(\mu_F) &= U_{is}(\mu_F, \mu_{Ci}) \tilde{C}_{is}(\mu_{Ci}), \\ \tilde{C}_{in}(\mu_F, \nu_F) &= U_{in}(\mu_F, \mu_{Ci}; \nu_F) V_{in}(\nu_F, \nu_C; \mu_{Ci}) \tilde{C}_{in}(\mu_{Ci}, \nu_C), \end{aligned} \quad (8.13)$$

where the evolution kernels are given as

$$\begin{aligned} U_{is}(\mu_F, \mu_{Ci}) &= \exp\left[4C_F S_\Gamma(\mu_F, \mu_{Ci}) - 2C_F a_\Gamma(\mu_F, \mu_{Ci}) \ln \frac{\omega_i Q_L}{\mu_{Ci}^2} - 2a_{\gamma_\ell}(\mu_F, \mu_{Ci})\right], \\ U_{in}(\mu_F, \mu_{Ci}; \nu_F) &= U_{is}(\mu_F, \mu_{Ci}) \exp\left[-2C_A S_\Gamma(\mu_F, \mu_{Ci}) + C_A a_\Gamma(\mu_F, \mu_{Ci}) \ln \frac{\nu_F Q_L}{\mu_{Ci}^2}\right], \\ V_{in}(\nu_F, \nu_C; \mu_{Ci}) &= \exp\left[C_A a_\Gamma(\mu_{Ci}, M) \ln \frac{\nu_F}{\nu_C}\right]. \end{aligned} \quad (8.14)$$

8.3 Soft function

The μ and ν anomalous dimensions for the soft function are given by eqs. (7.22) and (7.24) respectively. The evolution of the soft function can be proceeded as in the case of the hard function and the soft evolution with the k nonsinglets can be written as

$$\tilde{\mathbf{S}}_k(\mu_F, \nu_F) = \Pi_{Sk}(\mu_F, \mu_S; \nu_F, \nu_S) \mathbf{\Pi}_S^\dagger(\mu_F, \mu_S) \tilde{\mathbf{S}}_k(\mu_S, \nu_S) \mathbf{\Pi}_S(\mu_F, \mu_S), \quad (8.15)$$

where the evolution kernel $\Pi_{Sk}(\mu_F, \mu_S; \nu_F, \nu_S)$ comes from the identity matrix, and the evolution kernel $\mathbf{\Pi}_S(\mu_F, \mu_S)$ from \mathbf{M} .

Here we also evolve with respect to ν first, and then μ . The evolution kernel Π_{Sk} can be written as

$$\Pi_{Sk}(\mu_F, \mu_S; \nu_F, \nu_S) = U_{Sk}(\mu_F, \mu_S; \nu_F) V_{Sk}(\nu_F, \nu_S; \mu_S), \quad (8.16)$$

where

$$\begin{aligned} V_{Sk}(\nu_F, \nu_S; \mu_S) &= \exp\left[-kC_A a_\Gamma(\mu_S, M) \ln \frac{\nu_F}{\nu_S}\right], \\ U_{Sk}(\mu_F, \mu_S; \nu_F) &= \exp\left[-8C_F S_\Gamma(\mu_F, \mu_S) - 4C_F a_\Gamma(\mu_F, \mu_S) \ln \frac{\mu_S^2}{Q_L^2} \right. \\ &\quad \left. - 2C_F a_\Gamma(\mu_F, \mu_S) \ln(n_{12}n_{34}) + 2kC_A S_\Gamma(\mu_F, \mu_S) \right. \\ &\quad \left. - kC_A a_\Gamma(\mu_F, \mu_S) \ln \frac{\nu_F Q_L}{\mu_S^2}\right], \end{aligned} \quad (8.17)$$

and $\mathbf{\Pi}_S(\mu_F, \mu_S)$ is given by

$$\mathbf{\Pi}_S(\mu_F, \mu_S) = \exp\left[-a_\Gamma(\mu_F, \mu_S)\mathbf{M}\right]. \quad (8.18)$$

With the addition of nonsinglets, the anomalous dimension of the hard function is not affected, and the sum of all the other ν -anomalous dimensions for any number of nonsinglets is cancelled.

$$\left(\tilde{\Gamma}_S^\nu\right)_k^{(1)} + \left(\tilde{\gamma}_B^\nu(\omega_1) + \tilde{\gamma}_B^\nu(\omega_2) + \tilde{\gamma}_J^\nu(\omega_3) + \tilde{\gamma}_J^\nu(\omega_4)\right)_k = 0, \quad (8.19)$$

where it is understood that the soft function with the k nonsinglets should be employed, if there are k nonsinglets in the collinear parts.

9 Conclusion and outlook

The analysis of the N -jettiness in high-energy electroweak processes is more sophisticated due to the presence of the nonsinglet contributions. It may be looked upon as a mere copy of QCD, but the most notable distinction, compared with QCD, is that a lot of different channels involving nonsinglet contributions enter the expression of the N -jettiness. In QCD, only the projection to the color singlets for the collinear and the soft functions survives. As a result, the definitions of the factorized collinear and soft functions should be extended to the nonsinglet contributions to include all the possible channels. With these additional ingredients, we have established the factorization theorem for the N jettiness in weak interaction. We have chosen the simplest $SU(2)$ gauge interaction only to show the distinction of the participation of the nonsinglets in the initial and the final states. The extension to the full Standard Model is nontrivial due to the additional particles, the gauge mixing and the effect of the electroweak symmetry breaking, but is necessary for phenomenology. It will be the next subject to pursue, following this development.

According to the different hierarchy of scales, different effective theories are employed. When $\mathcal{T}^2 \sim M^2 \ll p_c^2 \sim Q\mathcal{T} \ll Q^2$, SCET_I is appropriate, and both the collinear and the soft functions contribute to the jettiness. On the other hand, when $\mathcal{T}^2 \sim M^2 \sim p_c^2 \ll Q\mathcal{T} \ll Q$, we employ SCET_{II}. In this case, the collinear functions are the PDF or the fragmentation functions, which do not contribute to the jettiness, and only the soft function seems to contribute to the jettiness. However, the effect of the hard-collinear modes by integrating out the SCET_I-collinear modes through the matching coefficients contributes to the jettiness. Though the detailed physics is different in SCET_I and in SCET_{II}, if we combine the contributions of the matching coefficients and the PDF or the fragmentation functions, and identify them as the beam functions or the FJFs, the jettiness in both cases can be obtained by computing the beam functions and the FJFs in SCET_I. Taking account of all the intricacies, we have established the factorization of the 2-jettiness both in SCET_I and in SCET_{II}. In the computation of the jettiness, the gauge boson mass is regarded as small, and we take the small mass limit in our final results. Note that there is no IR divergence due to the physical gauge boson mass M , however small that is.

When the nonsinglets participate in the scattering, the main distinction is the existence of the rapidity divergence in the collinear and soft functions. As in QCD, there is no rapidity

divergence in the singlet contributions. However, the rapidity divergence arises when the nonsinglets are involved in the factorized parts owing to the different group theory factors between the real and the virtual contributions. Of course, in the final expression for the N -jettiness when all the factorized parts are added, the rapidity divergence cancels for any number of nonsinglets. For the effective theory to be consistent, it should hold true because the full theory is free of the rapidity divergence. However, the effect of rapidity divergence in each collinear and soft sectors plays an important role in resumming large logarithms. Due to the presence of the double RG evolutions with respect to the renormalization scale μ and the rapidity scale ν for the nonsinglet contributions, we have to solve the coupled RG equation to evolve with respect to both of them, and the results have been presented here.

As mentioned in section 3, it is important to study the possible violation of the factorization in weak interaction due to the Glauber exchange between the spectator partons. It arises when the nonsinglets participate in the scattering because the group theory factors are not the same for different configurations of the Glauber gauge bosons across the unitarity cuts. The presence of the rapidity divergence due to the nonsinglets appear from a similar source. Therefore it is critical to look into the Glauber exchange in considering the factorization. It is beyond the scope of this paper, and we will investigate this topic in the future.

Despite the fact that we only employed the $SU(2)$ gauge interaction, we reiterate that this opens up a lot of possibilities in the phenomenology of the high-energy lepton colliders. The first task will be to include all the interactions to delineate the Standard Model completely. It also involves the electroweak symmetry breaking and the effect of the masses of the heavy particles. Next, the additional ingredients in the factorization should be provided to yield theoretical predictions. We have considered $e^-e^+ \rightarrow \mu^-\mu^+$, but other modes such as $e^-e^+ \rightarrow W^+W^-$, and the Higgs production should also be included for the study of the phenomenology. These topics will be our next areas of research.

A Laplace transforms of the distributions

It is convenient to consider the Laplace transform of the N -jettiness, in which the factorized parts are written as the products of the hard, collinear and soft functions. After the individual parts are evolved, we can make an inverse Laplace transformation [47] to obtain the original N -jettiness. Another advantage is that the anomalous dimensions with the Laplace transforms are ordinary functions, while the original anomalous dimensions may contain distributions. Therefore the solution of the RG equation in the Laplace transform can be written in a more tangible form.

Let us begin with the Laplace transform of the soft function, which is given as

$$\begin{aligned}\tilde{S}\left(\ln\frac{Q_L}{\mu}, M, \mu\right) &= \int_0^\infty dk e^{-sk} S(k, M, \mu), \quad s = \frac{1}{e^{\gamma_E} Q_L}, \\ S(k, M, \mu) &= \frac{1}{2\pi i} \int_{c-i\infty}^{c+i\infty} ds e^{sk} \tilde{S}\left(\ln\frac{1}{e^{\gamma_E} s\mu}, M, \mu\right).\end{aligned}\tag{A.1}$$

where the contour is chosen to stay to the right of all discontinuities ($c > 0$) in the inverse Laplace transform. The scale Q_L is a conjugate variable to s .

Note that the variable s in the Laplace transform should be common to all the factorized parts including the collinear part, that is, it should be conjugate to the jettiness. It is straightforward to express the Laplace transform of the collinear functions with the same form as in eq. (A.1) by noting that $t = \omega k$ in the beam functions and $p^2 = \omega k$ in the jet functions, where k represents the jettiness.

$$\begin{aligned}
\tilde{B}_i\left(\ln \frac{\omega Q_L}{\mu^2}, z, M, \mu\right) &= \int_0^\infty dk e^{-sk} B_i(\omega k, z, M, \mu), \\
B_i(\omega k, z, M, \mu) &= \frac{1}{2\pi i} \int_{c-i\infty}^{c+i\infty} ds e^{sk} \tilde{B}_i\left(\ln \frac{1}{e^{\gamma_E} s \mu}, M, \mu\right), \\
\tilde{J}_i\left(\ln \frac{\omega Q_L}{\mu^2}, M, \mu\right) &= \int_0^\infty dk e^{-sk} J_i(\omega k, M, \mu), \\
J_i(\omega k, M, \mu) &= \frac{1}{2\pi i} \int_{c-i\infty}^{c+i\infty} ds e^{sk} \tilde{J}_i\left(\ln \frac{1}{e^{\gamma_E} s \mu}, M, \mu\right), \tag{A.2}
\end{aligned}$$

with $s = 1/(e^{\gamma_E} Q_L)$.

In the collinear and the soft functions, the distributions arise from the expressions $\mu^{2\epsilon}/(\omega k)^{1+\epsilon}$ and $\mu^\epsilon/k^{1+\epsilon}$ respectively. They can be expanded in powers of ϵ , and can be written as

$$\begin{aligned}
\frac{\mu^{2\epsilon}}{(\omega k)^{1+\epsilon}} &= -\frac{1}{\epsilon} \delta(\omega k) + \frac{1}{\mu^2} \mathcal{L}_0\left(\frac{\omega k}{\mu^2}\right) - \epsilon \frac{1}{\mu^2} \mathcal{L}_1\left(\frac{\omega k}{\mu^2}\right) + \dots, \\
\frac{\mu^\epsilon}{k^{1+\epsilon}} &= -\frac{1}{\epsilon} \delta(k) + \frac{1}{\mu} \mathcal{L}_0\left(\frac{k}{\mu}\right) - \epsilon \frac{1}{\mu} \mathcal{L}_1\left(\frac{k}{\mu}\right) + \dots. \tag{A.3}
\end{aligned}$$

The Laplace transforms of these functions are given as

$$\int_0^\infty e^{-sk} dk \frac{\mu^{2\epsilon}}{(\omega k)^{1+\epsilon}} = \frac{1}{\omega} \left(\frac{s\mu^2}{\omega}\right)^\epsilon \Gamma(-\epsilon), \quad \int_0^\infty e^{-sk} dk \frac{\mu^\epsilon}{k^{1+\epsilon}} = (s\mu)^\epsilon \Gamma(-\epsilon). \tag{A.4}$$

By expanding eq. (A.4) in powers of ϵ and by comparing them with eq. (A.3), we can obtain the Laplace transforms of the distributions. If we denote the Laplace transform of the function $f(k)$ by $L[f(k)]$, the Laplace transforms of the first three terms for the collinear parts are given by

$$\begin{aligned}
L[\delta(\omega k)] &= \frac{1}{\omega}, \quad L\left[\frac{1}{\mu^2} \mathcal{L}_0\left(\frac{\omega k}{\mu^2}\right)\right] = -\frac{1}{\omega} \ln \frac{se^{\gamma_E} \mu^2}{\omega} = -\frac{1}{\omega} \ln \frac{\mu^2}{\omega Q_L}, \\
L\left[\frac{1}{\mu^2} \mathcal{L}_1\left(\frac{\omega k}{\mu^2}\right)\right] &= \frac{1}{\omega} \left(\frac{1}{2} \ln^2 \frac{se^{\gamma_E} \mu^2}{\omega} + \frac{\pi^2}{12}\right) = \frac{1}{\omega} \left(\frac{1}{2} \ln^2 \frac{\mu^2}{\omega Q_L} + \frac{\pi^2}{12}\right). \tag{A.5}
\end{aligned}$$

and the first three terms from the soft part are given as

$$\begin{aligned}
L[\delta(k)] &= 1, \quad L\left[\frac{1}{\mu} \mathcal{L}_0\left(\frac{k}{\mu}\right)\right] = -\ln(se^{\gamma_E} \mu) = -\ln \frac{\mu}{Q_L}, \\
L\left[\frac{1}{\mu} \mathcal{L}_1\left(\frac{k}{\mu}\right)\right] &= \frac{1}{2} \ln^2(se^{\gamma_E} \mu) + \frac{\pi^2}{12} = \frac{1}{2} \ln^2 \frac{\mu}{Q_L} + \frac{\pi^2}{12}. \tag{A.6}
\end{aligned}$$

B Beam functions and the matching coefficients for small M

The matrix element M_a in eq. (5.4) is given by

$$M_a = \frac{\alpha}{2\pi} \theta\left((1-z)t - zM^2\right) \theta(z) \theta(1-z) \frac{(1-z)t - zM^2}{(t - zM^2)^2}. \quad (\text{B.1})$$

It is regarded as a distribution both in t and z for small M . When M_a is integrated over t to an arbitrary renormalization scale μ^2 , it is given by

$$\int_{zM^2/(1-z)}^{\mu^2} dt M_a \rightarrow \frac{\alpha}{2\pi} (1-z) \left(-1 + \ln \frac{(1-z)\mu^2}{z^2 M^2}\right) \theta(z) \theta(1-z), \quad (\text{B.2})$$

which is regarded as the coefficient of $\delta(t)$. Because M_a in this limit behaves like $\sim 1/t$, it can be written as

$$M_a = \frac{\alpha}{2\pi} (1-z) \theta(z) \theta(1-z) \left[\left(-1 + \ln \frac{(1-z)\mu^2}{z^2 M^2}\right) \delta(t) + f(z, \mu) \frac{1}{\mu^2} \mathcal{L}_0\left(\frac{t}{\mu^2}\right) \right], \quad (\text{B.3})$$

where the function $f(z, \mu)$ is to be determined.

Note that we have the identity

$$\frac{\mu^{2\epsilon}}{t^{1+\epsilon}} = -\frac{1}{\epsilon} \delta(t) + \frac{1}{\mu^2} \mathcal{L}_0\left(\frac{t}{\mu^2}\right) - \epsilon \frac{1}{\mu^2} \mathcal{L}_1\left(\frac{t}{\mu^2}\right) + \dots. \quad (\text{B.4})$$

Taking the logarithmic derivative with respect to μ^2 , we get

$$\begin{aligned} \mu^2 \frac{d}{d\mu^2} \frac{\mu^{2\epsilon}}{t^{1+\epsilon}} &= \epsilon \frac{\mu^{2\epsilon}}{t^{1+\epsilon}} = -\delta(t) + \epsilon \frac{1}{\mu^2} \mathcal{L}_0\left(\frac{t}{\mu^2}\right) + \dots \\ &= \mu^2 \frac{d}{d\mu^2} \frac{1}{\mu^2} \mathcal{L}_0\left(\frac{t}{\mu^2}\right) - \epsilon \mu^2 \frac{d}{d\mu^2} \frac{1}{\mu^2} \mathcal{L}_1\left(\frac{t}{\mu^2}\right) + \dots. \end{aligned} \quad (\text{B.5})$$

Comparing the coefficients of the powers of ϵ , we obtain the result

$$\mu^2 \frac{d}{d\mu^2} \left[\frac{1}{\mu^2} \mathcal{L}_0\left(\frac{t}{\mu^2}\right) \right] = -\delta(t), \quad \mu^2 \frac{d}{d\mu^2} \left[\frac{1}{\mu^2} \mathcal{L}_1\left(\frac{t}{\mu^2}\right) \right] = -\frac{1}{\mu^2} \mathcal{L}_0\left(\frac{t}{\mu^2}\right), \dots. \quad (\text{B.6})$$

In order to determine $f(z, \mu)$, we use the fact that M_a in eq. (5.4) is independent of μ^2 , $\mu^2 dM_a/d\mu^2 = 0$. If we compare the coefficients of $\delta(t)$, we obtain $f(z, \mu) = 1$. The final result is given by

$$M_a = \frac{\alpha}{2\pi} (1-z) \theta(z) \theta(1-z) \left[\left(-1 + \ln \frac{(1-z)\mu^2}{z^2 M^2}\right) \delta(t) + \frac{1}{\mu^2} \mathcal{L}_0\left(\frac{t}{\mu^2}\right) \right]. \quad (\text{B.7})$$

The naive collinear contribution M_b in eq. (5.5) is given by

$$\tilde{M}_b = \frac{\alpha}{2\pi} \frac{z}{1-z} \frac{1}{t - zM^2} \theta\left((1-z)t - zM^2\right) \theta(z) \theta(1-z). \quad (\text{B.8})$$

For small M , it is proportional to $1/t(1-z)$, and should be regarded as distributions both in z and t . We first integrate over t , and it is given as

$$\int_{zM^2/(1-z)}^{\mu^2} dt \tilde{M}_b \rightarrow \frac{\alpha}{2\pi} \theta(z) \theta(1-z) \frac{z}{1-z} \ln \frac{(1-z)\mu^2}{z^2 M^2}, \quad (\text{B.9})$$

which should be regarded as a coefficient of $\delta(t)$, but it is also a distribution in z . Therefore the most general form can be written as

$$\begin{aligned} \tilde{M}_b = \frac{\alpha}{2\pi} \left\{ \delta(t) \left[A\delta(1-z) + z\mathcal{L}_0(1-z) \ln \frac{\mu^2}{z^2 M^2} + z\mathcal{L}_1(1-z) \right] \right. \\ \left. + g(z, \mu) \frac{1}{\mu^2} \mathcal{L}_0\left(\frac{t}{\mu^2}\right) + h(z, \mu) \frac{1}{\mu^2} \mathcal{L}_1\left(\frac{t}{\mu^2}\right) \right\}. \end{aligned} \quad (\text{B.10})$$

Because the integration of \tilde{M}_b over z yields a term proportional to $\ln(t/\mu^2)$, the distribution $\mathcal{L}_1(t/\mu^2)$ is included here. Or we can include \mathcal{L}_n with $n \geq 2$, but the coefficients of those functions turn out to be zero.

Eq. (B.9) is further integrated over z to yield

$$\int_0^{\mu^2/(\mu^2+M^2)} dz \frac{z}{1-z} \ln \frac{(1-z)\mu^2}{z^2 M^2} = -1 + \frac{\pi^2}{3} - \ln \frac{\mu^2}{M^2} + \frac{1}{2} \ln^2 \frac{\mu^2}{M^2}, \quad (\text{B.11})$$

and

$$\int_0^{\mu^2/(\mu^2+M^2)} dz \left(z\mathcal{L}_0(1-z) \ln \frac{\mu^2}{z^2 M^2} + z\mathcal{L}_1(1-z) \right) = -1 + \frac{\pi^2}{3} - \ln \frac{\mu^2}{M^2}. \quad (\text{B.12})$$

Therefore A is determined to be $A = [\ln^2(\mu^2/M^2)]/2$. The unknown quantities $g(z, \mu)$ and $h(z, \mu)$ are determined by requiring that \tilde{M}_b is independent of μ , that is, $\mu^2 d\tilde{M}_b/d\mu^2 = 0$. They are given by

$$f(z, \mu) = \delta(1-z) \ln \frac{\mu^2}{z^2 M^2} + z\mathcal{L}_0(1-z), \quad g(z, \mu) = \delta(1-z). \quad (\text{B.13})$$

The final result is given by

$$\begin{aligned} \tilde{M}_b = \frac{\alpha}{2\pi} \left[\delta(t) \delta(1-z) \frac{1}{2} \ln^2 \frac{\mu^2}{M^2} + \delta(t) z \left(\ln \frac{\mu^2}{z^2 M^2} \mathcal{L}_0(1-z) + \mathcal{L}_1(1-z) \right) \right. \\ \left. + \delta(1-z) \left(\frac{1}{\mu^2} \mathcal{L}_0\left(\frac{t}{\mu^2}\right) \ln \frac{\mu^2}{M^2} + \frac{1}{\mu^2} \mathcal{L}_1\left(\frac{t}{\mu^2}\right) \right) + \frac{z}{\mu^2} \mathcal{L}_0\left(\frac{t}{\mu^2}\right) \mathcal{L}_0(1-z) \right]. \end{aligned} \quad (\text{B.14})$$

C Semi-inclusive jet functions and FJF for small M in SCET_I

C.1 Semi-inclusive jet functions

In taking the limit of small M from eq. (5.30), we use the definition

$$\mathcal{L}_n(x) \equiv \left[\frac{\theta(x) \ln^n x}{x} \right]_+ = \lim_{\beta \rightarrow 0} \left[\frac{\theta(x-\beta) \ln^n x}{x} + \delta(x-\beta) \frac{\ln^{n+1} \beta}{n+1} \right], \quad (\text{C.1})$$

and the following identities:

$$\begin{aligned} \lim_{\beta \rightarrow 0} \left[\frac{\theta(x-\beta) \ln(x-\beta)}{x} + \frac{1}{2} \delta(x-\beta) \ln^2 \beta \right] &= \mathcal{L}_1(x) - \frac{\pi^2}{6} \delta(x), \\ \lim_{\beta \rightarrow 0} \frac{\theta(x-\beta) \beta}{x^2} &= \delta(x), \quad \lim_{\beta \rightarrow 0} \frac{\theta(x-\beta) \beta^2}{x^3} = \frac{1}{2} \delta(x). \end{aligned} \quad (\text{C.2})$$

Putting $x = p^2/\mu^2$ and $\beta = M^2/\mu^2$, and using the relations eqs. (C.1) and (C.2), M_a and M_b in eq. (5.30) are written as

$$\begin{aligned} M_a &= \frac{\alpha}{2\pi} \frac{1}{\mu^2} \left(\frac{1}{2x} - \frac{\beta}{x^2} + \frac{1}{2} \frac{\beta^2}{x^3} \right) \theta(x - \beta) = \frac{\alpha}{2\pi} \left[\delta(p^2) \left(-\frac{3}{4} + \frac{1}{2} \ln \frac{\mu^2}{M^2} \right) + \frac{1}{2\mu^2} \mathcal{L}_0 \left(\frac{p^2}{\mu^2} \right) \right], \\ M_b &= \frac{\alpha}{2\pi} \frac{1}{\mu^2} \left(-\frac{1 + \ln \beta}{x} + \frac{\ln x}{x} + \frac{\beta}{x^2} \right) \theta(x - \beta) \\ &= \frac{\alpha}{2\pi} \left[\delta(p^2) \left(1 - \ln \frac{\mu^2}{M^2} + \frac{1}{2} \ln^2 \frac{\mu^2}{M^2} \right) - \frac{1}{\mu^2} \mathcal{L}_0 \left(\frac{p^2}{\mu^2} \right) \left(1 - \ln \frac{\mu^2}{M^2} \right) + \frac{1}{\mu^2} \mathcal{L}_1 \left(\frac{p^2}{\mu^2} \right) \right]. \end{aligned} \quad (\text{C.3})$$

The contributions M_b^\emptyset and M_c , and the wavefunction renormalization with the residue remain the same.

C.2 Fragmenting jet functions

Out of the matrix elements in eq. (5.40) for the FJFs, we need to consider M_a and \tilde{M}_b in the limit of small M and the rest remains the same in the limit. Firstly, M_a is given by

$$\begin{aligned} M_a &= \frac{\alpha}{2\pi} \theta(z) \theta(1-z) \theta \left(p^2 - \frac{M^2}{1-z} \right) \frac{1}{p^2} \left(1 - z - \frac{M^2}{p^2} \right) \\ &= \frac{\alpha}{2\pi} \theta(z) \theta(1-z) \theta(z - \beta) \frac{1-z}{\mu^2} \left(\frac{1}{z} - \frac{\beta}{z^2} \right), \end{aligned} \quad (\text{C.4})$$

where the dimensionless variables $z = p^2/\mu^2$, $\beta = M^2/[(1-z)\mu^2]$ are introduced. Using the definitions of the distributions and their properties in eqs. (C.1) and (C.2), M_a is written as

$$M_a = \frac{\alpha}{2\pi} \theta(z) \theta(1-z) (1-z) \left[\delta(p^2) \left(\ln \frac{(1-z)\mu^2}{M^2} - 1 \right) + \frac{1}{\mu^2} \mathcal{L}_0 \left(\frac{p^2}{\mu^2} \right) \right]. \quad (\text{C.5})$$

In order to compute the limit of small M in

$$\tilde{M}_b = \frac{\alpha}{2\pi} \theta(z) \theta(1-z) \theta \left(p^2 - \frac{M^2}{1-z} \right) \frac{1}{p^2} \frac{z}{1-z}, \quad (\text{C.6})$$

we first expand $1/p^2$ as distributions in the form

$$\frac{1}{p^2} \frac{1}{1-z} \theta \left(p^2 - \frac{M^2}{1-z} \right) = \delta(p^2) h(z, \mu) + \frac{1}{\mu^2} \mathcal{L}_0 \left(\frac{p^2}{\mu^2} \right) g(z, \mu) + \frac{1}{\mu^2} \mathcal{L}_1 \left(\frac{p^2}{\mu^2} \right) f(z, \mu) + \dots, \quad (\text{C.7})$$

where the functions $h(z, \mu)$, $g(z, \mu)$ and $f(z, \mu)$ are to be determined. Following the procedure explained in appendix B, \tilde{M}_b is given as

$$\begin{aligned} \tilde{M}_b &= \frac{\alpha}{2\pi} \left[\delta(p^2) \delta(1-z) \frac{1}{2} \ln^2 \frac{\mu^2}{M^2} + \delta(p^2) \left(z \ln \frac{\mu^2}{M^2} \mathcal{L}_0(1-z) + z \mathcal{L}_1(1-z) \right) \right. \\ &\quad \left. + \delta(1-z) \left(\frac{1}{\mu^2} \mathcal{L}_0 \left(\frac{p^2}{\mu^2} \right) \ln \frac{\mu^2}{M^2} + \frac{1}{\mu^2} \mathcal{L}_1 \left(\frac{p^2}{\mu^2} \right) \right) + \frac{z}{\mu^2} \mathcal{L}_0 \left(\frac{p^2}{\mu^2} \right) \mathcal{L}_0(1-z) \right]. \end{aligned} \quad (\text{C.8})$$

D Color structures of the soft functions

D.1 Tree-level color matrices for the soft functions

We present the color factors for the tree-level soft functions with different number of nonsinglets.

$$\begin{aligned}
\mathbf{S}^{(0)}(0,0,0,0) &= \begin{pmatrix} C_A C_F/2 & 0 \\ 0 & C_A^2 \end{pmatrix}, & (D.1) \\
\mathbf{S}^{(0)}(1,1,0,0) &= \frac{1}{2} \begin{pmatrix} C_F - \frac{C_A}{2} & 0 \\ 0 & 2C_A \end{pmatrix} \quad (12), \quad \mathbf{S}^{(0)}(0,0,1,1) = \frac{1}{2} \begin{pmatrix} C_F - \frac{C_A}{2} & 0 \\ 0 & 2C_A \end{pmatrix} \quad (34), \\
\mathbf{S}^{(0)}(1,0,1,0) &= \frac{1}{2} \begin{pmatrix} 2C_F - \frac{C_A}{2} & 1 \\ 1 & 0 \end{pmatrix} \quad (13), \quad \mathbf{S}^{(0)}(0,1,0,1) = \frac{1}{2} \begin{pmatrix} 2C_F - \frac{C_A}{2} & 1 \\ 1 & 0 \end{pmatrix} \quad (24), \\
\mathbf{S}^{(0)}(1,0,0,1) &= \frac{1}{2} \begin{pmatrix} 2C_F - C_A & 1 \\ 1 & 0 \end{pmatrix} \quad (14), \quad \mathbf{S}^{(0)}(0,1,1,0) = \begin{pmatrix} C_F - \frac{C_A}{2} & \frac{1}{2} \\ \frac{1}{2} & 0 \end{pmatrix} \quad (23), \\
\mathbf{S}^{(0)}(1,1,1,0) &= \frac{1}{2} \begin{pmatrix} C_F - \frac{C_A}{2} & 0 \\ 1 & 0 \end{pmatrix} \quad (123) + \frac{1}{2} \begin{pmatrix} C_F - \frac{C_A}{2} & 1 \\ 0 & 0 \end{pmatrix} \quad (132), \\
\mathbf{S}^{(0)}(1,1,0,1) &= \frac{1}{2} \begin{pmatrix} C_F - \frac{C_A}{2} & 0 \\ 1 & 0 \end{pmatrix} \quad (124) + \frac{1}{2} \begin{pmatrix} C_F - \frac{C_A}{2} & 1 \\ 0 & 0 \end{pmatrix} \quad (142), \\
\mathbf{S}^{(0)}(1,0,1,1) &= \frac{1}{2} \begin{pmatrix} C_F - \frac{C_A}{2} & 0 \\ 1 & 0 \end{pmatrix} \quad (143) + \frac{1}{2} \begin{pmatrix} C_F - \frac{C_A}{2} & 1 \\ 0 & 0 \end{pmatrix} \quad (134), \\
\mathbf{S}^{(0)}(0,1,1,1) &= \frac{1}{2} \begin{pmatrix} C_F - \frac{C_A}{2} & 0 \\ 1 & 0 \end{pmatrix} \quad (243) + \frac{1}{2} \begin{pmatrix} C_F - \frac{C_A}{2} & 1 \\ 0 & 0 \end{pmatrix} \quad (234).
\end{aligned}$$

Here $(a_1 a_2 \dots a_n) = \text{Tr}(t^{a_1} t^{a_2} \dots t^{a_n})$, and the color indices are to be contracted with the corresponding collinear nonsinglet parts. Note that the soft color matrices with a single nonsinglet are zero due to weak charge conservation.⁷

$$\mathbf{S}(1,0,0,0) = \mathbf{S}(0,1,0,0) = \mathbf{S}(0,0,1,0) = \mathbf{S}(0,0,0,1) = 0. \quad (D.2)$$

The color structure with all the four nonsinglets is given by

$$\begin{aligned}
\mathbf{S}^{(0)}(1,1,1,1) &= \frac{1}{2} \begin{pmatrix} C_F - \frac{C_A}{2} & 0 \\ 1 & 0 \end{pmatrix} \quad (1243) + \frac{1}{2} \begin{pmatrix} C_F - \frac{C_A}{2} & 1 \\ 0 & 0 \end{pmatrix} \quad (1342) \\
&+ \begin{pmatrix} (C_F - \frac{C_A}{2})^2 & C_F - \frac{C_A}{2} \\ C_F - \frac{C_A}{2} & 1 \end{pmatrix} \quad (12)(34) + \begin{pmatrix} \frac{1}{4} & 0 \\ 0 & 0 \end{pmatrix} \quad (13)(24). & (D.3)
\end{aligned}$$

⁷In SU(2), all the color matrices with the odd number of nonsinglets become zero.

D.2 No mixing in the soft function at order α

We show that there is no mixing in the N -jettiness soft function for the case with all the four nonsinglets. In ref. [24], there are three independent functions and there is a mixing among these terms at order α . We treat the soft function in the operator basis as a 2×2 matrix. Here when we consider the jettiness, there is also a mixing in the real contributions, while there is no mixing in the virtual contributions. But it turns out that the mixing is cancelled in the sum.

The soft color matrix $\mathbf{S}^{(0)}(1, 1, 1, 1)$ in eq. (D.3) includes the color factors (1243), (1342), (13)(24) and (12)(34). There is mixing because there appear different color factors at one loop, which are not present at tree level. It is helpful to look at the soft part in eq. (3.30) with all the nonsinglets, which is given as

$$\langle 0 | \text{Tr} \left(t^c S_2^\dagger T_J S_1(0) t^d S_1^\dagger T_I S_2(x) \right) \cdot \text{Tr} \left(t^e S_3^\dagger T_J S_4(0) t^f S_4^\dagger T_I S_3(x) \right) | 0 \rangle. \quad (\text{D.4})$$

The contractions of the fields at 0 or x yield virtual contributions, while the contraction of the fields with 0 and x yield real contributions.

Each contraction of i and j in the virtual contributions in figure 5 (a) does not produce new color structures, while the real contributions produce new color structures. The contractions of i with j in the real contributions at one loop in figure 5 (b) produce the following color structures:

$$\begin{aligned} S_{12+21}^{R(1)}(1, 1, 1, 1) &= -\left(C_F - \frac{C_A}{2}\right) \mathbf{S}^{(0)}(1, 1, 1, 1) - \frac{1}{8} \begin{pmatrix} 1 & 0 \\ 0 & 0 \end{pmatrix} \left[(1423) + (1324) \right], \\ S_{13+31}^{R(1)}(1, 1, 1, 1) &= -\left(C_F - \frac{C_A}{2}\right) \mathbf{S}^{(0)}(1, 1, 1, 1) - \frac{1}{8N^2} \begin{pmatrix} 1 & -2N \\ -2N & 4N^2 \end{pmatrix} \left[(1432) + (1234) \right], \\ S_{14+41}^{R(1)}(1, 1, 1, 1) &= -\left(C_F - \frac{C_A}{2}\right) \mathbf{S}^{(0)}(1, 1, 1, 1) + \frac{1}{8} \begin{pmatrix} 1 & 0 \\ 0 & 0 \end{pmatrix} \left[(1423) + (1324) \right] \\ &\quad + \frac{1}{8N^2} \begin{pmatrix} 1 & -2N \\ -2N & 4N^2 \end{pmatrix} \left[(1432) + (1234) \right], \\ S_{23+32}^{R(1)}(1, 1, 1, 1) &= -\left(C_F - \frac{C_A}{2}\right) \mathbf{S}^{(0)}(1, 1, 1, 1) + \frac{1}{8} \begin{pmatrix} 1 & 0 \\ 0 & 0 \end{pmatrix} \left[(1423) + (1324) \right] \\ &\quad + \frac{1}{8N^2} \begin{pmatrix} 1 & -2N \\ -2N & 4N^2 \end{pmatrix} \left[(1432) + (1234) \right], \\ S_{24+42}^{R(1)}(1, 1, 1, 1) &= -\left(C_F - \frac{C_A}{2}\right) \mathbf{S}^{(0)}(1, 1, 1, 1) - \frac{1}{8N^2} \begin{pmatrix} 1 & -2N \\ -2N & 4N^2 \end{pmatrix} \left[(1432) + (1234) \right], \\ S_{34+43}^{R(1)}(1, 1, 1, 1) &= -\left(C_F - \frac{C_A}{2}\right) \mathbf{S}^{(0)}(1, 1, 1, 1) - \frac{1}{8} \begin{pmatrix} 1 & 0 \\ 0 & 0 \end{pmatrix} \left[(1423) + (1324) \right], \end{aligned} \quad (\text{D.5})$$

where the extra terms in each contraction represents the new color structures which are not present in $\mathbf{S}^{(0)}(1, 1, 1, 1)$. The first term $S_{12+21}^{R(1)}(1, 1, 1, 1)$, for example, represents the

sum of the contributions $i, j = 1, 2$ and $2, 1$, where the two contributions have different color factors (1423) and (1324).

When summed over all the contractions (ij), these additional contributions cancel in $d\mathbf{S}/d\ln\mu$ from eq. (7.20), because $dS_{ij,\text{hemi}}^R/d\ln\mu$ are independent of n_{ij} . Though $dS_{ij,\text{hemi}}^V/d\ln\mu$ depends on n_{ij} , there is no mixing in the color structure for the virtual contributions. As a consequence, there is no mixing in the soft anomalous dimensions at one loop. On the other hand, in inclusive cross sections in which both $dS_{ij}^R/d\ln\mu$ and $dS_{ij}^V/d\ln\mu$ depend on n_{ij} [24], there appears mixing in the contributions with four non-inglets.

Acknowledgments

This work is supported by Basic Science Research Program through the National Research Foundation of Korea (NRF) funded by the Ministry of Education (Grant No. NRF-2019R1F1A1060396).

References

- [1] C. W. Bauer, S. Fleming, and M. E. Luke, *Summing Sudakov logarithms in $B \rightarrow X_s \gamma$ in effective field theory*, *Phys. Rev.* **D63** (2000) 014006, [[hep-ph/0005275](#)].
- [2] C. W. Bauer, S. Fleming, D. Pirjol, and I. W. Stewart, *An Effective field theory for collinear and soft gluons: Heavy to light decays*, *Phys. Rev.* **D63** (2001) 114020, [[hep-ph/0011336](#)].
- [3] C. W. Bauer and I. W. Stewart, *Invariant operators in collinear effective theory*, *Phys. Lett. B* **516** (2001) 134–142, [[hep-ph/0107001](#)].
- [4] C. W. Bauer, D. Pirjol, and I. W. Stewart, *Soft collinear factorization in effective field theory*, *Phys. Rev.* **D65** (2002) 054022, [[hep-ph/0109045](#)].
- [5] D. d’Enterria, *Physics at the FCC-ee*, in *17th Lomonosov Conference on Elementary Particle Physics*, 2, 2016. [arXiv:1602.05043](#).
- [6] **ILC** Collaboration, G. Aarons et al., *International Linear Collider Reference Design Report Volume 2: Physics at the ILC*, [arXiv:0709.1893](#).
- [7] **FCC** Collaboration, A. Abada et al., *FCC-ee: The Lepton Collider: Future Circular Collider Conceptual Design Report Volume 2*, *Eur. Phys. J. ST* **228** (2019), no. 2 261–623.
- [8] **CLICdp**, **CLIC** Collaboration, T. K. Charles et al., *The Compact Linear Collider (CLIC) - 2018 Summary Report*, [arXiv:1812.06018](#).
- [9] J. Collins, *Foundations of Perturbative QCD*. Cambridge Monographs on Particle Physics, Nuclear Physics and Cosmology. Cambridge University Press, 2011.
- [10] A. Idilbi and T. Mehen, *On the equivalence of soft and zero-bin subtractions*, *Phys. Rev. D* **75** (2007) 114017, [[hep-ph/0702022](#)].
- [11] A. Idilbi and T. Mehen, *Demonstration of the equivalence of soft and zero-bin subtractions*, *Phys. Rev. D* **76** (2007) 094015, [[arXiv:0707.1101](#)].
- [12] T. Becher and G. Bell, *Analytic Regularization in Soft-Collinear Effective Theory*, *Phys. Lett. B* **713** (2012) 41–46, [[arXiv:1112.3907](#)].

- [13] J.-y. Chiu, A. Jain, D. Neill, and I. Z. Rothstein, *The Rapidity Renormalization Group*, *Phys. Rev. Lett.* **108** (2012) 151601, [[arXiv:1104.0881](#)].
- [14] J.-Y. Chiu, A. Jain, D. Neill, and I. Z. Rothstein, *A Formalism for the Systematic Treatment of Rapidity Logarithms in Quantum Field Theory*, *JHEP* **05** (2012) 084, [[arXiv:1202.0814](#)].
- [15] Y. Li, D. Neill, and H. X. Zhu, *An exponential regulator for rapidity divergences*, *Nucl. Phys. B* **960** (2020) 115193, [[arXiv:1604.00392](#)].
- [16] M. A. Ebert, I. Moulton, I. W. Stewart, F. J. Tackmann, G. Vita, and H. X. Zhu, *Subleading power rapidity divergences and power corrections for q_T* , *JHEP* **04** (2019) 123, [[arXiv:1812.08189](#)].
- [17] J. Chay and C. Kim, *Consistent treatment of rapidity divergence in soft-collinear effective theory*, *JHEP* **03** (2021) 300, [[arXiv:2008.00617](#)].
- [18] A. V. Manohar and I. W. Stewart, *Running of the heavy quark production current and $1/v$ potential in QCD*, *Phys. Rev. D* **63** (2001) 054004, [[hep-ph/0003107](#)].
- [19] A. H. Hoang, A. V. Manohar, and I. W. Stewart, *The Running Coulomb potential and Lamb shift in QCD*, *Phys. Rev. D* **64** (2001) 014033, [[hep-ph/0102257](#)].
- [20] M. Ciafaloni, P. Ciafaloni, and D. Comelli, *Bloch-Nordsieck violating electroweak corrections to inclusive TeV scale hard processes*, *Phys. Rev. Lett.* **84** (2000) 4810–4813, [[hep-ph/0001142](#)].
- [21] M. Ciafaloni, P. Ciafaloni, and D. Comelli, *Bloch-Nordsieck violation in spontaneously broken Abelian theories*, *Phys. Rev. Lett.* **87** (2001) 211802, [[hep-ph/0103315](#)].
- [22] P. Ciafaloni and D. Comelli, *The Importance of weak bosons emission at LHC*, *JHEP* **09** (2006) 055, [[hep-ph/0604070](#)].
- [23] A. Manohar, B. Shotwell, C. Bauer, and S. Turczyk, *Non-cancellation of electroweak logarithms in high-energy scattering*, *Phys. Lett. B* **740** (2015) 179–187, [[arXiv:1409.1918](#)].
- [24] A. V. Manohar and W. J. Waalewijn, *Electroweak Logarithms in Inclusive Cross Sections*, *JHEP* **08** (2018) 137, [[arXiv:1802.08687](#)].
- [25] I. W. Stewart, F. J. Tackmann, and W. J. Waalewijn, *N -Jettiness: An Inclusive Event Shape to Veto Jets*, *Phys. Rev. Lett.* **105** (2010) 092002, [[arXiv:1004.2489](#)].
- [26] T. T. Jouttenus, I. W. Stewart, F. J. Tackmann, and W. J. Waalewijn, *The Soft Function for Exclusive N -Jet Production at Hadron Colliders*, *Phys. Rev. D* **83** (2011) 114030, [[arXiv:1102.4344](#)].
- [27] I. W. Stewart, F. J. Tackmann, and W. J. Waalewijn, *The Beam Thrust Cross Section for Drell-Yan at NNLL Order*, *Phys. Rev. Lett.* **106** (2011) 032001, [[arXiv:1005.4060](#)].
- [28] D. Bertolini, D. Kolodrubetz, D. Neill, P. Pietrulewicz, I. W. Stewart, F. J. Tackmann, and W. J. Waalewijn, *Soft Functions for Generic Jet Algorithms and Observables at Hadron Colliders*, *JHEP* **07** (2017) 099, [[arXiv:1704.08262](#)].
- [29] G. Lusterians, J. K. L. Michel, F. J. Tackmann, and W. J. Waalewijn, *Joint two-dimensional resummation in q_T and 0-jettiness at NNLL*, *JHEP* **03** (2019) 124, [[arXiv:1901.03331](#)].
- [30] G. Buchalla, A. J. Buras, and M. E. Lautenbacher, *Weak decays beyond leading logarithms*, *Rev. Mod. Phys.* **68** (1996) 1125–1144, [[hep-ph/9512380](#)].

- [31] R. Kelley and M. D. Schwartz, *1-loop matching and NNLL resummation for all partonic 2 to 2 processes in QCD*, *Phys. Rev. D* **83** (2011) 045022, [[arXiv:1008.2759](#)].
- [32] C. W. Bauer, A. Hornig, and F. J. Tackmann, *Factorization for generic jet production*, *Phys. Rev. D* **79** (2009) 114013, [[arXiv:0808.2191](#)].
- [33] I. W. Stewart, F. J. Tackmann, and W. J. Waalewijn, *The Quark Beam Function at NNLL*, *JHEP* **09** (2010) 005, [[arXiv:1002.2213](#)].
- [34] Z.-B. Kang, F. Ringer, and I. Vitev, *The semi-inclusive jet function in SCET and small radius resummation for inclusive jet production*, *JHEP* **10** (2016) 125, [[arXiv:1606.06732](#)].
- [35] L. Dai, C. Kim, and A. K. Leibovich, *Fragmentation of a Jet with Small Radius*, *Phys. Rev. D* **94** (2016), no. 11 114023, [[arXiv:1606.07411](#)].
- [36] S. D. Ellis, C. K. Vermilion, J. R. Walsh, A. Hornig, and C. Lee, *Jet Shapes and Jet Algorithms in SCET*, *JHEP* **11** (2010) 101, [[arXiv:1001.0014](#)].
- [37] I. W. Stewart, F. J. Tackmann, and W. J. Waalewijn, *Factorization at the LHC: From PDFs to Initial State Jets*, *Phys. Rev. D* **81** (2010) 094035, [[arXiv:0910.0467](#)].
- [38] M. Baumgart, O. Erdoğan, I. Z. Rothstein, and V. Vaidya, *Breakdown of the naive parton model in super-weak scale collisions*, *Phys. Rev. D* **100** (2019), no. 9 096008, [[arXiv:1811.04120](#)].
- [39] Z. Ligeti, I. W. Stewart, and F. J. Tackmann, *Treating the b quark distribution function with reliable uncertainties*, *Phys. Rev. D* **78** (2008) 114014, [[arXiv:0807.1926](#)].
- [40] G. P. Korchemsky and A. V. Radyushkin, *Renormalization of the Wilson Loops Beyond the Leading Order*, *Nucl. Phys. B* **283** (1987) 342–364.
- [41] I. A. Korchemskaya and G. P. Korchemsky, *On lightlike Wilson loops*, *Phys. Lett. B* **287** (1992) 169–175.
- [42] M. Procura and I. W. Stewart, *Quark Fragmentation within an Identified Jet*, *Phys. Rev. D* **81** (2010) 074009, [[arXiv:0911.4980](#)]. [Erratum: *Phys.Rev.D* 83, 039902 (2011)].
- [43] A. Jain, M. Procura, and W. J. Waalewijn, *Parton Fragmentation within an Identified Jet at NNLL*, *JHEP* **05** (2011) 035, [[arXiv:1101.4953](#)].
- [44] J.-y. Chiu, A. Fuhrer, R. Kelley, and A. V. Manohar, *Factorization Structure of Gauge Theory Amplitudes and Application to Hard Scattering Processes at the LHC*, *Phys. Rev. D* **80** (2009) 094013, [[arXiv:0909.0012](#)].
- [45] J. Chay, C. Kim, Y. G. Kim, and J.-P. Lee, *Soft Wilson lines in soft-collinear effective theory*, *Phys. Rev. D* **71** (2005) 056001, [[hep-ph/0412110](#)].
- [46] M. Sjö Dahl, *ColorMath - A package for color summed calculations in SU(Nc)*, *Eur. Phys. J. C* **73** (2013), no. 2 2310, [[arXiv:1211.2099](#)].
- [47] T. Becher, M. Neubert, and B. D. Pecjak, *Factorization and Momentum-Space Resummation in Deep-Inelastic Scattering*, *JHEP* **01** (2007) 076, [[hep-ph/0607228](#)].